From the Department of Neuroscience
Karolinska Institutet, Stockholm, Sweden

WHO, WHEN & HOW

ELECTROPHYSIOLOGICAL STUDIES ON CONNECTIVITY OF STRIATAL NEURONS

Susanne Szydlowski

Karolinska Institutet

Stockholm 2014

Published by Karolinska Institutet. Printed by Åtta.45 Tryckeri AB

ISBN 978-91-7549-557-6

WHO, WHEN & HOW
Electrophysiological studies on connectivity of striatal neurons

THESIS FOR DOCTORAL DEGREE (Ph.D.)

By

Susanne Natalie Szydlowski

Principal Supervisor:
Assoc. Prof. Gilad Silberberg
Karolinska Institutet
Department of Neuroscience

Co-supervisor(s):
Prof. Sten Grillner
Karolinska Institutet
Department of Neuroscience

Assistant Prof. Marie Carlén
Karolinska Institutet
Department of Neuroscience

Opponent:
Dr. Enrico Bracci
University of Sheffield
Department of Psychology

Examination Board:
Assoc. Prof. Karima Chergui
Karolinska Institutet
Department of Physiology & Pharmacology

Assoc. Prof. Louise Adermark
Gothenburg University
Department of Neuroscience & Physiology
Division of Addiction Biology

Prof. Gilberto Fisone
Karolinska Institutet
Department of Neuroscience

ABSTRACT

The nervous system has been studied in many ways and in many different organisms. Organisms that have a brain and mind or a simpler nervous system use it to sense the environment, process this sensory input and make appropriate decisions on how to act or interact with the environment. The complexity of the nervous system varies with the type of organism but this basic function remains the same. This thesis aims to examine a part of the brain called the striatum that is tightly interlinked with action selection and motor control. The approach employed is a reductionist approach where we look at the different parts constituting the striatum, the striatal neuronal types (WHO), their interaction (HOW), temporal aspects of the interaction (WHEN) and by what means the interaction can be altered or modulated (HOW).

In the first study we investigated the striatal neuronal types (WHO) and more specifically the histochemical and electrophysiological properties of the 5HT3a-EGFP + neurons. We showed that they are interneurons and show little overlap with any of the classical striatal markers with the highest overlap being with parvalbumin. Furthermore we have showed that they fall into three categories of interneurons with resemblance to the classical striatal interneurons Fast spiking interneurons (FSIs), neurogliaform interneurons (NGF) and Low-threshold spiking interneurons (LTSIs). The LTS-like 5HT3a-EGFP+ interneurons show a strong and reliable response to nicotine, which is different from the one recorded in LTSIs from Lhx6-EGFP mice. With the findings from the studies we hypothesize that the 5HT3a-EGFP+, LTSIs and NGF interneurons are a novel subpopulation of striatal interneurons.

In the second study we investigated HOW the striatal neurons interact and the temporal aspects of this interaction (WHEN). More specifically we used the patch-clamp technique to investigate both intrastriatal feedforward and feedback connections and the dynamics of these synapses. We found that Medium spiny neuron to Medium spiny neuron (MSN) interconnectivity is sparse and that MSNs of both the indirect and direct pathway contact each other. The indirect pathway MSN is to a larger extent the presynaptic cell but contacts - MSNs of both types with similar probabilities. There is no difference in the connections when it comes to amplitudes or synaptic dynamics and they exhibit both facilitating and depressing components. We saw that FSIs contact MSNs with high probability and that these connections exhibit reliably depressing synaptic dynamics. Furthermore, they contact MSNs of both types and the same FSI even contacts MSNs of both types.
In the third study we extended our investigations of feedforward inhibition by FSIs. We used optogenetics and patch-clamp recordings to investigate which striatal interneurons the FSIs form connections with. We found that FSIs are target selective and completely avoid Cholinergic interneurons (AChIs) while forming sparse connections with LTSIs. This suggests that the functions and roles of the different types of striatal interneurons are separated and that the AChIs could be specifically involved in reinforcement learning and that the FSIs have a more specific role in action-selection.

In the last study we investigated HOW the striatal connections can be altered by membrane fluctuations. More specifically we investigated how the membrane potential of the presynaptic cell can modulate the connections formed between FSI-MSN and MSN-MSN. We found that it has an effect on the release probability of the synapse. The extent of the effect is dictated by the initial release probability of the synapse and this type of presynaptic modulation might serve to make synapses more precise and time-locked. The study indicates how the membrane potential fluctuations of striatal neurons seen in-vivo can alter the dynamics of the connectivity.

LIST OF PUBLICATIONS

I. Ana B. Muñoz-Manchado*, Claire Foldi*, **Susanne N Szydlowski***, Luke Sjulson, Michael Ferries, Charles Wilson, Gilad Silberberg and Jens Hjerling-Leffler. Neuronal population labelled in the 5HT3a^{EGFP} mouse doubles the amount of molecularly defined striatal GABAergic interneurons. *Submitted Manuscript*

II. Henrike Planert, **Susanne N Szydlowski**, Johannes J Hjorth, Sten Grillner* and Gilad Silberberg*. Dynamics of synaptic transmission between fast-spiking interneurons and striatal projection neurons of the direct and indirect pathways. J Neuroscience. 2010 March 30(9): 3499-507.

III. **Susanne N Szydlowski***, Iskra Pollak Dorocic*, Henrike Planert*, Marie Carlén, Konstantinos Meletis & Gilad Silberberg. Target Selectivity of feedforward inhibition by striatal fast-spiking interneurons. J Neuroscience. 2013 Jan 33(4):1678-1683

IV. Henrike Planert*, **Susanne N Szydlowski*** and Gilad Silberberg. Modulation of intrastriatal connections by presynaptic membrane potential. *Manuscript*

*These authors contributed equally

PUBLICATIONS NOT INCLUDED IN THE THESIS

Erik Norberg, Marie Karlsson, Olga Korenovska, **Susanne N Szydlowski**, Gilad Silberberg, Per Uhlén, Sten Orrenius and Boris Zhivotovsky. Critical role for hyperpolarization-activated cyclic nucleotide-gated channel 2 in the AIF-mediated apoptosis. The EMBO journal. 2010 Oct 29(22): 3869–3878.

TABLE OF CONTENTS

LIST OF ABBREVIATIONS

SNc	Substantia Nigra pars Compacta
GPi	Globus Pallidus Interna
SNr	Substantia Nigra pars Reticulata
GPe	Globus Pallidus Externa
STN	Subthalamic Nucleus
AP	Action Potential
GABA	ϒ Amino Butyric Acid
MSN	Medium Spiny Neuron
D1R/DRD1	Dopamine D1 Receptor
D2RDRD2	Dopamine D2 Receptor
SP	Substance P
ChAT	Choline Acetyl Transferase
AChI	Cholinergic Interneuron
TAN	Tonically Active Neuron
AHP	Afterhyperpolarization
PV	Parvalbumin
FSI	Fast Spiking Interneuron
SOM	Somatostatin
NPY	Neuropeptide Y
nNOS	Nitric Oxide Synthase
LTSI	Low Threshold Spiking Interneuron
NGF	Neurogliaform Interneuron
(E)GFP	(Enhanced) Green Fluorescent Protein
CR	Calretinin
TH	Tyrosine Hydroxylase
L-DOPA	L-3,4-Dihydroxyphenylalanin
5HT	5-hydroxytryptamine (Serotonin)
VGluT3	Vesicular Glutamate Transporter 3
FACS	Fluorescence Activated Cell Sorting
Ctip-2	Coup-TF Interacting Protein 2
DARPP-32	Dopamine and cAMP Regulated Phosphoprotein 32
Lhx6	LIM homeobox protein 6
iMSN	Indirect pathway Medium Spiny Neuron
dMSN	Direct pathway Medium Spiny Neuron
RMP	Resting Membrane Potential
LTP	Long Term Potentiation
LTD	Long Term Depression

STDP	Spike Timing Dependent Plasticity
STD	Short Term Depression
STP/STF	Short Term Potentiation/Short Term Facilitation
PPR	Paired Pulse Ratio
PSP	Postsynaptic Potential
ChR2	Channelrhodopsin 2
Cre	Causes Recombination
nAChRs	Nicotinic Acetylcholine Receptor
mAChRs	Muscarinic Acetylcholine Receptor
AChR	Acetylcholine Receptor
NK	Neurokinin
GPCR	G-Protein Coupled Receptor
DA	Dopamine
CPBG	Chloropheneylbiguanide
RT-PCR	Reverse Transcription Polymerase Chain Reaction
CNQX	6-Cyano-7-nitroquinoxaline-2,3-dione
AP-V	D-(-)-2-Amino-5-phosphonopentanoic acid
ANOVA	Analysis of Variance
ABC-DAB	Avidin-Biotin Complex- 3′,3′-diaminobenzidine
EGTA	Ethylene Glycol Tetraacetic Acid
BAPTA	1,2-bis(o-aminophenoxy)ethane-N,N,N′N′-tetraacetic acid

DECONSTRUCTING THE BRAIN- THE REDUCTIONIST BASIS OF MODERN NEUROSCIENCE

The mind has fascinated and perplexed thinkers of all times. Plato and Aristotle pondered about it and gave humans a so-called rational soul. The rational soul was thought to enable us to take in and act in the world. Descartes in the 17th century developed what we call Cartesian Dualism, which separates the brain into body and mind. This way of seeing the brain and mind, to a large part, still influences the way we think about the brain. Especially so in psychiatric disorders, where a bodily dysfunction in fact is not separated from the mind and can influence the mind, soul and what we perceive as personality.

In the 18th century the mind and brain was tackled by looking at the skull. It was subdivided, measured and according to the results, phrenologists thought they could deduce and decide the character of a person. During the same period Luigi Galvani first discovered what is commonly known as animal electricity. He discovered that muscles in the leg of a frog could twitch. Electrical signals as part of the nervous system is a fundamental principle of modern neuroscience, but it was not until the work of Santiago Ramón y Cajal that the real foundation of modern neuroscience was laid. He started the work of identifying the building blocks of the brain, namely the nerve cells or neurons. In order to do so he used a technique called a Golgi staining that he learnt from Camillo Golgi. With this technique the intricate anatomy of the building blocks were beautifully revealed and Ramon y Cajal proposed that what he saw were neurons rather than a continuous network. He also postulated that the neurons constitute different portions that serve various purposes for example linking them to other neurons.

Since then the nervous system has been studied in many ways and in many different organisms. Organisms that have a brain and mind or a simpler nervous system use it to sense the environment, process this sensory input and make appropriate decisions on how to act or interact with the environment. The complexity of the nervous system varies with the type of organism but this basic function remains the same. This thesis aims to examine a part of the brain called the striatum that is tightly interlinked with action selection and motor control. The striatum is part of a larger set of nuclei called the basal ganglia. The approach to understanding the striatum in this thesis is in line with the reductionist approach also employed by Ramón y Cajal and focuses on the different striatal neuronal types (WHO), their interaction (HOW), temporal aspects of the interaction (WHEN) and by what means the interaction can be altered or modulated (HOW).t striatal neuronal types (WHO), HOW they interact, temporal aspects of the interaction (WHEN) and HOW the interaction can be altered or modulated.

WHO

DECONSTRUCTING THE BASAL GANGLIA

The basal ganglia are a group of subcortical nuclei that are grouped together because of their interconnectivity and involvement in similar processes and functions. They are thought to be involved in functions ranging from action selection and motor learning to reinforcement learning and reward(English et al., 2012; Frank, 2004; Middleton and Strick, 2000; Schultz, 2002; Sullivan et al., 2008; Turner and Desmurget, 2010). They are involved in many disease states such as Parkinson's disease, Huntington's disease, Tourette's syndrome, ADHD addiction disorders and schizophrenia(Albin et al., 1989; 1995; Alexander et al., 1986; Hsu et al., 2010; Koob and Volkow, 2010; Mink, 2001; Olson, 2004). The striatum is the input structure of the basal ganglia and receives glutamatergic input from the whole cortical mantle(Carman et al., 1965; Kemp and Powell, 1970; Knook, 1965; Webster, 1961). The input comes primarily from layer 5 pyramidal neurons and is topographically and somatotopically organized although not in a continuous fashion(Jones et al., 1977; Kincaid et al., 1998; Kincaid and Wilson, 1996; Kunzle, 1975; 1977; Malach and Graybiel, 1986). Apart from the cortex the striatum also receives glutamatergic input from the thalamus, serotonergic input from the dorsal raphe nucleus and dopaminergic input from the Substantia Nigra pars Compacta (SNc) (Anden et al., 1965; 1964; Bedard et al., 1969; Bolam et al., 2000; Grofová, 1979; Hokfelt and U, 1969; Jones and Leavitt, 1974; Lavoie and Parent, 1990; Vertes, 1991). The dopaminergic connections are denervated in Parkinson's disease due to selective degeneration of dopaminergic neurons in the SNc(Albin et al., 1989). Dopamine signaling is involved in reward or reinforcement learning and plays a role in motor control at the level of the striatum(Gerfen, 2003; Gerfen and Surmeier, 2011; Schultz, 2002). Serotonin signalling is involved in cognitive and motor functions and has interactions with dopamine signalling(Di Matteo et al., 2008a). Whether and how this interaction also exists at the level of the striatum is not fully understood.

The striatum sends projections via two different pathways called the indirect and the direct pathway. The direct pathway is thought to promote movement while the indirect pathway is thought to inhibit movement(Alexander and Crutcher, 1990; Penney and Young, 1986; Smith et al., 1998). The balance between the two pathways is regulated by the dopaminergic projections from the SNc, with dopamine facilitating the direct pathway and inhibiting the indirect pathway(Gerfen, 2003; Gerfen and Surmeier, 2011). The direct pathway projects directly to the output nuclei of the basal ganglia; the Globus pallidus interna (GPi) and the Substantia Nigra pars Reticulata(SNr) (Bunney and Aghajanian, 1976). The indirect pathway projects indirectly to the output nuclei via Globus Pallidus externa (GPe), which in turn, projects to the Subthalamic Nucleus (STN)(Sato et al., 2000). The output structures of the basal ganglia project to the brain stem but also back to the thalamus, thus regulating the activity in the cortex. This pattern of projections creates a loop of which there are several. They consist of the motor, sensory, associative and limbic loop (see figure 1)(Alexander and Crutcher, 1990; Alexander et al., 1986). The loops are parallel, segregated and control different higher brain functions.. Although they are segregated, there is crosstalk between the loops(Haber, 2008). Furthermore, evolution-oriented studies have shown that the basic architecture of the loop-circuitry exists in lower vertebrates and that this basic circuitry might have been multiplied to form the additional loops seen in mammals (Stephenson-Jones et al., 2012; 2011).

Additional basal ganglia loops and projections

In addition to the classical basal ganglia nuclei, their projections and role in motor control there are some more recently described projections. These include the "hyperdirect pathway" and the GPe direct projections to the striatum (Nambu et al., 2000; 2002). The hyperdirect pathway consists of the classical indirect loop of the STN and GPi/SNr but skips the striatum and GPe. The STN receives input from the cortex, which implies that the striatum is not the only input structure of the basal ganglia. It has been suggested that the role of this pathway is to inhibit irrelevant motor programs and changing motor plans(Isoda and Hikosaka, 2008; Leblois et al., 2006; Nambu et al., 2002). Furthermore the STN also innervates the GPe, which forms a new projection that is not a part of any of the classical pathways. As mentioned the GPe projects to the striatum but also to the GPi. The GPe-striatal projection is made up of a different population of neurons than those projecting to the STN(Beckstead, 1983; Bevan et al., 1998; Kita and Kitai, 1994; Mallet et al., 2012; 2008; Shu and Peterson, 1988; Staines and Fibiger, 1984; Staines et al., 1981). To make matters even more complex the striatum is not the sole projection of the dopaminergic terminals arising from the SNc but they also innervate the GPe, GPi and STN(Nambu, 2008). How these different additional projections affect the processing within the basal ganglia remains to be seen but it challenges the simplistic model of action selection.

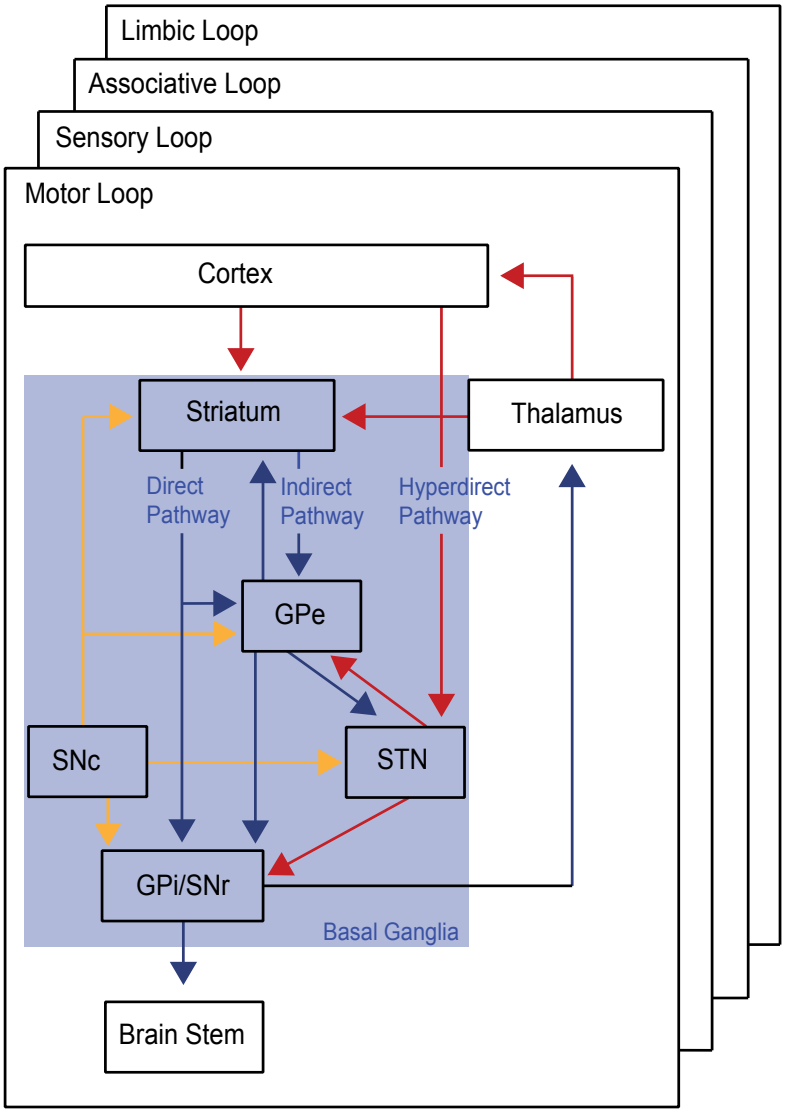

Figure 1. *Schematic showing the projections to, from and within the basal ganglia and the different loops that they form. GPe= Globus Pallidus Externa, SNc= Substantia Nigra pars Reticulata, STN= Subthalamic nucleus, GPi= Globus Pallidus Interna and SNr= Substantia Nigra pars Reticulata. Red arrows indicate an excitatory glutamatergic projection, Blue arrows an inhibitory GABAergic projection and yellow arrows dopaminergic projections.*

DECONSTRUCTING THE STRIATUM

Striatal Projection Neurons

The striatum consists of both projection neurons and interneurons. These different neuronal types were first studied using different histological methods and therefore classified according to their morphology. The morphological classification was done according to their size and dendritic spines(Chang et al., 1982). With these methods including the study of nuclei indentation the most abundant type of neuron found was the medium-sized densely spiny neuron and it makes up 90-95 % of all neurons(Graveland and DiFiglia, 1985; Wilson and Groves, 1980). They were found to be GABAergic and are divided into two separate groups depending on where they project(Kita and Kitai, 1988; Smith et al., 1998). Their electrophysiological characteristics cannot be dissected apart and these include a hyperpolarized membrane potential, strong inward rectification and a delay to the first Action Potential (AP)(Kita et al., 1985; 1984; Koós and Tepper, 1999). They can however be set apart according to the receptors they express which are Dopamine D1 receptors (D1R) or Dopamine D2 receptors (D2R). The D1 MSNs are a part of the already mentioned direct pathway and also co-express Substance-P (SP)(Bolam et al., 1983; Izzo et al., 1987). The D2 MSNs are a part of the indirect pathway and co-express enkephalin(DiFiglia et al., 1982; Izzo et al., 1987; Pickel et al., 1980). This division is however, somewhat of an oversimplification since almost all D1 MSNs send projections not only to the GPi but also send axon collaterals to the GPe(Fujiyama et al., 2011; Kawaguchi et al., 1990). Furthermore there are some findings that suggest that there are neurons that express both types of Dopamine receptors although this still remains controversial(Gerfen and Surmeier, 2011; Nambu, 2008).

Striatal Interneurons

The interneurons in the striatum are sparse in quantity but have been predicted to play an important role in striatal processing because of their large axonal arborizations(Kita et al., 1990; Kubota and Kawaguchi, 2000; Tepper and Bolam, 2004). The interneuronal type that has been much studied due to its size is the large aspiny neuron(Chang et al., 1982). They express the enzyme Choline Acetyl Transferase (ChAT), release acetylcholine during neurotransmission and are therefore called cholinergic interneurons (AChI)(Bolam et al., 1984; Kawaguchi, 1993; Phelps and Vaughn, 1986; Phelps et al., 1985). Early in vivo studies identified tonically active neurons that were named TANs and these were confirmed to be the AChI(Kimura et al., 1984; Raz et al., 1996; Wilson et al., 1990). They have also been shown to be tonically active in-vitro (Bennett and Wilson, 1998; 1999; Lee et al., 1998)Apart from their tonic activity they have a depolarized membrane potential, exhibit a sag (Ihcurrent) and have long and deep afterhyperpolarization (AHP)(Kawaguchi, 1993). In addition to being tonically active in vivo they are highly synchronized, have been shown to be play a functional role in reinforcement learning and respond to salient stimuli with a pause and a burst(Aosaki et al., 1995; 1994; Joshua et al., 2008; Kimura et al., 1984; Morris et al., 2004).

The presence of GABAergic interneurons was confirmed through the early histological studies but the subdivision of them was not confirmed until later and is still under constant revision(Ibanez-Sandoval et al., 2010; 2011; Kita and Kitai, 1988; Kubota et al., 1993; Oorschot, 2013; Ribak et al., 1979). The most classical of these interneuronal types is the one that expresses the calcium binding protein parvalbumin (PV). They have medium sized somata, aspiny dendrites and dense local axonal arborizations(Bennett and Bolam, 1994; Cowan et al.,

1990; Kita et al., 1990). They have later been confirmed to be so called Fast spiking interneurons (FSIs), which are similar to their frequently encountered counterpart in the cortex and hippocampus(Kawaguchi, 1997; Markram et al., 2004). Their electrophysiological characteristics include a more depolarized resting membrane potential than the MSNs, short and deep AHP, high frequency spiking and a stuttering or non-accommodating firing pattern(Kawaguchi, 1993).

Another classical GABAergic interneuronal-type is the one expressing somatostatin (SOM), nitric oxide synthase (nNOS) and Neuropeptide Y (NPY)(Dawson et al., 1991; Smith and Parent, 1986; Vincent et al., 1983; 1982; Vuillet et al., 1990). Their morphological characteristics are an elongated soma, aspiny dendrites that are poorly branched and less dense and branched axons. They are distributed throughout the striatum although sometimes encountered in more dense clusters(Chesselet and Graybiel, 1986; DiFiglia and Aronin, 1982; Ibanez-Sandoval et al., 2011; Takagi et al., 1983). The expression of nNOS has been paired with electrophysiolgical recordings and indicates that these interneurons belong to the Low threshold spiking interneuron type (LTSI) The electrophysiological characteristics of the LTSI include a depolarized resting membrane potential, high input resistance, low firing threshold and an accommodating firing pattern (Kawaguchi, 1993). Recently it was shown that they are spontaneously and tonically active (Beatty et al., 2012). It was previously assumed that nNOS expression in striatal interneurons is completely colocalized with SOM and NPY expression but histochemical studies suggest that there are nNOS and SOM positive interneurons that are NPY negative (Figueredo-Cardenas et al., 1996b; Smith and Parent, 1986). NPY is however, not restricted to the LTSIs and is expressed by another interneuron type, the Neurogliaform interneuron (NGF)(Ibanez-Sandoval et al., 2011).

The NGF interneuron was an early discovered but very sparsely dispersed striatal interneuron (Chang et al., 1982; Ibanez-Sandoval et al., 2011; Sancesario et al., 1998). This neuronal type was first encountered in the Central Nervous System by Ramón y Cajal (1904) and was then called dwarf cell. In early morphological studies their dendrites and axons could not be identified easily, but were described as spherical, and it was therefore not clear whether they were glial cells or neurons, hence their name(Chang et al., 1982). Electrophysiological studies have confirmed their presence in the striatum and concluded that their characteristics are similar to the NGF found in the cortex and hippocampus(Markram et al., 2004). They were electrophysiogically defined as Late Spiking neurons in the cortex and their electrophysiological characteristics are partly similar to the striatal MSNs with Inward rectification, low input resistance and hyperpolarized resting membrane potential. Moreover, they have longer duration APs and large amplitude AHP (Ibanez-Sandoval et al., 2011; Karagiannis et al., 2009; Karayannis et al., 2010; Markram et al., 2004; Povysheva et al., 2007; Sancesario et al., 1998). In one of the studies identifying striatal NGF, NPY-EGFP transgenic mice were used and a proportion of the GFP+ cells were NGF. This shows that NPY is not specific or restricted to the LTSIs (Ibanez-Sandoval et al., 2011).

There is a group of striatal interneurons expressing Calretinin (CR) that have been shown to colocalize PV to a small extent but not any of the other known markers (Bennett and Bolam, 1993; Figueredo-Cardenas et al., 1996a; Jacobowitz and Winsky, 1991; Rymar et al., 2004). They have not been classified electrophysiologically and it is still not known whether they group into any of the already known interneuronal types or if they make up their own electrophysiologically distinct group.

Other neuronal types include the Tyrosine Hydroxylase (TH) positive neurons. TH is an enzyme that catalyzes the reaction of L-Tyrosine to L-DOPA and is often used to identify dopaminergic neurons. The striatal TH+ neurons were first discovered in the monkey and gained interest because they become more numerous in animal models of Parkinson's disease. One of the hypothesis was that these neurons could be a compensatory mechanism for the striatum to replace the lost nigral dopaminergic signaling(Dubach et al., 1987; Huot and Parent, 2007). Recently this hypothesis was rejected with the help of voltammetry(Tepper, 2013). The fact still remains that these neurons exist but their role in striatal processing remains unclear. They have been proposed to form 4 different subtypes of interneurons based on their electrophysiological characteristics and that they have spines on their dendrites (Ibanez-Sandoval et al., 2010). Whether and if so, where they project has not been established and it can therefore not be said with certainty if they are in fact interneurons or projections neurons. They do respond to dopaminergic signaling so a role there would be feasible(ibanez-Sandoval et al., 2013).

Relative size of the interneuronal population

Many studies have tried to address the issue of percentages of the different striatal interneuronal types. The early studies used Golgi impregnation combined with immunohistochemistry, a method that does not label all neurons, and therefore presumably not accurate (Oorschot, 2013). Recent studies have used sterology combined with in-situ hybridization or immunohistochemistry. The total number of neurons has been quantified in three different studies and percentages of interneurons have been calculated accordingly (Luk and Sadikot, 2001; Oorschot, 1996)The four classical interneuronal types have been examined and their percentages are as follows: SOM+ LTSIs 0.8 %, AChI 0.4 %, PV+ FSIs 0.6% and CR+ interneurons 0.5 % (Bennett and Bolam, 1993; Oorschot et al., 1999; Rymar et al., 2004; West et al., 1996).This amounts to 2.3% of all striatal neurons, which is less than the prediction from the MSN percentages (Graveland and DiFiglia, 1985). There have been speculations that this in fact proves that the MSN percentages are wrong but there has been no direct evidence that this is the case (Oorschot, 2013). Another explanation is that all striatal neurons are not encompassed by the already described types and that others are to be discovered.

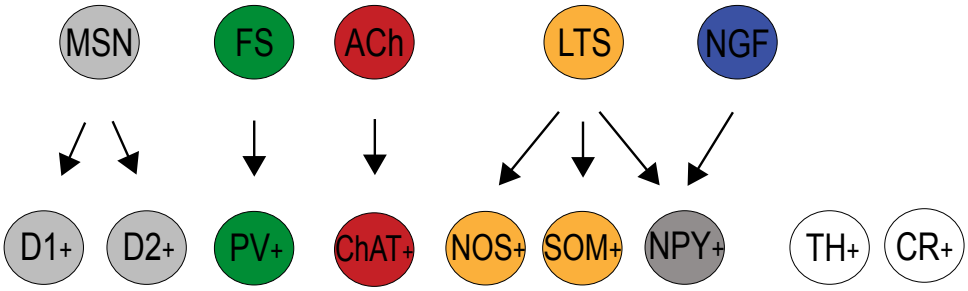

Figure 2. *Schematic showing the different striatal neuron types. The upper row segregates the neurons according to their name used, based on either morphological or electrophysiological properties. The lower row indicates what specific neuropeptides, enzymes, receptors or proteins that have been used to identify the neurons. MSN= Medium Spiny Neuron, FS=Fast spiking interneuron, ACh=(Acetylcholine,) Cholinergic interneuron LTS= Low threshold spiking interneuron, NGF=Neurogliaform interneurons, D1=Dopamine D1 receptor, D2= Dopamine D2 receptor, PV= Parvalbumin, ChAT=Choline Acetyl Transferase, NOS(nNOS)= Nitric oxide synthase, SOM=Somatostatin, NPY=Neuropeptide Y, TH=Tyrosine hydroxylase, CR=Calretinin.*

Paper I

Although extensive research has been put into identifying all the interneuronal types in the striatum the predicted and experimentally identified percentages still do not match (Oorschot, 2013). In the cortex the 5HT3a population encompasses all the interneurons that cannot be identified otherwise(Lee et al., 2010; Rudy et al., 2011). The aim of paper I was, to with the help of a 5HT3a transgenic mouse model, characterize the GFP+ neurons both histochemically and electrophysiologically. Below follows a brief summary of this study. Further details can be found in the paper.

We used in-situ hybridization, immunohistochemistry and FACS sorting to quantify and characterize the cells with regard to their molecular markers. All of the labelled neurons were GABAergic (100%, n=4 animals). A portion of the cells were labelled by Ctip2 (6.84 ±1.58%, n=7 animals), none of them expressed DARPP-32 and the neurons did not exhibit spines on their dendrites, indicating that they are not MSNs but interneurons. In order to further characterize this interneuronal population we examined the expression of different known striatal interneuronal markers (SOM, nNOS, NPY & TH) and their overlap with the 5HT3a-EGFP+ interneurons. This characterization showed that there is very little overlap between the different markers and the GFP-populations. PV showed the most overlap (19.78 ± 0.26%, n=3 animals), TH very little (2.48% ±0.51, n=5) and almost no overlap with the remaining markers. When quantifying the number of 5HT3a interneurons and adding the non-overlapping interneurons labeled by the other markers the amount adds up to 4.46 % of all striatal neurons.

We also did electrophysiological recordings and postvisualization of the recorded interneurons to further characterize them. The electrophysiological characterization showed that these interneurons fall into three different types of and that these are similar to the already described FSIs, NGF and LTSIs. The FS-like interneurons (32%, n=41 cells) exhibited short AP half-width, low input resistance, deep after-hyperpolarizations, a high maximum firing rate, and non-accommodating, often stuttering firing pattern. The NGF-like interneurons (16%; n=20 cells) exhibited delayed firing, slightly larger AP half widths with a slower more rounded AHP and an accommodating firing pattern. The LTS-like interneurons (53%, n=68/129) exhibited a higher resting membrane potential, input resistance and membrane time constants. Moreover, they exhibited diverse properties with some of them corresponding to classical LTSIs. In a set of direct comparison experiments the FSIs were compared to the FSIs recorded in Lhx6-EGFP transgenic mice and they showed very similar properties.

The possible connectivity of the interneurons to AChIs was tested by puffing with 100 μM nicotine. None of the FS-like interneurons (n=0/13), a portion of the NGF-like (25%, 2/8) and the majority of the LTS-like interneurons (86%, n=18/21) responded to the puffing. Only one of the FSIs recorded and puffed in the Lhx6-EGFP mouse responded. Furthermore, It showed that the LTS-like 5HT3a-EGFP + interneurons respond to nicotine to a larger extent than the LTSIs recorded in the Lhx6-EGFP mouse (27%, n=4/15). Although this does not confirm direct connectivity it does show the possibility of a connection. It does, however, show that these interneurons to a large extent would be affected by cholinergic volume transmission.

WHEN & HOW

HOW THE DECONSTRUCTED PARTS INTERACT- INTRASTRIATAL CONNECTIVITY

Connections on the Projection Neurons

With the help of staining and electron microscopy much of the intrastriatal connectivity has been anatomically explored(Bennett and Bolam, 1994; Kitai and Wilson, 1982; Somogyi et al., 1981; Takagi et al., 1983; Wilson and Groves, 1980; Yung et al., 1996). The first neuronal type characterized in the striatum was the MSN and thus the first synapses identified were on these neuronal types. They are the projection neurons and any connections on these neurons would influence the information going out of the striatum and would therefore be of high importance. The projection neurons were predicted to form GABAergic synapses on each other (Kitai and Wilson, 1982; Park et al., 1980; Somogyi et al., 1981; Wilson and Groves, 1980; Yung et al., 1996). For a long time this could not be confirmed electrophysiologically (Jaeger et al., 1994; Stern et al., 1998) and it is only fairly recently that these connections were found to be functional (Czubayko and Plenz, 2002; Koos et al., 2004; Tunstall et al., 2002; Venance et al., 2004). Surprisingly, the connections were much sparser than predicted, the interconnectivity is only about 10-19 %, and they were unidirectional (Czubayko and Plenz, 2002; Koos et al., 2004; Tunstall et al., 2002; Venance et al., 2004). In addition to chemical synapses, one of the studies found that MSNs interconnect via electrical synapses, this finding has however not been reproduced and was contradicted recently when all MSN-MSN transmission could be abolished with a GABAa blocker (Chuhma et al., 2011; Venance et al., 2004).

FSIs or PV+ neurons were predicted to form synapses on the perikarya of MSNs and these were in fact functional and frequently encountered (Bennett and Bolam, 1994; Koós and Tepper, 1999).They were identified to be a candidate for providing so called feedforward inhibition, a concept further discussed in the section "Does the winner take it all", to the MSNs since they receive cortical input and respond to this with a shorter delay than the MSNs (Koos et al., 2004; Koós and Tepper, 1999; Mallet et al., 2005; Taverna et al., 2007; Tepper et al., 2008).

LTSIs were also predicted to form synapses on dendrites, dendritic spines and shafts of striatal neurons and have been found to form functional connections with MSNs(Takagi et al., 1983). This interconnectivity seems to be higher in rats than in mice and is possibly long-range (Gittis et al., 2010; Ibanez-Sandoval et al., 2011; Koós and Tepper, 1999). TH+ neurons form contacts on to MSNs but because their exact type and role is not well established one cannot predict what the role of this connection can be (Ibanez-Sandoval et al., 2010). It could be of high importance in Parkinson's disease since the TH+ neurons are more numerous in the disease (Huot and Parent, 2007).

In other parts of the nervous system as well as the striatum cholinergic influence on processing has mainly been thought to be via volume transmission (Descarries et al., 1997; Zoli et al., 1998). Although histological studies could confirm that the large aspiny neurons form synapses onto other striatal neurons functional studies on their interconnectivity have lagged (Bolam et al., 1984; Phelps and Vaughn, 1986; Phelps et al., 1985). The first studies on the subject indeed examined their role through applying cholinergic receptor (AChR) agonists (Calabresi et al., 1998a; Koos and Tepper, 2002; Malenka and Kocsis, 1988; Sugita et al., 1991). AChIs have recently been shown to indeed form functional connections and they do contact MSNs. These contacts have different temporal components and are therefore most likely made up by different types of connections. There is a disynaptic connection that is mediated by the NGF and TH+

neurons. The AChIs excite the NGF and TH+ neurons and these in turn inhibit the MSNs (English et al., 2012; Luo et al., 2013). In addition to this disynaptic connection the AChIs have been shown to drive GABA-release from dopaminergic terminals (Nelson et al., 2014; Threlfell et al., 2012; Tritsch et al., 2012). Moreover, the AChIs express the vesicular glutamate transporter 3 (VGluT3) and there is evidence suggesting that they make direct glutamatergic contacts with MSNs (Gras et al., 2008; 2002; Higley et al., 2011). Because the AChIs have been implicated in reinforcement learning this could be an important way in which their role in this process is transferred to the MSNs.

Connections on the Interneurons

AChIs contact MSNs and this connectivity is reciprocal with MSNs contacting AChIs (Chuhma et al., 2011). A part from contacting MSNs, AChIs send feedback connections onto other AChIs. This feedback connection is mediated via GABAergic transmission because it is abolished when applying GABAergic blockers but what interneuron or terminal mediates this has not been established (Sullivan et al., 2008). It has been shown that dopaminergic terminals co-release GABA so it could be these (Tritsch et al., 2012). Another hypothesis is that it is mediated by one of the known or yet unknown interneuron types. Candidates that have been mentioned are the FSIs or LTSIs (Sullivan et al., 2008).

A part from contacting the MSNs with high probability, the FSIs are also interconnected via gap-junctions (Koós and Tepper, 1999). The role of these gap-junctions is not completely understood, but for example the cortical FSIs gap-junctions have been proposed to play a role in synchronizing the neurons (Galarreta and Hestrin, 2001; Gibson et al., 2005; Mancilla et al., 2007). The same has been proposed for striatal FSIs although recent studies suggest otherwise and instead synchronicity could be greater among directly coupled striatal FSIs (Berke, 2008; Hjorth et al., 2009).

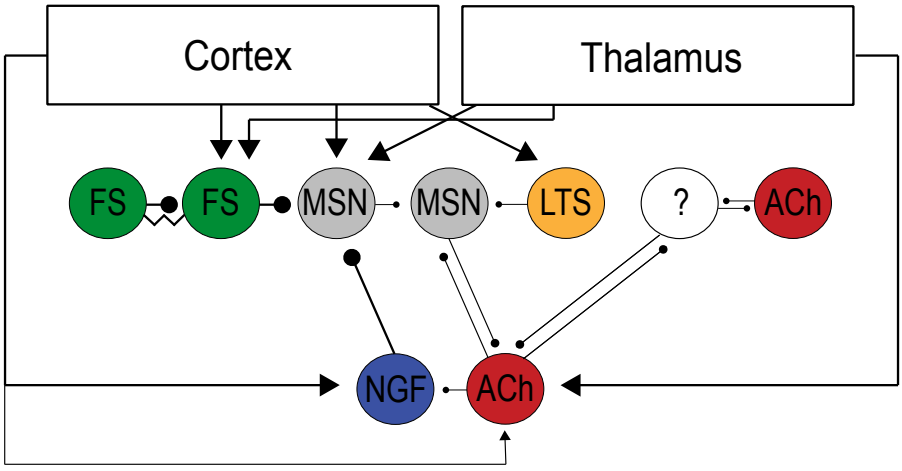

Figure 3*. A summary of the striatal microcircuitry. Lower weight connection symbols indicate relatively weaker connections. MSN= Medium Spiny Neuron, FS=Fast spiking interneuron, ACh=(Acetylcholine,) Cholinergic interneuron, LTS= Low threshold spiking interneuron, NGF=Neurogliaform interneurons*

Does the winner take it all?

The indirect and direct pathways have been shown to be a feasible model on the global scale but the question is how this model translates into individual neuronal function and predictions on when and how the projection neurons are interconnected.

Based on the logic of Darwinism or natural selection Edelman developed a framework regarding the development of the nervous system (Edelman, 1993).The idea was that much like natural selection nerve cells are also selected according to their viability. Indeed the nervous system goes through major pruning during development where half to two thirds of all nerve cells die. This type of framework could be called "the winner takes it all" where all "weak" nerve cells are deleted. It could and has also been translated in the framework of a network (Edelman, 2006; McDowell, 2010). In the case of the striatum it could be translated in the case of corticostriatal function. MSNs receive The MSNs with the largest response or largest input "take it all". Since MSNs are inhibitory neurons the ones with the largest input or response would inhibit their neighbours and only their responses would be passed on or project out, a process also called lateral inhibition (Groves, 1983; Plenz et al., 1996; Wickens et al., 1995)

It was in fact shown that cortical stimulation induces an excitatory as well as an inhibitory response in MSNs (Park et al., 1980). The way of further proving this hypothesis would be to look at the interconnectivity of MSNs. The interconnectivity has as already mentioned been proven but it has been reported to be sparse and interestingly also unidirectional (Czubayko and Plenz, 2002; Koos et al., 2004; Tunstall et al., 2002; Venance et al., 2004). Another conclusion that could be drawn from this hypothesis is that there would be a difference in the activation pattern of the iMSNs versus dMSNs. The early MSN interconnectivity studies were conducted in wild type animals so the connectivity of the D1 versus D2 MSN types could not be examined. Recent studies have however shown that the iMSNs form synapses onto dMSN to a higher extent but also contact iMSNs arguing against the model (Taverna et al., 2008) When it comes to in vivo activation of the different types of MSNs surprisingly, a very recent study by Cui et al showed that both D1 and D2 MSNs are activated during movement (Cui et al., 2013). This would also argue against the hypothesis about lateral inhibition and the indirect and direct pathway. However, the anatomical resolution of the neurons activated was not great enough to draw this conclusion. The concurrent activation could therefore be explained by that activation of iMSNs serves to inhibit competing movements. Moreover, there is an indication that there is no difference in the way that the D1 and D2 MSNs are innervated or respond to cortical activation (Ballion et al., 2008; Kress et al., 2013), although some studies suggest otherwise (Flores-Barrera et al., 2010).

The strongest evidence supporting the separated pathways and possibly also the lateral inhibition hypothesis was done using optogenetics. In this study Channelrhodopsin (ChR2) was preferentially targeted to D1 or D2 MSNs. The ChR2-expressing neurons were activated by light. The activation of D1 MSNs started movement and the activation of D2 MSNs inhibited movement (Kravitz et al., 2010).

The winner takes it all model does not however, have to rely on interconnected projection neurons. In theory this could also be mediated through interneurons and they would be the source of inhibitory responses seen in MSNs upon cortical activation (Park et al., 1980). They would have to be innervated by the cortex and either receive input before or have electrophysiological characteristics that would enable them to respond quicker than and inhibit the projection neurons. Fast spiking interneurons fit into this criterion. They receive glutamatergic input from the

cortex and have also been shown to form synapses onto the soma of MSNs. The type of effect that they exert on the MSNs has been called feedforward inhibition (Koos et al., 2004; Koós and Tepper, 1999; Mallet et al., 2005; Taverna et al., 2007; Tepper et al., 2008). The role of feedforward inhibition in the striatal microcircuit has been proposed to be temporal control and gain control (Wilson, 2007). When it comes to temporal control the idea is that the fast spiking interneurons would inhibit responses of certain timings and allow responses at other times. This would function to create a temporal filter and synchronize the network. Gain control on the other hand shares the same idea as the "winner takes it all" concept. The role of the FSIs would be to inhibit weak responses and only strong responses would be filtered through.

PUTTING THE WHEN INTO CONNECTIVITY

The effect of Intrinsic properties of striatal neurons on temporal aspects of connectivity

The different neuronal types have different electrophysiological properties or intrinsic properties. Some of these properties can and do contribute to their physiological role in processing . The LTSIs for example have a very high input resistance(Kawaguchi, 1993). This would potentially make them more responsive to weaker input of any type but has been specifically shown to be true for cortical input (Gittis et al., 2010; Ibanez-Sandoval et al., 2011). They do however, not respond with shorter latencies than do MSNs (Fino et al., 2009)The MSNs on the other hand have a lower input resistance, relatively hyperpolarized RMP, inward rectification and show a delay to the first AP (Kawaguchi, 1993). This would mean that they need much and strong convergent excitatory input to be activated and that this activation could be delayed in comparison to other neurons (Mallet et al., 2005; Stern et al., 1998; 1997; Wilson, 1993). Inhibitory ionotropic GABAergic activation is coupled to Cl- channels that have a reversal potential at approximately -60 mV. Since the MSNs have a more hyperpolarized RMP than that, it has been proposed that inhibitory input to the MSNs could actually be serving to activate the MSNs (Bracci and Panzeri, 2006). However, the functional significance of this is unclear and is yet to be established. The FSIs have a comparable input resistance to the MSNs and also partially exhibit inward rectification(Kita et al., 1985; 1984; Koós and Tepper, 1999). They do not have a delay to the first AP and would therefore respond quicker to incoming input than the MSNs, which was also shown in vivo (Mallet et al., 2005). FSIs also show a stuttering or non-accommodating firing pattern but this behaviour was shown to be overridden with cortical input (Klaus et al., 2011). AChIs display a sag or Ih current and slow AHPs which enables them to be tonically active(Bennett and Wilson, 1999; Bennett et al., 2000; Oswald et al., 2009). They are also highly synchronized in vivo and respond to salient stimuli with a pause and a burst (Aosaki et al., 1994; 1995; Joshua et al., 2008; Kimura et al., 1984; Morris et al., 2004). It has been suggested that their intrinsic properties might mitigate this but it has also been shown that common glutamatergic input and dopaminergic input are involved in this behaviour(Bennett and Wilson, 1999; Chuhma et al., 2014; Ding et al., 2010; Lapper and Bolam, 1992; Oswald et al., 2009; Watanabe and Kimura, 1998).

Long term synaptic plasticity

Other than the intrinsic electrophysiological properties of individual neurons there are other mechanisms that can change the temporal aspect of connectivity. One such aspect is the dynamics of synapses that could either work to strengthen or weaken synapses over time. Two such mechanisms that work on a longer time-scale, in the magnitude of hours, days, weeks or longer, are Long term depression (LTD) and Long term Potentiation (LTP). They have long have been known to be related to memory (Bliss and Gardner-Medwin, 1973; Bliss and Lomo, 1973). These mechanisms are more widespread in the nervous system than initially thought and also take place in the striatum. A way of inducing these types of plastic changes is spike timing dependent plasticity (STDP). STDP is based on the Hebbian synaptic learning ("Cells that fire together wire together") where either LTP or LTD is induced depending on the timing of the paired activities of the pre-synaptic and post-synaptic cell (Abbott and Nelson, 2000). At corticostriatal synapses this type of mechanisms has been studied extensively and has been shown to take place for MSNs as well as for the LTSIs, AChI and FSI(Adermark and Lovinger, 2009;

Calabresi et al., 1992b; 1996; Charpier and Deniau, 1997; Fino et al., 2009; 2008; Wickens et al., 1996). A part from LTP and LTD taking place in striatal interneurons it has also been shown that the striatal interneurons influence and modulate the LTP and LTD of MSNs(Calabresi et al., 1992a; Wang et al., 2006). This type of synaptic plasticity is of high functional significance for striatal processing and most certainly dictates and modulates the information flow out from the striatum.

Short term synaptic plasticity

Other mechanisms that take place on a shorter time-scale, in the scale of milliseconds to minutes, are Short term depression (STD) and short term-potentiation or facilitation (STP/STF), also referred to as "synaptic dynamics" (Katz and Miledi, 1968). They potentially play a large role in shaping neuronal processing since they have great influence on the temporal aspects of connectivity. STD entails that connections are initially larger and diminish over time, which means that these types of connections will be more precise or time-locked. STP entails that connections are initially smaller and grow over time, which means that these types of connections will play a role and even strengthen their role over time. To be able to examine these mechanisms different models and experimental protocols have been used. Paired Pulse Ratios is the most commonly used model (Katz and Miledi, 1968). We have used both that and a model developed by Tsodyks and Markram. I explain both these models in the following paragraphs (Katz and Miledi, 1970; Tsodyks and Markram, 1997).

In the model with Paired Pulse Ratios, connectivity is examined using a paired pulse. The pulses can be delivered at different frequencies depending on what time scale the dynamics want to be studied at. With a paired pulse one can investigate if the amplitude of the synapse becomes stronger or weaker in the second pulse. The paired pulse ratio is calculated commonly according to this formula:

$$PPR = PSP_2 / PSP_1$$

It can be applied to both excitatory and inhibitory synapses. From the formula you can read that a second pulse with greater amplitude than the first will results in a PPR greater than 1. These synapses become stronger and are called facilitating. There are different mechanisms for why the second pulse is either greater but they are all presynaptic mechanism and depend on if all resources (in the form of vesicles and neurotransmitters) are used in the first pulse. Conversely if the amplitude of the second pulse is smaller, the PPR is smaller than 1 and the synapse is called depressing. There are different mechanisms for why the second pulse is smaller and these can be of both presynaptic and postsynaptic origin.

In the model developed by Tsodyks and Markram the short-term dynamics of individual connections can be assessed in greater detail (Tsodyks and Markram, 1997). It includes a longer stimulation of the presynaptic neuron with a train of pulses followed by a recovery test pulse approximately 1s after the train. The model also assesses the resources and how efficiently they are used. It divides the resources into three different states 1. Effective, 2. Inactive and 3. Recovered. The effective state is when the resources can be utilized, the inactive state is when the resources have just been used and are inactive and the recovered state is when the resources are recovered from inactivation. The inactivation happens on a time scale of a few milliseconds and the recovery from inactivation happens on a time scale of about 1s, which is the reason for the recovery test pulse being at 1s after the train of pulses. The parameters or components of

the synaptic dynamics that can be extracted from the model include the rate of depression and facilitation and come in the form of the Utilization factor (Use). The higher this factor is the more efficient is the utilization of resources, which means that the rate of depression is higher.

Neuronal oscillations

In addition to the dynamics of connectivity another temporal aspect of the neuronal networks and connectivity are neuronal oscillations. The brain is always active and the spontaneous rhythmic activity generates a pattern of oscillations. The oscillations have been classified in ranges of frequencies and correlate to different brain states. These frequencies are slow (< 1 Hz), delta (1-4Hz), theta (4-8), alpha (8-13Hz), beta (13-20Hz) and gamma (30-80Hz) (Steriade et al., 2001). In cortical neurons the oscillations generate periods characterized by high spontaneous activity and a depolarized membrane potential (up states) which are alternated with silent intervals and hyperpolarized membrane potential (down states)(Steriade et al., 1993). The oscillations are generated in the cortex and propagated to for example the thalamus and the striatum(Sanchez-Vives and McCormick, 2000; Timofeev et al., 2000). The striatal neurons also undergo these shifts in membrane potential and they are driven by glutamatergic input from the cortex and thalamus (Wilson, 1986; 1993; Wilson and Kawaguchi, 1996; Wilson et al., 1983). Most of the different types of striatal neurons exhibit this pattern of behaviour but they are most prominent in the neurons that have a more hyperpolarized membrane potential and that are not tonically active. MSNs and FSIs especially exhibit prominent up and down states. The MSNs have a RMP of around -80 mV and this is the value that the down states cluster in. The up states cluster in values around -60 mV(Reig and Silberberg, 2012; Sharott et al.2012). Recent studies in rodents using in vivo awake patch clamp recordings show that the up and down states is not only a phenomenon that occur during anesthesia or slow-wave sleep, but also awake and behaving animals have shifts in membrane potential. The shifts are not as pronounced as in the case of the slow-wave sleep but still occur (Kasanetz et al., 2002; Mahon et al., 2006).

Neuronal oscillations most likely have substantial impact on the processing of information in the striatal circuit. The MSNs have a more hyperpolarized RMP and an inwardly rectifying potassium channel. This makes them less responsive to cortical input. Cortical oscillations and coherent gamma oscillations across cortical areas seen in perception processing might ensure the response of MSNs to stimuli(Engel et al., 2001; Stern et al., 1997). Interneurons in other brain areas have been shown to fire in different and set phases of the oscillation. This behaviour could define the role of interneurons in the circuitry(Klausberger et al., 2003). Furthermore, it has been shown in other model organisms that the membrane potential of the presynaptic neuron has significant influence on the properties of connections and this has also recently been shown in the cortex, hippocampus and cerebellum of rodents(Alle and Geiger, 2008; Angstadt and Calabrese, 1991; Christie et al., 2011; Katz and Miledi, 1967; Maynard and Walton, 1975; Shimahara and Tauc, 1975; Shu et al., 2006; Zhu et al., 2011). This is another way in which oscillations can have a substantial impact on the striatal circuit and processing. How the shifts in the membrane potential of presynaptic neurons and activity of interneurons in different phases of oscillation, affect the dynamics and strength of striatal connections and temporal aspects of connectivity has not yet been explored.

Paper II

To further assess the feasibility of the "winner takes it all" model in paper II we examined the interconnectivity of the iMSNs and dMSNs and the synaptic dynamics of that connectivity. We also examined the synaptic dynamics and connectivity of the FSIs to the two types of MSNs. Below follows a brief summary of this study. Further details can be found in the paper.
The experiments were done in either wild type and unlabelled or retrogradely labelled rats where the dMSNs were labelled. In addition to this, a set of experiments were performed in Drd1-EGFP mice, making it possible to compare connectivity and synaptic dynamics in the two models. In the unlabelled rat experiments we found that the MSN-MSN connectivity was much sparser (20%, n=40/202) and with both facilitating and depressing connections as compared to the FSI-MSN connectivity (74%, n=29/39). The FSI-MSN connectivity showed high probability of connectivity and was strongly depressing.

We used and adapted the model developed by Tsodyks and Markram, previously described here, for synaptic dynamics to extract different facilitating and depressing components of the connections (for more detailed information please see material & methods of paper II). With this model we revealed that the recovery test pulse showed strong depression for the FSI-MSN connections and strong facilitation for the MSN-MSN connection. The MSN-MSN connection had a high F/D ratio and mixed facilitating and depressing components. The FSI-MSN connections on the other hand had purely depressing components. The experiments done in retrogradely labeled rats showed similar properties as the ones done in unlabeled rats. Both labelled and unlabeled MSNs received input from FSIs.

Experiments done in transgenic mice showed even sparser MSN-MSN interconnectivity than in the rats (7.8%, n=23/294). The presynaptic cell was to a larger extent an iMSN (74%, n=17/23) and to a lesser extent a dMSN (26%). The connections showed similar amplitudes and synaptic dynamics with varying components similar to what was found in the rat experiments. iMSNs contacted both dMSNs (23 %) and iMSNs (13%) and no apparent difference could be seen between the connections. This suggests that the synaptic dynamics were neither decided by the presynaptic neuron type nor the postsynaptic neuron type.

FSI-MSN connectivity was also investigated in the Drd1-EGFP mouse. It showed similar properties to the one in the rat with depressing synaptic dynamics, high release probability and it was unidirectional. The relative connectivity of the FSIs to the MSNs of the different types is 67% (indirect pathway)-89%(direct pathway). Furthermore, the inhibition seems to not be significantly differential for dMSNs and iMSNs and even the same FSI contact MSNs of both pathways.

Paper III

To further examine the phenomenon of feedforward inhibition and its selectivity in paper III we examined the connectivity of FSIs. The FSIs have been implicated to transmit this type of inhibition to the MSNs but other postsynaptic neurons have not been investigated. Below follows a brief summary of this study. Further details can be found in the paper.

To selectively target the FSIs we used PV-Cre transgenic mice that were injected with an Adeno-associated viral vector that expresses a ChR2-mCherry fusion in a Cre dependent manner. Immunohistochemistry confirmed that 97% of the mCherry-expressing neurons were PV+. We also confirmed that these neurons were FSIs and that they responded to light stimulation with an AP by targeted patch-clamp recordings of the labelled neurons (n=18). We recorded from MSNs and were able to elicit responses in the MSNs by light-stimulating the FSIs (n=42/66). The responses were three-fold larger compared to those from direct connections and confirmed that we stimulated a population of FSIs. We could confirm previous results regarding FSI-MSN connectivity and its synaptic dynamics. Time constants corresponded to depressing connections but the utilization factor was higher which indicated that the release probability was higher. This is likely due to AP doublets elicited during light stimulation. We recorded from pairs and triplets of MSNs and AChIs or LTSIs and found that FSI are not connected to Cholinergic and to a very small degree to LTSIs.

Paper IV

As described in the section on neuronal oscillations, a network is seldom static and fluctuations in membrane potential of individual neurons and networks of neurons occur constantly. In paper IV we wanted to examine how the membrane potential of the presynaptic neuron can influence the strength and dynamics of the connection. Below follows a brief summary of this study. Further details can be found in the paper.

We therefore used a transgenic mouse that labels FSIs and LTSIs with GFP. We could then target recordings of pairs, triplets and quadruplets of FSIs and MSNs (n=39 pairs). We examined both FS-MSN and MSN-MSN connections. We recorded the neurons and kept the presynaptic cell at a more hyperpolarized or depolarized potential to stimulation. The FS-MSN connections were modulated by presynaptic voltage and keeping the presynaptic cell at a more depolarized membrane potential increased the amplitude and the release probability of the synaptic response (Amplitudes, 2.52 ± 1.19 mV->2.92 ± 1.22 mV , PPR, 0.88 ± 0.18 -> 0.76 ± 0.16). Moreover, there was a correlation between the initial release probability and amount of modulation ($r2 = 0.32$, $p = 0.014$). We did experiments where we changed the synaptic dynamics of the connections by lowering the extracellular concentration of Calcium from 2 mM to 1 mM. The preliminary results show that when the initial release probability is decreased by lowering extracellular calcium, the amount of modulation increases.

The MSN-MSN connections (n=4), showed a similar trend to the FSI-MSN connections, with an increase in amplitude (0.91 ± 0.18 mV -> 1.00 ± 0.24 mV) and an increase in PPR (0.76 ± 0.11 -> 0.63 ± 0.09). The number of connections are too small to draw any definitive conclusions from.

Preliminary Results-
Neurons expressing 5HT3a receptors and their connectivity

In addition to the data presented in paper I we have also obtained some preliminary results on the direct connectivity of 5HT3a-GFP+ neurons. We recorded from pairs and triplets of GFP+ neurons (n=27) and AChIs (n=14) and checked their connectivity with the protocol described in paper I (n=50 pairs). We examined the connectivity of both AChIs and GFP+ pairs in both directions (n=28/50) and between GFP+ neurons (n=12/50). The GFP+ neurons were of both LTS-like (n=13) and FS-like type (n=14). We did not find any connections between AChIs and the FS-like interneurons (n=18) and one LTS-like to AChI connection of low amplitude (n=1/18). Although we did not find any or very sparse connectivity in this study, in paper III we do show that LTS-like 5HT3a-EGFP+ interneurons respond to nicotine puffing. It therefore raises the possibility that this subpopulation is interconnected to the AChIs and that they are the interneurons that mediate the recurrent inhibition between the AChIs. The direct connectivity was done with all GFP+ neurons regardless of type and we also concluded that the 5HT3a interneurons are a very diverse population of neurons. It is possible that only a subpopulation of the LTS-like interneurons contact the AChIs. To clearly conclude whether they are in fact mediating recurrent inhibition a more precise method of examining the connectivity of 5HT3a interneurons would be needed.

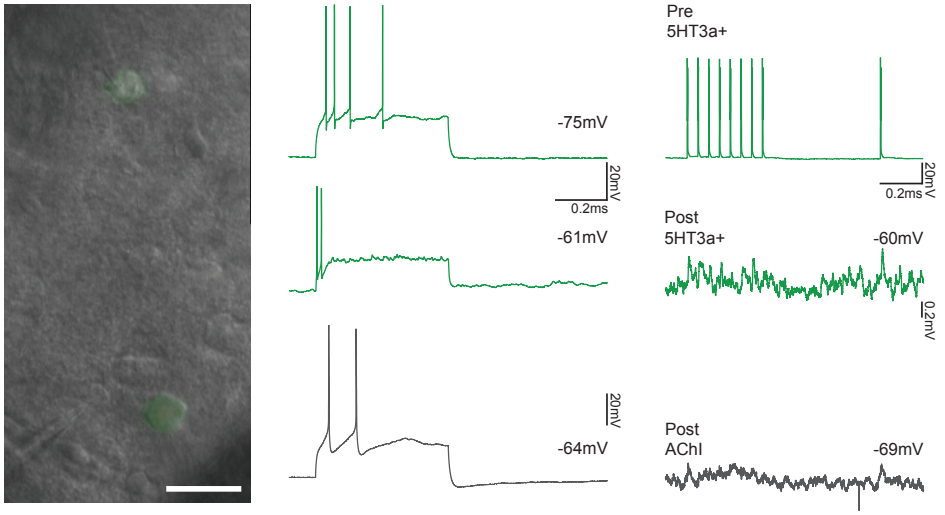

Figure 4. *Connectivity of 5HT3a+ interneurons. Left: Overlayed IR-DIC and fluorescent photomicrograph. Scalebar=20 µm. Top Middle: Trace from a 5Ht3a+ interneuron showing an accommodating firing pattern and a low firing threshold (most likely an LTS-like interneuron). Middle middle: Trace from a 5HT3a+ interneuron showing a fast onset of firing and subthreshold oscillations. Bottom Middle: Trace from an AChI showing long and deep AHP and relatively depolarized RMP. Top Right: Average trace from stimulation of the presynaptic 5HT3a interneuron. Middle Right: The response of a possible postsynaptic 5HT3a interneuron, to the stimulation of the presynaptic 5HT3a interneuron. Bottom Left: Response of the postsynaptic AChI to the stimulation of the presynaptic 5HT3a interneuron.*

HOW THE INTERACTIONS CAN BE ALTERED- MODULATION OF INTRASTRIATAL CONNECTIVITY

Processing within the striatum is composed of many parts including the different types of interneurons and the projection neurons. So far I have only described these different parts, how they are directly connected and the possible effects of the connections on striatal processing. There are however, other ways of how the different parts can be affected and these include various types of modulation. Receptors of different kinds are not limited to postsynaptic terminals but can be expressed at presynaptic terminals, at various parts of the dendrites, the soma and even the axon. Moreover, some neurotransmitters and neuropeptides are not degraded instantly and can therefore diffuse and cause volume transmission. This poses a potential way of how neurotransmitters and neuropeptides can affect processing without directly contacting the neurons. In addition to this, presynaptic terminals can be innervated by modulatory input. Anatomical studies have shown that the striatum is rich in Cholinergic, Dopaminergic, Serotonergic and SP receptors and that these neurotransmitters and neuropeptides respectively therefore can exert a powerful modulatory effect on striatal transmission (Gerfen and Wilson, 1996; Hokfelt et al., 1975; Jakab and Goldman-Rakic, 1996; Steinbusch, 1981).

Dopamine in the striatum

As mentioned before striatum receives dopaminergic input from the SNc. Its receptors consist of the D1-D5 and are divided into D1-like and D2-like receptors. The D1-like comprise the D1 and D5 and the D2-like the D2, D3, D4(Neve and Neve, 1997). In the striatum they are expressed on MSNs, AChIs and Dopaminergic axons. D1 receptors are restricted to the dMSNs and AChIs although there have been studies suggesting that there are MSNs that co-express D2 and D1 receptors (Bertran-Gonzalez et al., 2010; Gerfen and Surmeier, 2011). AChI also express the D5 receptors and studies indicate that they express D2 receptors. In general, D1 receptor activation increases excitability of neurons and D2 activation decreases it which is the case in the dMSNs and iMSNs(Alexander and Crutcher, 1990; Liu et al., 2004; Neve et al., 2004; Surmeier et al., 2007). The extent of this excitability is however, dependent on the membrane potential of the neuron (Flores-Barrera et al., 2010; Planert et al., 2013).

One study shows that AChIs are not directly affected by D2 receptor agonists but are depolarized by D1-like receptor agonists (Aosaki et al., 1998) However, other studies have showed that D2 receptor activation induces pauses in AChIs strongly arguing for D2 receptor expression(Chuhma et al., 2014; Deng et al., 2007). It has also been shown that AChIs do in fact express D2 receptors (Lemoine et al., 1990)

Acetylcholine in the striatum

The main source of Acetylcholine in the striatum are the AChIs. The AChIs are tonically active and therefore contribute with a constant Cholinergic tone(Kimura et al., 1984; Raz et al., 1996; Wilson et al., 1990). AChRs consist of the ionotropic nicotinic receptors (nAChRs) and the metabotropic muscarinic receptors (mAChRs). The mAChRS comprise of M1-M5 and are subdivided into M1-class and M2-class according to which G-protein they express. M1-class contains the M1, M3 and M5 and the M2-class contains M2 and M4. (Bonner et al., 1987; 1988; Kubo et al., 1986; Peralta et al., 1987). AChIs, LTSIs and FSIs express M2 receptors and MSNs and glutamatergic terminals express M1 receptors. The expression of M4 is limited to

dMSNs. nAChRs are expressed on dopaminergic terminals, glutamatergic terminals and striatal interneurons(Aosaki et al., 2010; Threlfell and Cragg, 2011). There is no clear anatomical evidence of nAChR expression on striatal interneurons but pharmacological evidence suggests that these striatal interneurons are LTSIs, NGF, PV+ FSIs and TH+ neurons (Hill et al., 1993; Jones et al., 1999; Koos and Tepper, 2002; Luo et al., 2013).

Serotonin in the striatum

As mentioned previously the striatum receives serotonergic input from the Dorsal Raphe Nucleus(Lavoie and Parent, 1990; Vertes, 1991).. There are 6 families of Serotonin receptors the 5HT1, 2, 3, 4, 5, 6 and 7. All of the receptors with the exception of the 5HT3 are metabotropic G-Protein Coupled receptors (GPCRs). The 5HT3 is a ligand gated ionotropic receptor similar to other ionotropic receptors found throughout the nervous system(Hoyer et al., 2002). Since the striatum receives input from the Dorsal Raphe Nucleus these could be of high functional importance. In immunohistochemical studies it has been shown that 5HT receptors are widely distributed on the dopaminergic terminals coming from the Substantia nigra. Those receptors are of the 5HT2A, 5HT2C and 5HT1a. Striatal neurons also express 5HT receptors(Di Matteo et al., 2008b). These have been discovered through immunohistochemical studies and have been shown to be functionally relevant through electrophysiological studies. Serotonin receptor activation inhibits both MSNs and LTSIs (Cains et al., 2012; Mansari and Blier, 1997). The LTSI inhibition is mediated through 5HT2c receptors. The FSIs and AChIs are depolarized and excited by serotonin respectively and both events are mediated by 5HT2 receptors (Blomeley and Bracci, 2005; 2009; Bonsi et al., 2007). The AChI depolarizing events are more specifically due to the activation of 5HT2C, 5HT6, and 5HT7 serotonin receptors and the FSI events are due to activation of the 5HT2c receptor (Blomeley and Bracci, 2005; Bonsi et al., 2007). In studies investigating 5HT receptor expression it was found that MSNs express 5HT2a, 5HT2c, 5HT4, 5HT5a and 5HT6 receptors and AChIs express 5HT2C, 5HT6 and 5HT7 (Bonsi et al., 2007; Gérard et al., 1997; Hamon et al., 1999; Ward and Dorsa, 1996).

Substance P in the striatum

The primary source of SP in the striatum are the dMSNs, although some early studies indicated external sources (Bolam et al., 1983). SP has three receptors in the brain NK1, NK2 and NK3 whereof the NK1 has the highest affinity for the neuropeptide (Almeida et al., 2004). In the striatum all of these receptors are expressed and the AChIs, LTSIs, MSNs and glutamatergic terminals preferentially express the high affinity NK1 receptor (Blomeley and Bracci, 2008; Gerfen, 1991; Jakab and Goldman-Rakic, 1996; Kaneko et al., 1993; Ritter et al., 1985). SP immunoreactive terminals are symmetrical and contact dendritic shafts and spines of medium-sized neurons and perikarya and proximal dendrites of AChIs (Bolam and Izzo, 1988; Bolam et al., 1986). The AChIs show no direct pure SP connectivity response but a depolarizing response to exogenous SP, which presumably is mediated by a Sodium current (Aosaki and Kawaguchi, 1996). It has recently been shown that the medium sized neurons that are contacted by SP terminals are likely to also include MSNs since functional studies show direct depolarizing effects of SP on MSNs but no detectable direct MSN interconnectivity mediated by it (Blomeley and Bracci, 2008; Bolam and Izzo, 1988; Galarraga et al., 1999) The medium-sized neurons that contain SP receptors most likely include the LTSIs since they also show a direct depolarizing response to SP (Aosaki and Kawaguchi, 1996).

Modulation of Corticiostriatal synaptic transmission

Corticostriatal transmission onto the MSNs is directed to the dendritic spines. It has been shown that these spines and areas around them contain several types of receptors. These include DA, ACh, and SP receptors (Aosaki et al., 2010; Jakab and Goldman-Rakic, 1996; Threlfell and Cragg, 2011). Although tested there has been no evidence pointing towards modulation of glutamatergic transmission onto AChI by SP (Govindaiah et al., 2010). On the other hand, both bath application of NK1 receptor agonists and direct activation of SP expressing MSNs, modulates glutamatergic transmission with an increase in the amplitude of the Excitatory postsynaptic potential (EPSP) (Blomeley and Bracci, 2008; Blomeley et al., 2009). Conversely AChR activation either through pharmacology or direct control of nearby AChIs decreases EPSPs in MSNs (Calabresi et al., 1998a; Malenka and Kocsis, 1988; Pakhotin and Bracci, 2007; Sugita et al., 1991).

In addition to the modulatory effect exerted by the neurotransmitters and neuropeptides described, GABA can also have a modulatory affect on corticostriatal transmission (Calabresi et al., 1991; Nisenbaum et al., 1993). More specifically this effect is conveyed through the metabotropic GABAb receptors and the activation of NGF interneurons (Logie et al., 2013). As described before, the AChIs are interconnected with the NGF, which makes it feasible that this modulatory effect of GABAb is conveyed via the activation of AChIs (English et al., 2012).

Modulation of intrastriatal Inhibitory synaptic transmission

Acetylcholine also affects and modulates inhibitory transmission more specifically the connections between the FSIs and MSNs by decreasing their amplitude (Koos and Tepper, 2002). Likewise SP not only produces direct effects on individual neurons and a modulation of corticostriatal transmission but it also modulates intrastriatal inhibitory transmission. It is however only transmission to AChIs that is affected and it is likely that also endogenous SP can have this affect since adding NK1 receptor antagonist while recording Inhibitory postsynaptic currents (IPSCs) in AChIs increases the responses. Transmission to both FSIs and MSNs was also tested but exhibited no change (Govindaiah et al., 2010).

The interplay between Acetylcholine and Dopamine

Except for modulating corticostriatal and intrastriatal inhibitory transmission alone the different striatal modulatory neurotransmitters and neuropeptides interact with each other in complex ways to modulate striatal processing. Serotonin and most likely also SP interact with both acetylcholine and dopamine but the most studied interaction is the one between dopamine and acetylcholine (Anderson et al., 1994; Aosaki et al., 2010; Butcher et al., 1976; Di Matteo et al., 2008b; Threlfell and Cragg, 2011). The reasons being that patients with Parkinson's disease, where the dopaminergic projections to the striatum are degenerated, have been treated for symptoms with both dopamine replacement and anti-cholinergic substances. This has led to a view on dopamine and acetylcholine as antagonists in action. Dopamine has high initial release probability in the striatum, which is followed by a STD. This STD is linked to AChI activity and the activation of nAChRs expressed on dopaminergic terminals. Acetylcholine through the activation of nAChRs increases initial release probability, which is followed by STD. There is also evidence showing that DA receptor activation inhibits or induces pauses in AChIs. Although AChIs on a shorter time-scale are inhibited by dopamine, the mechanisms for enhanced acetyl-

choline release in Parkinson's disease might not be as simplistic. Rather it is believed that basal ganglia oscillatory activity could be the culprit since dopamine depletion does not change the frequency of firing of AChIs (Aosaki et al., 2010; Threlfell and Cragg, 2011).

Recent studies have also shown that AChIs can induce dopamine transmission locally which challenges the view of dopamine and acetylcholine as antagonistic in action(Surmeier and Graybiel, 2012; Threlfell et al., 2012). Other than these interactions dopamine and AChIs are also thought to be crucial for the induction of LTD in MSNs. It has indeed been shown that LTD depends on the activation of the D2 receptor (Calabresi et al., 1996; Wang et al., 2006).

Preliminary Results- Effect of 5HT3a receptor agonist on 5HT3a-EGFP positive neurons

Much of the 5HT receptor expression of striatal neurons has been mapped out both through immunohistochemical, single cell RT-PCR and functional pharmacological studies. The 5HT3 receptor is expressed in the striatum but its functional significance has not been elucidated. A reason for this is that it is an ionotropic fast inactivating receptor making it impossible to use traditional pharmacological techniques to study its action(Rudy et al., 2011). In Paper I we used a 5HT3a-EGFP transgenic mouse to show that a subset of striatal interneurons express the 5HT3a receptor. The interneurons share electrophysiological characteristics of FSI, NGF and LTSIs. We could not rule out that the LTSIs make up a novel subtype of the classical LTSIs since they for example show a stronger and more reliable response to nicotine puffing. In addition to the nicotine puffing experiments presented in Paper I we also puffed the 5HT3a-EGFP+ neurons with CPBG (a 5HT3a receptor agonist). 5/8 neurons recorded responded to the puffing which of 3 were LTS-like and 2 FS-like. All FSIs responded with a depolarization and surprisingly, 1/3 LTSIs respond with a depolarization to CPBG puffing which is the opposite effect of previously described response to 5HT(Cains et al., 2012). More experiments would have to be done to verify this and it would also be interesting to see if they are the same interneurons that respond strongly to nicotine puffing. If in fact so, this would further strengthen the hypothesis that these are a novel LTSI subtype.

Preliminary Results- Modulation of intrastriatal connectivity by Cholinergic interneurons

It has been shown that AChR activation modulates corticostriatal transmission onto MSNs both by endogenous and exogenous acetylcholine (Calabresi et al., 1998a; 1998b; Malenka and Kocsis, 1988; Pakhotin and Bracci, 2007; Sugita et al., 1991). It has also been shown that exogenous application of Acetylcholine reduces the connection amplitude of FSI to MSN synaptic transmission(Koos and Tepper, 2002). It has however not been shown if the same is true for endogenous acetylcholine. To further examine this we patched pairs of MSNs and AChIs. We placed a stimulating electrode at approximately 200 μm distance from the patched pair of neurons and GABAergic responses were reliably evoked in the MSN. We controlled that they were purely GABAergic by blocking glutamatergic responses with CNQX and AP-V. To examine how the evoked responses are modulated by AChI activation we evoked APs on the AChI prior to extracellular stimulation at different time intervals 20, 30 and 40 ms.

The results show that there is a trend (p=0.0659, Repeated Measures ANOVA) that AChI stimulation 20 ms prior to extracellular stimulation reduces the amplitude of the connection. This time course of AChI modulation is in agreement to what was found on the AChI modulatory effect on corticostriatal transmission (Pakhotin and Bracci, 2007)

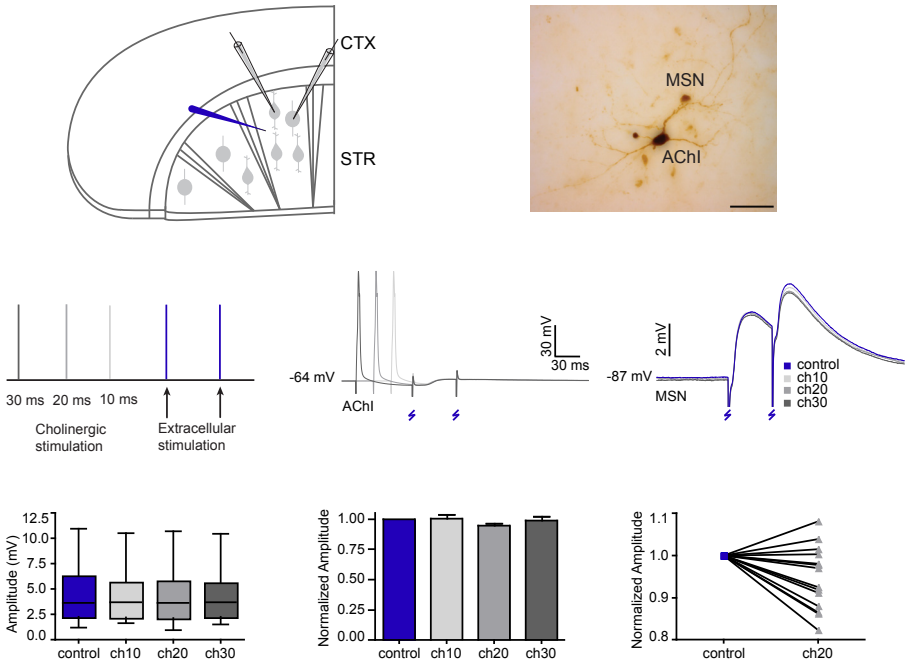

Figure 5. *Extracellular activation of non-glutamatergic transmission to MSNs. Top Left: Schematic showing the experimental set-up. Top Right: Photomicrograph of a pair of recorded neurons, post-visualized with ABC-DAB Scalebar=50 µm. Middle left: Schematic showing the experimental paradigm. Middle middle: Averaged traces from AChI showing elicited AP at 30, 20 and 30 ms prior to extracellular stimulation. Middle Right: Traces from responses of the MSNs with light stimulation alone (blue) or combined with prior AChI stimulation (grey). Bottom Left: Box and whisker plot of amplitudes of responses from all experiments in all conditions. Bottom Middle: Normalized amplitudes of all responses in the different conditions. Bottom Right: Individual amplitudes taken from experiments with AChI stimulation 20 ms prior to extracellular stimulation*

In the second part of the project we used transgenic mice of PV-Cre type that were virally injected and that express ChR2 and mCherry in a Cre-dependent manner (for details see material &methods paper II). The ChR2 and mCherry confirmed to be reliably expressed and confined to FSIs (see paper II). We recorded from pairs of MSNs and AChIs and light stimulated the FSIs. We recorded the responses in the MSNs and they were found to be reliable and of comparable synaptic dynamics as previously reported responses recorded through direct connectivity. We examined the modulation of AChI on the MSN responses by evoking APs in the patched AChI 20 ms prior to light stimulation (n=8). We saw a slight increase of the response with AChI modulation in a portion of the MSNs recorded (n=5/8, 38 %). This contradicts the results obtained with extracellular stimulation and the results presented in the previous paper with exogenous acetylcholine application (Koos and Tepper, 2002).

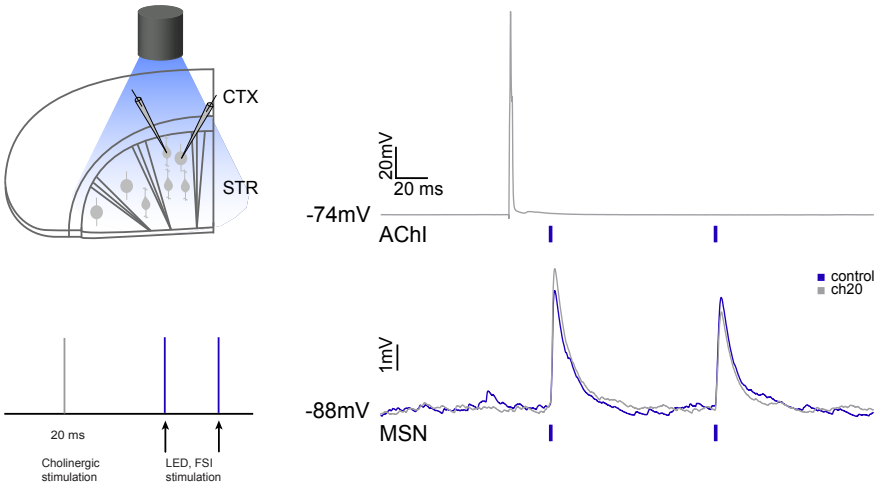

Figure 6. *Optogenetic activation of FSI-MSN connections and its modulation by single AChI activation. Top Left: Schematic showing the experimental set-up. Bottom Left: Schematic showing the experimental paradigm. Top Left: Averaged trace from an AChI showing elicited AP at 20 ms prior to light stimulation. Bottom Right: Traces from responses of the MSNs with light stimulation alone (blue) or combined with prior AChI stimulation (grey).*

WHO, WHEN & HOW & WHAT IT MEANS

NEUROSCIENCE IN THE AGE OF TECHNIQUES

After the introduction of animal electricity and the nerve cells as discrete building blocks of the nervous system much has happened in the way we study the system. Especially, at present the development and discoveries of new and better techniques are immense. Below I briefly summarize and discuss the different techniques used in the thesis. For further information and detailed descriptions see material & methods of the individual papers.

To further study animal electricity, an area now named electrophysiology, thin, sharp electrodes have been used to perturb and measure from individual neurons and nerve fibers. Neher and Sakmann further advanced this technique when they developed the patch-clamp technique, enabling recordings from individual neurons and even the small ion-channels that shape their electrical properties(Sakmann and Neher, 1984). It is this technique together with in vitro slice recordings that I have predominantly used in my thesis. The slices are 250 μm thick and inevitably some parts of the neuronal branches are cut off in the process. This could of course potentially mean that some connections are severed as well. Therefore the percentages and number of connectivity could likely differ in vivo and should only be taken as a directional value rather than absolute. Moreover, we used the patch-clamp technique by patching the soma of the neurons. This would allow for correct measurement of all input that is large enough to be detected in the soma. There could therefore be weak connectivity of distal dendrites that we cannot detect with our method. We focus on the connectivity that could be transmitted and passed on. Although, not strong enough to be passed on we do not exclude that this weak connectivity can have substantial impact on local processing.

Many different model organisms can and have been used to study the nervous system. Of the lower vertebrates and invertebrates these include Aplysia, Squid, Leech, Lobster, Drosophila, C. Elegans, Zebrafish and Lamprey(Castellucci et al., 1970; Hartline and Maynard, 1975; Hodgkin and Huxley, 1952; Kimmel et al., 1982; McClellan and Grillner, 1984; Quinn et al., 1974; Stent et al., 1978; White et al., 1986). The advantage of them is that you can derive general principles regarding the function of the nervous system. Moreover, they are easier to keep intact and still manipulate. Higher vertebrates have also been used including cats, zebra-finches, primates and rodents(Brown and Sherrington, 1912; Farries and Perkel, 2000; Hubel and Wiesel, 1968). In this thesis we have used rodents with an emphasis on mice. In addition to the advantage regarding breading, mice genetics are easily manipulated to create transgenic mouse lines. There is a wealth of transgenic mouse models and we have used ones that help us identify and specifically target certain types and subtypes of striatal neurons (Gittis et al., 2010; Heintz, 2001; Hippenmeyer et al., 2005)..

Another transgenic mouse model, which we used in paper II, is the PV-Cre transgenic mouse(Cardin et al., 2009). We used it to target a light-activated opsin and a fluorescent protein to the striatal interneurons FSI (Deisseroth et al., 2006). This enabled us to with the help of blue light stimulate a population of these specific interneurons. We used it to detect connections in a more efficient way and also because it gives a more in vivo like stimulation where populations of neurons are stimulated at the same time instead of individual neurons. It can and is being used to manipulate specific groups of neurons in an intact animal.

Ramon y Cajal beautifully visualized individual and networks of neurons. In this thesis we have used different visualization techniques. These include immunohistochemistry and histochemistry. Immunohistochemistry has been used to visualize and compare striatal interneurons of different types. This has been done to quantify and assess different interneuronal populations. It has also been used as a control to the different transgenic mouse models used. Histochemistry has been used to label and post-visualize recorded cells. This has been done using both fluorescence and the ABC-DAB technique (Horikawa and Armstrong, 1988; Kita and Armstrong, 1991).

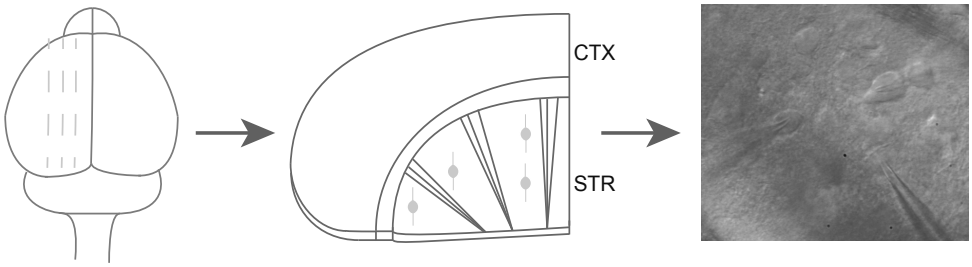

Figure 7. *Schematic showing the steps in the in-vitro preparation, used in the projects of the thesis. From dissection, slicing and finally to patch-clamping. The photomicrograph to the right shows 3 neurons patched at the same time.*

CONCLUSIONS

With the studies included in this thesis we have investigated the immunohistochemical and electrophysiological properties of the 5HT3a-EGFP + neurons. We showed that they are interneurons and show little overlap with any of the classical striatal markers with the highest overlap being with PV. Furthermore we have showed that they fall into three categories of interneurons with resemblance to FSI, NGF and LTSIs. The FSI-like interneurons constituted 32 % of all recorded neurons and the overlap of PV with 5HT3a was 19.78 ± 0.26%. This together with the fact that the FSIs showed pronounced similarities with FSIs recorded in the Lhx6-EGFP mouse (see paper I, supplementary figure 2) suggests that they are not a novel subpopulation.

NPY show little overlap with 5HT3a expression (1.67 ±0.48) and because a substantial amount of the recorded 5HT3a-EGFP + neurons are NGF-like (16%), which have previously been identified via their NPY expression (Ibanez-Sandoval et al., 2011), we hypothesize that the NGF-like 5HT3a-EGFP + neurons are a novel subpopulation.

The LTS-like 5HT3a-EGFP+ interneurons show a strong and reliable response to nicotine, which is different from the one recorded in LTSIs from Lhx6-EGFP mice. Furthermore, a proportion of them respond to 5HT3a agonists with a depolarization, which is opposite to responses previously recorded on serotonin responses of LTSIs. This further strengthens the hypothesis that these LTS-like neurons are a novel subpopulation of the LTSIs. They show no direct connectivity with AChIs but further experiments will have to be done to confirm these preliminary results.

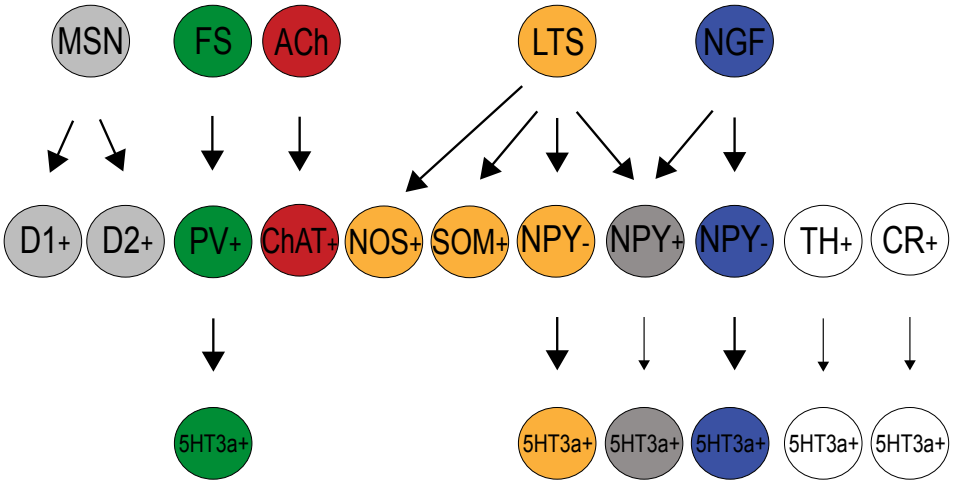

Figure 8. *Conclusion regarding the striatal neuron types reached in the thesis. It shows an extension of the striatal neuron types that also shows their 5HT3a expression. Note the novel subpopulations of the LTS that are NPY- and the NGF that are NPY-. Lower weight arrows indicate that not all of the neurons expressing the protein in question also express the 5HT3a receptor. MSN= Medium Spiny Neuron, FS=Fast spiking interneuron, ACh=(Acetylcholine,) Cholinergic interneuron, LTS= Low threshold spiking interneuron, NGF=Neurogliaform interneurons, D1=Dopamine D1 receptor, D2= Dopamine D2 receptor, PV= Parvalbumin, ChAT=Choline Acetyl Transferase, NOS(nNOS)= Nitric oxide synthase, SOM=Somatostatin, NPY=Neuropeptide Y.*

We also investigated both intrastriatal feedforward and feedback connections. We found that MSN-MSN interconnectivity is sparse and that MSNs of both indirect and direct type contact each other. The iMSN is to a larger extent the presynaptic cell but contact MSNs of both types with similar probabilities. There is no difference in the connections when it comes to amplitudes or synaptic dynamics and they exhibit both facilitating and depressing components.

We found that FSIs contact MSNs with high probability and reliably depressing synaptic dynamics. They contact MSNs of both types and the same FSI even contacts MSNs of both types. Furthermore FSIs are target selective and completely avoid AChIs while forming sparse connections with LTSIs. This shows that there is a separation between the AChI network and the feedforward inhibition. Likely because of segregation in function where the AChIs are involved in reinforcement learning and motor learning while the feedforward inhibition probably has a role in action selection.

Lastly we showed that in MSN-MSN and FSI-MSN connections the membrane potential of the presynaptic neuron has an effect on the release probability of the synapse. The extent of the effect is dictated by the initial release probability of the synapse and this type of presynaptic modulation might serve to make synapses more precise and time-locked.

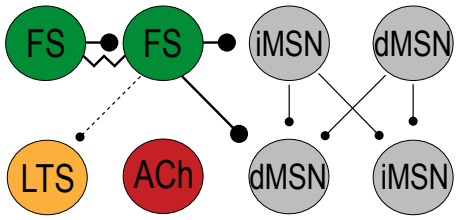

Figure 9. A schematic of the conclusions reached in the thesis regarding connectivity. Lower weight connections symbols indicate a relatively weaker connection. iMSN= Indirect pathway Medium Spiny Neuron, dMSN=Direct pathway Medium Spiny Neuron, FS=Fast spiking interneuron, ACh=(Acetylcholine,) Cholinergic interneuron LTS= Low threshold spiking interneuron.

FUTURE PERSPECTIVES

In paper I we study the 5HT3a-EGFP+ interneurons. It would be interesting to investigate their connectivity using for example optogenetics and also to further study their role in striatal serotonergic processing.

In paper II we show that the synaptic dynamics of MSN interconnectivity is varying with both facilitating and depressing components. One explanation for this could be that when stimulating dMSNs there is release of SP, which could affect these parameters. The variability in synaptic dynamics could perhaps be eliminated by blocking SP receptors and would be an interesting topic to explore further. Other neuropeptides that I have not explored in this thesis are enkephalin and dynorphin, which are expressed and transmitted from iMSNs and dMSNs respectively (DiFiglia et al., 1982; Izzo et al., 1987; Reiner and Anderson, 1990). Since they are also stimulated during the experiments they could potentially also have an effect on the synaptic dynamics.

In paper III we showed that FSIs are target selective and only innervate LTSIs sparsely. The number of LTSIs recorded in the optogenetic experiments was low due to the relatively low LTSIs percentages and because we could not specifically target them for recording. Although we did confirm the low connectivity in a different transgenic mouse model it would be interesting to further test their connectivity in targeted recordings combined with optogenetics. Furthermore, it would be interesting to look at FSI connectivity with regards to neuronal cell assemblies and the connectivity between and within these assemblies.

In paper IV we showed that presynaptic membrane potential affects amplitudes and paired pulse ratios of synapses specifically in FSI-MSN connections and most likely also in MSN-MSN connections. It would be interesting to further examine the mechanism of this and elucidate the role of Calcium-channels by chelating intracellular Calcium (EGTA or BAPTA) and/or by targeting specific Calcium channels pharmacologically. Moreover, it would be interesting to test a protocol that mimics the up and down states seen in vivo to further elucidate the physiological significance of this phenomenon. Furtermore, to in greater detail study how the synaptic dynamics are influenced by presynaptic membrane potential, we could use the model and experimental protocol developed by Tsodyks and Markram.

In addition to the papers, I presented preliminary results regarding modulation of intrastriatal inhibitory transmission. In the first part of the study inhibitory synaptic transmission was elicited through extracellular stimulation and responses recorded in MSNs. The transmission therefore most likely comprised of presynaptic neurons of both MSN and FSI type. In the second part of the study we studied only FSI to MSN transmission. It would therefore be interesting to also explore if MSN to MSN transmission is modulated by AChR activation. Because AChIs are tonically active even in slice preparations it would be interesting to further explore the modulation by silencing these neurons either by optogenetics, pharmacological means or by lowering extracellular concentrations of K^+. To examine how direct AChI modulation one could patch and stimulate single AChIs while activating the FSI to MSN, or MSN to MSN synaptic transmission. It would also be interesting to see how simultaneous stimulation of several AChIs modulates intrastriatal inhibitory transmission but because AChIs are directly and disynaptically connected to MSNs it would not be possible to discriminate between a direct synaptic and a modulatory effect.

RECONCILING THE DECONSTRUCTED BRAIN WITH ITS GLOBAL FUNCTIONS

One of the most difficult questions to answer, which arises with the reductionist way of studying the brain, is how all of these deconstructed parts act in concert. In research concerning vision this problem has been especially articulated and is known as the binding problem. It addresses how different components of visual input (colour, shape & motion) are being processed in different areas but combined into a single coherent perception. Firstly it questions how a set of input that are of different colour, shape and motion are intermixed. Secondly, it questions how the different components can form a uniform experience(Crick, 1995; Revonsuo and Newman, 1999; SmythiesPlaton, 1994).. A solution to that problem that has been proposed is the phenomenon of neuronal oscillations (Milner, 1974; Shadlen and Movshon, 1999). Oscillations occur at different brain states and have been observed at frequencies corresponding to delta (1-4 Hz), theta (4-8), alpha (8-13Hz) and gamma (13-30Hz). The slower frequencies have been associated with sleep and especially gamma is associated with cognition and awareness. The way that the oscillations would potentially solve the binding problem is that the neurons that oscillate together at the gamma frequency would be bound together and code for the same part of the visual input (Engel et al., 1990). This idea could be extrapolated to different brain processes that also partly deal with the same issue of different parts being activated for the same task. Whether it is in fact oscillations that are the answer remains unsolved(Kauffman, 2012).

Another problem that arises is how we can extrapolate the findings on a deconstructed level to also hold on a global level. The usual problems of the way we study these phenomena, which also holds for the studies in the thesis, are that the conditions during the studies vary significantly from the ones encountered in real life or physiological situations. In addition to this problem there is the problem of laws on the micro level that can be broken on the global level, a phenomenon called broken symmetry. This phenomenon can be nicely and intuitively illustrated with crystals. They are indeed highly organized and have a very intricate organization on the microscopic level but on the global level this organization is not to be seen (Anderson, 1972). I have tried to illustrate this problem in the cover picture of the thesis where I have taken a schematic of the known circuitry of the striatum and multiplied it into a different shape.

New techniques including optogenetics and others, that allow manipulation of the building blocks, offer a starting ground and platform for how to start tackling these issues (Armbruster et al., 2007; Deisseroth et al., 2006; Wall et al., 2010). It will be interesting to see how neuroscience in the future translates the deconstructed parts into a more global perspective.

SAMMANFATTNING PÅ SVENSKA

För att kunna förstå, manipulera och bota ett system såsom hjärnan behöver man insikt i dess olika beståndsdelar och hur dessa fungerar. Den moderna forskningen om hjärnan och neurovetenskapsforskningen grundlades i och med Ramón y Cajals fantastiska arbete med att visualisera dessa beståndsdelar, nervcellerna. Det var under den här tiden och med hjälp av det arbetet som neurondoktrinen accepterades. Neurondoktrinen bygger på att nervceller kan delas in i olika delar. Dessa är dendriten, som är den del av nervcellerna som tar emot information från andra nervceller. Cellkroppen, som är den del där cellkärnan finns. Och till sist axonet, som är den del varigenom nervcellen skickar vidare information till andra nervceller.

Senare visade man att hjärnan kan delas in i olika delar och att det sker informationsutbyte mellan olika hjärndelar, såväl som inom olika hjärndelar. Informationsutbytet eller kommunikationen mellan nervceller sker med hjälp av substanser som kallas neurotransmittorer.

Nervsystemet och hjärnan har studerats på olika sätt och i olika organismer. Det som alla organismer har gemensamt är att de använder nervsystemet för att känna av omgivningen och bearbeta den informationen för att sedan ta beslut om hur de ska agera eller interagera med omgivningen. Den del av den processen som studeras i den här avhandlingen är hur man påbörjar ett agerande.

Parkinsons sjukdom är ett exempel på en sjukdom där detta förlopp är stört. Ett av symptomen vid sjukdomen är svårigheter med att påbörja och att avsluta en rörelse. Den har förknippats med den grupp av hjärndelar, de s.k. basala ganglierna, som jag studerar i den här avhandlingen. Det finns två så kallade projektionsbanor eller kommunikationsvägar i de basala ganglierna, den indirekta och direkta banan. Den indirekta banan hämmar rörelse och är överaktiv i Parkinsons sjukdom, medan den direkta banan främjar rörelse och är underaktiv. Striatum är den del av hjärnan som har studerats i den här avhandlingen och är den del av basala ganglierna som tar emot information från andra hjärngrupper som hjärnbarken och thalamus.

Hjärnans nervceller kan klassificeras och delas in olika grupper. Indelningen är baserad på vilka proteiner som nervcellerna uttrycker och hur de beter sig rent elektrofysiologiskt (till exempel vad de har för resistans, vilomembranpotential och hur de svarar när man aktiverar dem med hjälp av olika spänningsprotokoll). Den största delen, 90-95%, av alla nervceller i striatum är så kallade projektionsneuron. Projektionsneuronen för vidare information från striatum till andra delar av hjärnan och är antingen en del av den direkta eller indirekta banan.

Förutom dessa projektionsneuron finns även så kallade interneuron. Dessa påverkar informationsbearbetningen inom striatum men sänder inte vidare information till andra delar av hjärnan. Striatums interneuron delas klassiskt in i cholinerga interneuron, FS (fast spiking) interneuron, LTS (low threshold spiking) interneuron och neurogliaform (NGF).

Det övergripande målet med avhandlingen var att studera nervcellerna i striatum och deras kommunikationsmönster. Mer specifikt var det att studera indelningen av de olika interneuronen, hur de kommunicerar både med varandra och projektionsneuronen och dessutom se hur kommunikationen på olika sätt kan ändras inom en kort tidsperiod.

Vi har använt oss av en rad olika tekniker för att studera detta. Den centrala tekniken är patch-clamp där vi har mätt elektrisk aktivitet från upp till fyra individuella nervceller samtidigt. Detta har vi gjort i hjärnsnitt från råtta och mus där vi hållit vävnaden levande i flera timmar. För att lättare kunna mäta och aktivera specifika nervellstyper har vi använt oss av transgena möss, bl. a möss som uttrycker ett fluorescerande protein, GFP (green fluorescent protein), i specifika interneuron eller i de två olika typerna av projektionsneuron. Vidare har vi använt transgena möss där vi riktat uttrycket av ett protein till FS-interneuron. Proteinet gör det möjligt att aktivera dessa interneuron med hjälp av ljus. Dessutom har vi använt oss av olika immunohistokemiska och histokemiska metoder för att klassificera och visualisera nervcellerna.

I den första studien har vi tittat på förekomsten av kommunikation mellan projektionsneuronen tillhörande den direkta och indirekta banan och hur styrkan på denna förändras över tiden. Vi såg att kommunikationen är sparsam, initialt svag och att den tilltar i styrka över en kort tidsperiod. Dessutom såg vi att nervceller från den direkta banan i högre grad än nervceller från den indirekta banan kommunicerar med nervceller både från den direkta och indirekta banan. Vidare studerade vi kommunikationen mellan FS-interneuronen och de två typerna av projektionsneuron. Vi såg att FS-interneuronen kontaktar de två typerna i liknande utsträckning och att till och med samma FS-interneuron kontaktade projektionsneuron av olika typ.

I den fjärde studien har vi vidare studerat i hur hög utsträckning FS-interneuronen kontaktar andra interneuron. Vi såg att de helt undviker cholinerga interneuron men kontaktar LTS-interneuron med låg sannolikhet.

I den tredje studien använde vi oss av en specifik transgen mus där neuron som uttrycker en viss serotonin-receptor, 5HT3a, även uttrycker det gröna fluorescerande proteinet GFP. Vi har karaktäriserat dessa neuron och funnit att de kan delas in i tre olika typer som har liknande egenskaper som de klassiska interneuronen FS, LTS och NGF. Vi såg att LTS-interneuronen skiljer sig från de klassiska genom att de svarar starkare och till högre grad på neurotransmittorn acetylcholine.

Membranpotentialen hos nervcellerna varierar beroende på hjärnans tillstånd. I den fjärde studien har vi tittat hur kommunikationen förändras när membranpotentialen hos den nervcell som för vidare information är förhöjd.

Vi studerade kommunikationen mellan de två typerna av projektionsneuron och mellan FS interneuron och projektionsneuronen. Vi såg att när membranpotentialen är förhöjd så ökar styrkan på kommunikationen i båda kommunikationstyperna. Detta är speciellt sant för de kontakter där styrkan från början är låg.

I många studier inom neurovetenskap och också i den här avhandlingen studeras de olika nervcellerna, hur de kommunicerar och hur kommunikationen förändras över tid. Med hjälp av dess typer av studier får man kunskap som gör det möjligt att förändra och manipulera processer som nervcellerna är inblandade i. Dessutom ger det möjlighet att ta fram läkemedel som riktas mot delar av dessa processer. Kommunikationsmönster och processer som gäller på mikronivån behöver dock inte gälla i ett större perspektiv. Det exemplifieras elegant av P.W Anderson i artikeln ”More is different” (”Mer är annorlunda”) med hjälp av kristallen. Kristallstrukturen är ju väldigt ordnad och ger ett exakt mönster på mikronivån men man ser inte ett spår av detta mönster när man tittar på den i lägre förstoring. Den stora utmaningen

för neurovetenskap i framtiden, och som till viss grad redan påbörjats, är att förstå hur alla dessa mönster ser ut i ett större perspektiv. Den här utmaningen eller det här problemet har jag försökt avbilda med hjälp av bilden på avhandlingens framsida. Där har jag utgått från kommunikationsmönstret för nervcellerna i striatum, multiplicerat detta och skapat en form som skiljer sig från den ursprungliga. Hur formen på kommunikationsmönstret verkligen ser ut i ett större perspektiv återstår att se.

STRESZCZENIE PO POLSKU

Aby zrozumieć, manipulować i wyleczyć takiego systemu jakim jest mózg, trzeba mieć wgląd w jego różne składniki i jego działalność. Współczesne badania mózgu i neurologia badań, opierają się na Ramón y Cajal niesamowitej pracy, aby wizualizować te elementy czyli komórki nerwowe. Przy pomocy tej pracy doktryna neuronowa została przyjęta. Podstawa doktryny neuronowej jest, ze komórki nerwowe można podzielić na różne części. Dendryty, częścią komórek które odbierają informacje z innych komórek. Soma komórki, jest częścią w której znajduje się jądro. I wreszcie aksona jest częścią przez która komórka nerwowa przesyła informacje do innych komórek.

Później wykazano, że mózg może być podzielony na wiele części i wymiana informacji następuje pomiędzy różnymi częściami mózgu, a także w różnych częściach mózgu. Wymiana informacji i komunikacji pomiędzy neuronami odbywa się za pomocą substancji zwanej neuroprzekaźnikami.

System nerwowy i mózg badano na różne sposoby i w różnych organizmach. Wspólnota wszystkich organizmów jest to, że za pomocą układu nerwowego wyczulają otoczenie, przetwarzają ta informacje i później podejmują decyzje o tym, czy i jak rozpocząć akcję i interakcje z otoczeniem. Częścią procesu badanego w tej pracy jest to, jak rozpocząć akcję.

Choroba Parkinsona jest przykładem zaburzenia, w których proces ten jest zakłócony. Jednym z objawów choroby są trudności w rozpoczęciu i zakończeniu ruchu. To jest związane z grupa części mózgu, Basal Ganglia, które studiowałam w tej pracy. Istnieją dwie tak zwane linie projekcyjne albo szlaki komunikacyjne w tych grupach, droga bezpośrednia i pośrednia. Ścieżka pośrednia hamuje ruch i powoduje nadczynność w chorobie Parkinsona, natomiast bezpośrednia droga przepływu promuje ruch i jest pod aktywna. Striatum jest ta częścią mózgu, które było badane w tej pracy i jest częścią basal ganglia, która otrzymuje informacje od innych grup mózgu, cortex i thalamus.

Neurony mózgu mogą być klasyfikowane i podzielone na kilka grup. Klasyfikacja oparta jest na tym które proteiny te komórki nerwowe zawierają i jak się zachowują czysto elektrofizjologicznie (na przykład jaki maja opor, oraz jakie maja napięcie spoczynkowej i jak reagują, gdy je aktywujemy za pomocą różnych protokołów napięć). Największa część 90-95% wszystkich neuronów striatum to tak zwane neurony projekcji . Neurony projekcji wysyłają informacje z striatum do innych części mózgu droga ścieżki bezpośredniej lub pośredniej. Oprócz tych neuronów projekcyjnych są tez tak zwane interneurony. One maja wpływ na przetwarzanie informacji w striatum, lecz nie wysyłają dodatkowych informacji do innych części mózgu. Interneurony w striatum są klasycznie podzielone do cholinergicznych interneuronow, FS (Fast-spiking) interneuronow, LTS (Low threshold spiking) Neurogliaform (NGF) interneuronow.

Ogólnym celem pracy było zbadanie komórek nerwowych w striatum i ich wzorców komunikacyjnych. Bardziej szczegółowym celem było zbadanie podziału różnych interneuronow oraz jak komunikują się ze sobą i z neuronami projekcji i jak komunikacja może w różny sposób zmieniać się w krótkim okresie czasu.

Korzystaliśmy z różnych technik do badania tego zjawiska. Kluczową technologią jest patch-clamp, gdzie mierzyliśmy elektryczną aktywność w aż do czterech pojedynczych neuronów jednocześnie. Używaliśmy do pomocy plasterków mózgu ze szczurów i mysz, których tkanki zachowywaliśmy przy życiu przez kilka godzin. Aby łatwiej można było mierzyć i aktywować konkretny typ komórek nerwowych używaliśmy transgenicznych myszy, specyficznie używaliśmy rodzaj transgenicznych mysz gdzie specjalna fluorescencyjna proteina, GFP (green fluorescent protein), była w określonych interneuronach albo w dwóch różnych typach neuronów projekcyjnych. Ponadto, myszy transgeniczne używaliśmy w ktorym specjalna proteina była z która można aktywować neurona z pomoczą światła. My mieliśmy ta proteinę specyficznie w interneuronow FS. Ponadto, używaliśmy różne metody immunohistochemiczne i histochemiczne w celu klasyfikacji i wizualizacji komórek nerwowych.

W pierwszym badaniu przyjrzeliśmy się występowaniu komunikacji między neuronami projekcyjnymi powiązanych droga bezpośrednia i pośrednia oraz zmiany się ich siły w czasie. Zauważyliśmy, że komunikacja jest rzadka, początkowo słaba i że jest zwiększenie intensywności w ciągu krótkiego okresu czasu. Ponadto dowiedzieliśmy się, że komórki nerwowe z bezpośredniej ścieżki komunikują się z neuronami zarówno z bezpośredniej jak i pośredniej ścieżki. Ponadto, badaliśmy komunikację interneuronow FS z dwoma rodzajami neuronów projekcyjnych. Widzieliśmy, że FS interneurony kontaktują się dwoma typami w podobnym stopniu, a nawet FS interneuron kontaktował neurony projekcyjne różnych typów.

Ponadto studiowaliśmy na ile FS interneuron kontaktował się z drugimi interneuronami. Widzieliśmy, że całkowicie unikał interneuronow cholinergicznych ale kontaktował się z interneuronami LTS z małym prawdopodobieństwem.

W trzecim badaniu używaliśmy konkretne transgeniczne myszy, w których neurony daja ekspresję określonego receptora 5HT3a serotoniny, jak również ekspresję GFP. Scharakteryzowaliśmy neurony i stwierdziliśmy, że można je podzielić na trzy różne rodzaje, które mają właściwości podobne do tych klasycznych interneuronow FS LTS i NGF. Okazało to że interneurony LTS są różne od klasycznego, że reagują one silniej, i w większym stopniu na acetylocholiny neuroprzekaźnikowe.

Napięcie komórek nerwowych zmienia się w zależności od stanu mózgu. W czwartym badaniu, sprawdziliśmy wpływ zmian komunikacji kiedy napięcie komórki, która wydaje informacje nerwowej, jest podwyższone. Badaliśmy te zjawisko w komunikację między dwoma typami neuronów projekcyjnych i między interneuronami FS i neuronach projekcyjnym. Zauważyliśmy, że gdy napięcie komórki wzrasta, to wzrasta tez siła komunikacji w obu typach komunikacyjnych. Dotyczy to specjalnie tych typów gdy komunikacja od początku jest bardzo niski .

W wielu badaniach w dziedzinie neurologii , a także w niniejszej pracy badaliśmy różne komórki nerwowe , ich komunikacje oraz zmianę ich komunikacji w czasie. Informacje która się otrzymuje dzięki takich badań pomaga aby wynaleźć jak można zmieniacz i manipulować procesy zaangażowanych komórek nerwowych. Zapewnia to możliwość opracowania leków, które są skierowane przeciwko składnikom tych procesów. Wzorce komunikacyjne i procesy które mają zastosowanie na poziomie mikro nie mają zastosowania w szerszej perspektywie . Przykład stylowo zaprezentował Anderson PW w artykule “Bardziej różni “ (“More is different”) za pomocą kryształu. Struktura krystaliczna jest bardzo uporządkowana i daje dokładny wzór na poziomie mikro , ale nie widać śladu tego wzoru , gdy patrzymy na
mniejszym powiększeniu. Głównym wyzwaniem dla neurologii w przyszłości jest zrozumienie,

w jaki sposób wzory te wyglądają w większej perspektywie. To wyzwanie , albo ten problem , próbowałam odtworzyć wykorzystując zdjęcia na początku pracy doktorskiej . Zaczęłam od wzorca komunikacji komórek nerwowych w striatum, pomnożyłam ich i tak stworzyłam nowy kształt inny od oryginału. Jak kształt wzorca komunikacyjnego w większej perspektywie naprawdę wygląda pozostaje do udowodnienia

ACKNOWLEDGEMENTS

I would like to thank all the co-workers, collaborators, family and friends who have been a part of this rollercoaster PhD journey. Thanks for all the scientific and non-scientific discussions, the inspiration, the support through the tough and not-so tough times, the laughter, the jokes, the dinners, the drinks and all the shared litres of coffee and tea.

Thanks to all the people that helped with the making of this thesis; my supervisor and co-supervisor for their comments; Ramón Reig for help with the part about neuronal oscillations; Will Jones for help with the English, formatting and front-cover; Gill Jones for help with the introduction; Peter Löw for help with formatting the manuscripts; Brita Robertson and Linus Larsson for help with the summary in Swedish "Sammanfattning på svenska"; Alina Szydlowski, Roman Szydlowski and Agnes Jaskiel for help with the summary in polish "Streszczenie po polsku".

Thank you to my supervisor Gilad Silberberg for always pushing me to be better, for teaching me how to become a master patcher and for the opportunity of attending all the inspiring scientific conferences and courses.

Thank you to my co-supervisor Sten Grillner for the scientific inspiration, all the feedback and discussions and for providing such a good atmosphere at the level 5 coffee group.

Thanks to my co-supervisor Marie Carlén for all the discussions, guidance and for being an excellent female scientist role model.

Thanks to my mentor Ewa Ehrenborg for guiding me through the jungle of science and for giving med the confidence and push to find my own way through it.

Thanks to the past and present members of the Silberberg lab: Henrike Planert, Jesper Ericsson, Ramón Reig, Ming Zhou, Maya Ketzef, Yvonne Johansson and Matthijs Dorst, for all the feedback, help, support, discussion, team-work and cakes. A special thanks to co-author Henrike Planert for all the team-work throughout.

Thanks to Brita Robertson for teaching me different histochemical methods and for the conversations about English literature and culture.

Thanks to all my collaborators on the different projects, for the team-work and inspiring discussion. A special thanks to collaborators Marie Carlén, Dinos Meletis and Iskra Pollak Dorocic, Jens Hjerling-Leffler, Claire Foldi and Ana Belen Munoz Manchado and Johannes Hjorth.

Thanks to the half-time committee members; Karima Chergui, Peter Wallén and Jens Hjeling-Leffler for all the excellent feedback, suggestions and comments during my half-time seminar.

Thanks to the members of the different departmental committees that I was in, for the opportunity to discuss important issues. A special thanks to Lennart Brodin and Peter Wallén in the educational board who listened to, commented and supported new ideas and ways of teaching the biomedical students and medical students.

Thanks to Iris Sylvander for all the help with administrative issues and all the conversations about plants and life.

Thanks to the past and present members from the Grillner, Silberberg, Kiehn, El-Manira, Deliagina and Hellgren-Kotaleski labs of the level 5 coffee-group and lunch seminars. For all the fun, interesting and educational conversations and discussions. For all the easter egg-rolling, Christmas glögg drinking, decorating and "julbording".

Thanks to the Ole Kiehn lab espresso corner for taking me up as their guest-coffee drinker and for providing the best espresso at the department. A special thanks to barista Peter Löw for all the mentoring, IT help and support and for making the department a more fun place to be. Thanks to Ann-Charlotte Westerdahl for all the help and support with ethical applications, protocols and PCR:ing and for all the fun chats. Thanks to Kim Dougherty for all the scientific feedback and discussions. Thanks to Natalie Sleiers for all the help on animal-related issues and for all the fun. Thanks to barista Carmello Bellardita for all the discussion on science, art and for helping me keep my italian up to speed. Thanks to Julien Bouvier for introducing me to the tips and tricks of Image J. Thanks to Lotta Borgius, Anna Kasagiannis, Adolfo Talpalar and Vanessa Caldeira for all the shared coffees and chats.

Thanks to past and present members of the El-Manira Lab for all the feedback and discussions and for the coffee-drinking-times. A special thanks to Jessica Ausborn, Rebecka Björnfors, Sabine Haupt and Emma Eklöf Ljunggren for all the coffee-chats.

Thanks to the Broberger lab for all the fun joint lab-outings. A special thanks to Lovisa Case for sharing brains, both literally and sometimes figuratively.

Thanks to the Basal Ganglia Journal Club : Marcus Jones, Ebba Samuelsson, Jesper Ericsson, Henrike Planert and Kai Du for all the interesting and educational discussions on basal ganglia related articles.

Thanks to all my office-mates throughout the years; Ebba Samuelsson, Jesper Ericsson, Andreas Klaus, Li-Ju Hsu, Anastasia Karayannidou, Chus Abalo, Andreas Kardamakis, Kai Du, Ramón Reig, Henrike Planert, Maya Ketzef, Ming Zhou, Yvonne Johansson and Matthijs Dorst. A special thanks to Ebba Samuelsson for all the discussions on science, teaching and plants. I miss you and wish you were still here to share this with me.

Thanks to all set-up mates; Carolina Thörn-Perez, Ebba Samuelsson, Jesper Ericsson, Isaac Shemer, Henrike Planert and Lorenza Capantini for their patience when hearing all my patching complaints and for the company during all those long hours of patching.

Thanks to PhD students at and outside the department and outside for all the meetings, dicussions, fun times and chats; Caroline Ran, Robert Karlsson, Adina Feldman, Kristoffer Sahlholm, Richard Andersson, Sophia Savage, Giulia Gaudenzi, Michalina Lewicka-Yammine, Iskra Pollak Dorocic, Andreas Kalckert, Sandra Gelhaar and Tobias Karlsson,

Thanks to my friends at the beginning of my PhD Emilia Horjales-Araujo and Hui Min Tan for all the chats and for the shared experience of the Crete conference and the works of Dr. Evans
Thanks to Ida Engqvist for help with all it-related issues and for saving me and my data on several occasions.

Thanks to Anders Lindquist for all the help on equipment making and set-up-building and Filip Lindholm for all the help with the hardware of equipment.

Thanks to all the administrative personnel; Chritina Ingvarsson, Anna Hammervik, Elzbieta Holmberg, Karin Lagerman and Thomas Johansson for all the help on administration-related issues.

Thanks to all the animal staff for all the help. A special thanks to Martina Andersson and Anna Lindberg.

Thanks to my family Mum Alina Szydlowski, Dad Roman Szydlowski and brother Martin Szydlowski for all their love and support. Thanks to my grandparents Mieczyslaw and Anna Hanczyc for their love and support from afar. A thanks to all my extended family and in particular my aunties Maria Grinberg, Bozena Hanczyc and Agnes Jaskiel for their love, help and support.

Thanks to my friends outside of science; Juliana Fritzhand, Ann-Sofi Silberstein, Petter Jansson, Linus Larsson, Joel Westerholm, Katrin Ingelstedt, Jon Skogens, Karin Morian, Karl Morian, Sofia Hällsten, Helena Sundin, Marcus Niemann, Ada Fredelius, David Borgström, Hanna Andersdotter-Eriksson, Signe Lidén, Johan Holkers and Johanna Wadshtorp for not letting me forget about the world outside of the lab. And for keeping me updated on what's going on. Thanks to those of you that are also members of the book-club for all the super-interesting discussions, for being my "vent" and for helping me sharpen my argumentation skills.

Thanks to my old and reliable laptop that made it through the thesis writing when the younger colleague gave up.

Lastly, but certainly not least, I would like to thank my friend, sambo, life partner and husband Will Jones for being my greatest supporter, for never doubting me and for all the immense love, help and patience during these years. And of course for always talking about the future.

REFERENCES

Abbott, L.F., and Nelson, S.B. (2000). Synaptic plasticity: taming the beast. Nature Neuroscience 3 Suppl, 1178–1183.

Adermark, L., and Lovinger, D.M. (2009). Frequency-Dependent Inversion of Net Striatal Output by Endocannabinoid-Dependent Plasticity at Different Synaptic Inputs. Journal of Neuroscience 29, 1375–1380.

Albin, R.L., Young, A.B., and Penney, J.B. (1989). The functional anatomy of basal ganglia disorders. Trends in Neurosciences 12, 366–375.

Albin, R.L., Young, A.B., and Penney, J.B. (1995). The functional anatomy of disorders of the basal ganglia. Trends in Neurosciences 18, 63–64.

Alexander, G.E., and Crutcher, M.D. (1990). Functional architecture of basal ganglia circuits: neural substrates of parallel processing. Trends in Neurosciences 13, 266–271.

Alexander, G.E., DeLong, M.R., and Strick, P.L. (1986). Parallel organization of functionally segregated circuits linking basal ganglia and cortex. Annual Review of Neuroscience 9, 357–381.

Alle, H., and Geiger, J.R.P. (2008). Analog signalling in mammalian cortical axons. Current Opinion in Neurobiology 18, 314–320.

Almeida, T.A., Rojo, J., Nieto, P.M., Pinto, F.M., Hernandez, M., Martin, J.D., and Candenas, M.L. (2004). Tachykinins and tachykinin receptors: Structure and activity relationships. Curr. Med. Chem. 11, 2045–2081.

Anden, N.E., A, D., Fuxe, K., and Larsson, K. (1965). Further Evidence for Presence of Nigro-Neostriatal Dopamine Neurons in Rat. American Journal of Anatomy 116, 329–&.

Anden, N.E., Carlsson, A., Dahlstrom, A., Fuxe, K., Hillarp, N.A., and Larsson, K. (1964). Demonstration and Mapping Out of Nigro-Neostriatal Dopamine Neurons. Life Sci. 3, 523–530.

Anderson, J.J., Kuo, S., Chase, T.N., and Engber, T.M. (1994). Dopamine D1 receptor-stimulated release of acetylcholine in rat striatum is mediated indirectly by activation of striatal neurokinin1 receptors. The Journal of Pharmacology and Experimental Therapeutics 269, 1144–1151.

Anderson, P.W. (1972). More is different. Science (New York, NY) 177, 393–396.

Angstadt, J.D., and Calabrese, R.L. (1991). Calcium currents and graded synaptic transmission between heart interneurons of the leech. The Journal of Neuroscience : the Official Journal of the Society for Neuroscience 11, 746–759.

Aosaki, T., and Kawaguchi, Y. (1996). Actions of substance P on rat neostriatal neurons in vitro. The Journal of Neuroscience : the Official Journal of the Society for Neuroscience 16, 5141–5153.

Aosaki, T., Kimura, M., and Graybiel, A.M. (1995). Temporal and spatial characteristics of tonically active neurons of the primate's striatum. Journal of Neurophysiology 73, 1234–1252.

Aosaki, T., Kiuchi, K., and Kawaguchi, Y. (1998). Dopamine D1-like receptor activation excites rat striatal large aspiny neurons in vitro. The Journal of Neuroscience : the Official Journal of the Society for Neuroscience 18, 5180–5190.

Aosaki, T., Tsubokawa, H., Ishida, A., Watanabe, K., Graybiel, A.M., and Kimura, M. (1994). Responses of tonically active neurons in the primate's striatum undergo systematic changes during behavioral sensorimotor conditioning. The Journal of Neuroscience : the Official Journal of the Society for Neuroscience 14, 3969–3984.

Aosaki, T., Miura, M., Suzuki, T., Nishimura, K., and Masuda, M. (2010). Acetylcholine-dopamine balance hypothesis in the striatum: An update. Geriatrics & Gerontology International 10, S148–S157.

Armbruster, B.N., Li, X., Pausch, M.H., Herlitze, S., and Roth, B.L. (2007). Evolving the lock to fit the key to create a family of G protein-coupled receptors potently activated by an inert ligand. Proceedings of the National Academy of Sciences of the United States of America 104,

5163–5168.
Ballion, B., Mallet, N., Bézard, E., Lanciego, J.L., and Gonon, F. (2008). Intratelencephalic corticostriatal neurons equally excite striatonigral and striatopallidal neurons and their discharge activity is selectively reduced in experimental parkinsonism. The European Journal of Neuroscience 27, 2313–2321.
Beatty, J.A., Sullivan, M.A., Morikawa, H., and Wilson, C.J. (2012). Complex autonomous firing patterns of striatal low-threshold spike interneurons. Journal of Neurophysiology 108, 771–781.
Beckstead, R.M. (1983). A Pallidostriatal Projection in the Cat and Monkey. Brain Research Bulletin 11, 629–632.
Bedard, P., L, L., Parent, A., and Poirier, L.J. (1969). Nigrostriatal Pathway - a Correlative Study Based on Neuroanatomical and Neurochemical Criteria in Cat and Monkey. Experimental Neurology 25, 365–&.
Bennett, B.D., and Bolam, J.P. (1993). Characterization of Calretinin-Immunoreactive Structures in the Striatum of the Rat. Brain Research 609, 137–148.
Bennett, B.D., and Bolam, J.P. (1994). Synaptic input and output of parvalbumin-immunoreactive neurons in the neostriatum of the rat. Neuroscience 62, 707–719.
Bennett, B.D., and Wilson, C.J. (1998). Synaptic regulation of action potential timing in neostriatal cholinergic interneurons. Journal of Neuroscience 18, 8539–8549.
Bennett, B.D., and Wilson, C.J. (1999). Spontaneous activity of neostriatal cholinergic interneurons in vitro. The Journal of Neuroscience : the Official Journal of the Society for Neuroscience 19, 5586–5596.
Bennett, B.D., Callaway, J.C., and Wilson, C.J. (2000). Intrinsic membrane properties underlying spontaneous tonic firing in neostriatal cholinergic interneurons. The Journal of Neuroscience : the Official Journal of the Society for Neuroscience 20, 8493–8503.
Berke, J.D. (2008). Uncoordinated firing rate changes of striatal fast-spiking interneurons during behavioral task performance. Journal of Neuroscience 28, 10075–10080.
Bertran-Gonzalez, J., Hervé, D., Girault, J.-A., and Valjent, E. (2010). What is the Degree of Segregation between Striatonigral and Striatopallidal Projections? Frontiers in Neuroanatomy 4.
Bevan, M.D., Booth, P.A.C., Eaton, S.A., and Bolam, J.P. (1998). Selective Innervation of Neostriatal Interneurons by a Subclass of Neuron in the Globus Pallidus of the Rat. 19, 1–15.
Bliss, T.V., and Gardner-Medwin, A.R. (1973). Long-lasting potentiation of synaptic transmission in the dentate area of the unanaestetized rabbit following stimulation of the perforant path. J. Physiol. (Lond.) 232, 357–374.
Bliss, T.V., and Lomo, T. (1973). Long-Lasting Potentiation of Synaptic Transmission in Dentate Area of Anesthetized Rabbit Following Stimulation of Perforant Path. J. Physiol. (Lond.) 232, 331–356.
Blomeley, C., and Bracci, E. (2005). Excitatory effects of serotonin on rat striatal cholinergic interneurones. The Journal of Physiology 569, 715–721.
Blomeley, C., and Bracci, E. (2008). Substance P depolarizes striatal projection neurons and facilitates their glutamatergic inputs. The Journal of Physiology 586, 2143–2155.
Blomeley, C.P., and Bracci, E. (2009). Serotonin excites fast-spiking interneurons in the striatum. The European Journal of Neuroscience 29, 1604–1614.
Blomeley, C.P., Kehoe, L.A., and Bracci, E. (2009). Substance P mediates excitatory interactions between striatal projection neurons. The Journal of Neuroscience : the Official Journal of the Society for Neuroscience 29, 4953–4963.
Bolam, J.P., and Izzo, P.N. (1988). The postsynaptic targets of substance P-immunoreactive terminals in the rat neostriatum with particular reference to identified spiny striatonigral neurons. Experimental Brain Research Experimentelle Hirnforschung Expérimentation Cérébrale 70, 361–377.

Bolam, J.P., Hanley, J.J., Booth, P.A., and Bevan, M.D. (2000). Synaptic organisation of the basal ganglia. Journal of Anatomy 196 (Pt 4), 527–542.
Bolam, J.P., Ingham, C.A., Izzo, P.N., Levey, A.I., Rye, D.B., Smith, A.D., and Wainer, B.H. (1986). Substance P-containing terminals in synaptic contact with cholinergic neurons in the neostriatum and basal forebrain: a double immunocytochemical study in the rat. Brain Research 397, 279–289.
Bolam, J.P., Somogyi, P., Takagi, H., Fodor, I., and Smith, A.D. (1983). Localization of Substance P-Like Immunoreactivity in Neurons and Nerve-Terminals in the Neostriatum of the Rat - a Correlated Light and Electron-Microscopic Study. J. Neurocytol. 12, 325–344.
Bolam, J.P., Wainer, B.H., and Smith, A.D. (1984). Characterization of cholinergic neurons in the rat neostriatum. A combination of choline acetyltransferase immunocytochemistry, Golgi-impregnation and electron microscopy. Neuroscience 12, 711–718.
Bonner, T.I., Buckley, N.J., Young, A.C., and Brann, M.R. (1987). Identification of a family of muscarinic acetylcholine receptor genes. Science 237, 527–532.
Bonner, T.I., Young, A.C., Brann, M.R., and Buckley, N.J. (1988). Cloning and expression of the human and rat m5 muscarinic acetylcholine receptor genes. Neuron 1, 403–410.
Bonsi, P., Cuomo, D., Ding, J., Sciamanna, G., Ulrich, S., Tscherter, A., Bernardi, G., Surmeier, D.J., and Pisani, A. (2007). Endogenous Serotonin Excites Striatal Cholinergic Interneurons via the Activation of 5-HT 2C, 5-HT6, and 5-HT7 Serotonin Receptors: Implications for Extrapyramidal Side Effects of Serotonin Reuptake Inhibitors. Neuropsychopharmacology 32, 1840–1854.
Bracci, E., and Panzeri, S. (2006). Excitatory GABAergic effects in striatal projection neurons. Journal of Neurophysiology 95, 1285–1290.
Brown, T.G., and Sherrington, C.S. (1912). The rule of reflex response in the limb reflexes of the mammal and its exceptions. J. Physiol. (Lond.) 44, 125–130.
Bunney, B.S., and Aghajanian, G.K. (1976). The precise localization of nigral afferents in the rat as determined by a retrograde tracing technique. Brain Research 117, 423–435.
Butcher, S.H., Butcher, L.L., and Cho, A.K. (1976). Modulation of neostriatal acetylcholine in the rat by dopamine and 5-hydroxytryptamine afferents. Life Sci. 18, 733–743.
Cains, S., Blomeley, C.P., and Bracci, E. (2012). Serotonin inhibits low-threshold spike interneurons in the striatum. The Journal of Physiology 590, 2241–2252.
Calabresi, P., Centonze, D., Gubellini, P., Pisani, A., and Bernardi, G. (1998a). Blockade of M2-like muscarinic receptors enhances long-term potentiation at corticostriatal synapses. European Journal of Neuroscience 10, 3020–3023.
Calabresi, P., Centonze, D., Gubellini, P., Pisani, A., and Bernardi, G. (1998b). Endogenous ACh enhances striatal NMDA-responses via M1-like muscarinic receptors and PKC activation. European Journal of Neuroscience 10, 2887–2895.
Calabresi, P., Maj, R., Mercuri, N.B., and Bernardi, G. (1992a). Coactivation of D1 and D2 Dopamine-Receptors Is Required for Long-Term Synaptic Depression in the Striatum. Neuroscience Letters 142, 95–99.
Calabresi, P., Mercuri, N.B., Demurtas, M., and Bernardi, G. (1991). Involvement of Gaba Systems in Feedback-Regulation of Glutamate-Mediated and Gaba-Mediated Synaptic Potentials in Rat Neostriatum. J. Physiol. (Lond.) 440, 581–599.
Calabresi, P., Pisani, A., Mercuri, N.B., and Bernardi, G. (1992b). Long-term Potentiation in the Striatum is Unmasked by Removing the Voltage-dependent Magnesium Block of NMDA Receptor Channels. The European Journal of Neuroscience 4, 929–935.
Calabresi, P., Pisani, A., Mercuri, N.B., and Bernardi, G. (1996). The corticostriatal projection: from synaptic plasticity to dysfunctions of the basal ganglia. Trends in Neurosciences 19, 19–24.
Cardin, J.A., Carlén, M., Meletis, K., Knoblich, U., Zhang, F., Deisseroth, K., Tsai, L.-H., and

Moore, C.I. (2009). Driving fast-spiking cells induces gamma rhythm and controls sensory responses. Nature 459, 663–667.
Carman, J.B., Cowan, R.L., Powell, T.P., and Webster, K.E. (1965). A Bilateral Cortico-Striate Projection. J. Neurol. Neurosurg. Psychiatr. 28, 71–77.
Castellucci, V., Pinsker, H., Kupfermann, I., and Kandel, E.R. (1970). Neuronal mechanisms of habituation and dishabituation of the gill-withdrawal reflex in Aplysia. Science 167, 1745–1748.
Chang, H.T., Wilson, C.J., and Kitai, S.T. (1982). A Golgi-Study of Rat Neostriatal Neurons - Light Microscopic Analysis. J. Comp. Neurol. 208, 107–126.
Charpier, S., and Deniau, J.M. (1997). In vivo activity-dependent plasticity at cortico-striatal connections: Evidence for physiological long-term potentiation. Proceedings of the National Academy of Sciences of the United States of America 94, 7036–7040.
Chesselet, M.F., and Graybiel, A.M. (1986). Striatal neurons expressing somatostatin-like immunoreactivity: evidence for a peptidergic interneuronal system in the cat. Nsc 17, 547–571.
Christie, J.M., Chiu, D.N., and Jahr, C.E. (2011). Ca(2+)-dependent enhancement of release by subthreshold somatic depolarization. Nature Neuroscience 14, 62–68.
Chuhma, N., Mingote, S., Moore, H., and Rayport, S. (2014). Dopamine Neurons Control Striatal Cholinergic Neurons via Regionally Heterogeneous Dopamine and Glutamate Signaling. Neuron 81, 901–912.
Chuhma, N., Tanaka, K.F., Hen, R., and Rayport, S. (2011). Functional Connectome of the Striatal Medium Spiny Neuron. The Journal of Neuroscience : the Official Journal of the Society for Neuroscience 31, 1183–1192.
Cowan, R.L., Wilson, C.J., Emson, P.C., and Heizmann, C.W. (1990). Parvalbumin-containing GABAergic interneurons in the rat neostriatum. The Journal of Comparative Neurology 302, 197–205.
Crick, F. (1995). Astonishing Hypothesis: The Scientific Search for the Soul - Francis Crick - Google Books.
Cui, G., Jun, S.B., Jin, X., Pham, M.D., Vogel, S.S., Lovinger, D.M., and Costa, R.M. (2013). Concurrent activation of striatal direct and indirect pathways during action initiation. Nature 494, 238–242.
Czubayko, U., and Plenz, D. (2002). Fast synaptic transmission between striatal spiny projection neurons. Proceedings of the National Academy of Sciences of the United States of America 99, 15764–15769.
Dawson, T.M., Bredt, D.S., Fotuhi, M., Hwang, P.M., and Snyder, S.H. (1991). Nitric oxide synthase and neuronal NADPH diaphorase are identical in brain and peripheral tissues. Proceedings of the National Academy of Sciences of the United States of America 88, 7797–7801.
Deisseroth, K., Feng, G., Majewska, A.K., Miesenböck, G., Ting, A., and Schnitzer, M.J. (2006). Next-generation optical technologies for illuminating genetically targeted brain circuits. Journal of Neuroscience 26, 10380–10386.
Deng, P., Zhang, Y., and Xu, Z.C. (2007). Involvement of I(h) in dopamine modulation of tonic firing in striatal cholinergic interneurons. The Journal of Neuroscience : the Official Journal of the Society for Neuroscience 27, 3148–3156.
Descarries, L., Gisiger, V., and Steriade, M. (1997). Diffuse transmission by acetylcholine in the CNS. Progress in Neurobiology 53, 603–625.
Di Matteo, V., Di Giovanni, G., Pierucci, M., and Esposito, E. (2008a). Serotonin control of central dopaminergic function: focus on in vivo microdialysis studies. Progress in Brain Research 172, 7–44.
Di Matteo, V., Pierucci, M., Esposito, E., Crescimanno, G., Benigno, A., and Di Giovanni, G. (2008b). Serotonin modulation of the basal ganglia circuitry: therapeutic implication for Parkinson's disease and other motor disorders. Progress in Brain Research 172, 423–463.

DiFiglia, M., and Aronin, N. (1982). Ultrastructural features of immunoreactive somatostatin neurons in the rat caudate nucleus. Journal of Neuroscience 2, 1267–1274.
DiFiglia, M., Aronin, N., and Martin, J.B. (1982). Light and Electron-Microscopic Localization of Immunoreactive Leu-Enkephalin in the Monkey Basal Ganglia. Journal of Neuroscience 2, 303–320.
Ding, J.B., Guzman, J.N., Peterson, J.D., Goldberg, J.A., and Surmeier, D.J. (2010). Thalamic Gating of Corticostriatal Signaling by Cholinergic Interneurons. Neuron 67, 294–307.
Dubach, M., Schmidt, R., Kunkel, D., Bowden, D.M., Martin, R., and German, D.C. (1987). Primate Neostriatal Neurons Containing Tyrosine-Hydroxylase - Immunohistochemical Evidence. Neuroscience Letters 75, 205–210.
Edelman, G.M. (1993). Neural Darwinism: selection and reentrant signaling in higher brain function. Neuron 10, 115–125.
Edelman, G.M. (2006). The embodiment of mind. Daedalus 135, 23–32.
Engel, A.K., Fries, P., and Singer, W. (2001). Dynamic predictions: oscillations and synchrony in top-down processing. Nature Reviews Neuroscience 2, 704–716.
Engel, A.K., König, P., Gray, C.M., and Singer, W. (1990). Stimulus-Dependent Neuronal Oscillations in Cat Visual Cortex: Inter-Columnar Interaction as Determined by Cross-Correlation Analysis. The European Journal of Neuroscience 2, 588–606.
English, D.F., Ibanez-Sandoval, O., Stark, E., Tecuapetla, F., Buzsáki, G., Deisseroth, K., Tepper, J.M., and Koos, T. (2012). GABAergic circuits mediate the reinforcement-related signals of striatal cholinergic interneurons. Nature Publishing Group 15, 123–130.
Farries, M.A., and Perkel, D.J. (2000). Electrophysiological properties of avian basal ganglia neurons recorded in vitro. Journal of Neurophysiology 84, 2502–2513.
Figueredo-Cardenas, G., Medina, L., and Reiner, A. (1996a). Calretinin is largely localized to a unique population of striatal interneurons in rats. Brain Research 709, 145–150.
Figueredo-Cardenas, G., Morello, M., and Sancesario, G. (1996b). Colocalization of somatostatin, neuropeptide Y, neuronal nitric oxide synthase and NADPH-diaphorase in striatal interneurons in rats. Brain Research.
Fino, E., Paille, V., Deniau, J.M., and Venance, L. (2009). Asymmetric spike-timing dependent plasticity of striatal nitric oxide-synthase interneurons. Neuroscience 160, 744–754.
Fino, E., Deniau, J.-M., and Venance, L. (2008). Cell-specific spike-timing-dependent plasticity in GABAergic and cholinergic interneurons in corticostriatal rat brain slices. The Journal of Physiology 586, 265–282.
Flores-Barrera, E., Vizcarra-Chacón, B.J., Tapia, D., Bargas, J., and Galarraga, E. (2010). Different corticostriatal integration in spiny projection neurons from direct and indirect pathways. Frontiers in Systems Neuroscience 41, 457–462.
Frank, M.J. (2004). By Carrot or by Stick: Cognitive Reinforcement Learning in Parkinsonism. Science (New York, NY) 306, 1940–1943.
Fujiyama, F., Sohn, J., Nakano, T., Furuta, T., Nakamura, K.C., Matsuda, W., and Kaneko, T. (2011). Exclusive and common targets of neostriatofugal projections of rat striosome neurons: a single neuron-tracing study using a viral vector. European Journal of Neuroscience 33, 668–677.
Galarraga, E., Hernández-López, S., Tapia, D., Reyes, A., and Bargas, J. (1999). Action of substance P (neurokinin-1) receptor activation on rat neostriatal projection neurons. Synapse (New York, NY) 33, 26–35.
Galarreta, M., and Hestrin, S. (2001). Electrical synapses between Gaba-Releasing interneurons. Nature Reviews Neuroscience 2, 425–433.
Gerfen, C.R. (1991). Substance P (neurokinin-1) receptor mRNA is selectively expressed in cholinergic neurons in the striatum and basal forebrain. Brain Research 556, 165–170.
Gerfen, C.R., and Wilson, C.J. (1996). Gerfen: Chapter II The basal ganglia. Handbook of

Chemical Neuroanatomy.
Gerfen, C.R. (2003). D1 dopamine receptor supersensitivity in the dopamine-depleted striatum animal model of Parkinson's disease. The Neuroscientist : a Review Journal Bringing Neurobiology, Neurology and Psychiatry 9, 455–462.
Gerfen, C.R., and Surmeier, D.J. (2011). Modulation of Striatal Projection Systems by Dopamine. Annual Review of Neuroscience 34, 441–466.
Gérard, C., Martres, M.P., Lefèvre, K., Miquel, M.C., Vergé, D., Lanfumey, L., Doucet, E., Hamon, M., and Mestikawy, el, S. (1997). Immuno-localization of serotonin 5-HT6 receptor-like material in the rat central nervous system. Brain Research 746, 207–219.
Gibson, J.R., Beierlein, M., and Connors, B.W. (2005). Functional properties of electrical synapses between inhibitory interneurons of neocortical layer 4. Journal of Neurophysiology 93, 467–480.
Gittis, A.H., Nelson, A.B., Thwin, M.T., Palop, J.J., and Kreitzer, A.C. (2010). Distinct Roles of GABAergic Interneurons in the Regulation of Striatal Output Pathways. The Journal of Neuroscience : the Official Journal of the Society for Neuroscience 30, 2223–2234.
Govindaiah, G., Wang, Y., and Cox, C.L. (2010). Substance P selectively modulates GABA(A) receptor-mediated synaptic transmission in striatal cholinergic interneurons. Neuropharmacology 58, 413–422.
Gras, C., Amilhon, B., Lepicard, E.M., Poirel, O., Vinatier, J., Herbin, M., Dumas, S., Tzavara, E.T., Wade, M.R., Nomikos, G.G., et al. (2008). The vesicular glutamate transporter VGLUT3 synergizes striatal acetylcholine tone. Nature Neuroscience 11, 292–300.
Gras, C., Herzog, E., Bellenchi, G.C., Bernard, V., Ravassard, P., Pohl, M., Gasnier, B., Giros, B., and Mestikawy, El, S. (2002). A third vesicular glutamate transporter expressed by cholinergic and serotoninergic neurons. The Journal of Neuroscience : the Official Journal of the Society for Neuroscience 22, 5442–5451.
Graveland, G.A., and DiFiglia, M. (1985). The frequency and distribution of medium-sized neurons with indented nuclei in the primate and rodent neostriatum. Brain Research 327, 307–311.
Grofová, I. (1979). Extrinsic Connections of the Neostriatum (Pergamon Press Ltd).
Groves, P.M. (1983). A theory of the functional organization of the neostriatum and the neostriatal control of voluntary movement. Brain Research 286, 109–132.
Haber, S. (2008). Parallel and integrative processing through the Basal Ganglia reward circuit: lessons from addiction. Biological Psychiatry 64, 173–174.
Hamon, M., Doucet, E., Lefèvre, K., Miquel, M.C., Lanfumey, L., Insausti, R., Frechilla, D., Del Rio, J., and Vergé, D. (1999). Antibodies and antisense oligonucleotide for probing the distribution and putative functions of central 5-HT6 receptors. Neuropsychopharmacology 21, 68S–76S.
Hartline, D.K., and Maynard, D.M. (1975). Motor patterns in the stomatogastric ganglion of the lobster Panulirus argus. J. Exp. Biol. 62, 405–420.
Heintz, N. (2001). BAC to the future: the use of bac transgenic mice for neuroscience research. Nature Reviews Neuroscience 2, 861–870.
Higley, M.J., Gittis, A.H., Oldenburg, I.A., Balthasar, N., Seal, R.P., Edwards, R.H., Lowell, B.B., Kreitzer, A.C., and Sabatini, B.L. (2011). Cholinergic interneurons mediate fast VGluT3-dependent glutamatergic transmission in the striatum. PLoS ONE 6, e19155.
Hill, J.A., Zoli, M., Bourgeois, J.P., and Changeux, J.P. (1993). Immunocytochemical localization of a neuronal nicotinic receptor: the beta 2-subunit. The Journal of Neuroscience : the Official Journal of the Society for Neuroscience 13, 1551–1568.
Hippenmeyer, S., Vrieseling, E., Sigrist, M., Portmann, T., Laengle, C., Ladle, D.R., and Arber, S. (2005). A developmental switch in the response of DRG neurons to ETS transcription factor signaling. PLoS Biology 3, e159.

Hjorth, J., Blackwell, K.T., and Kotaleski, J.H. (2009). Gap Junctions between Striatal Fast-Spiking Interneurons Regulate Spiking Activity and Synchronization as a Function of Cortical Activity. Journal of Neuroscience 29, 5276–5286.
Hodgkin, A.L., and Huxley, A.F. (1952). Currents carried by sodium and potassium ions through the membrane of the giant axon of Loligo. J. Physiol. (Lond.) 116, 449–472.
Hokfelt, T., and U, U. (1969). Electron and Fluorescence Microscopical Studies on Nucleus Caudatus Putamen of Rat After Unilateral Lesions of Ascending Nigro-Neostriatal Dopamine Neurons. Acta Physiol Scand 76, 415–&.
Hokfelt, T., Kellerth, J.O., Nilsson, G., and Pernow, B. (1975). Substance-P - Localization in Central Nervous-System and in Some Primary Sensory Neurons. Science 190, 889–890.
Horikawa, K., and Armstrong, W.E. (1988). A versatile means of intracellular labeling: injection of biocytin and its detection with avidin conjugates. Journal of Neuroscience Methods 25, 1–11.
Hoyer, D., Hannon, J.P., and Martin, G.R. (2002). Molecular, pharmacological and functional diversity of 5-HT receptors. Pharmacol. Biochem. Behav. 71, 533–554.
Hsu, J.-W., Lee, L.-C., Chen, R.-F., Yen, C.-T., Chen, Y.-S., and Tsai, M.-L. (2010). Striatal volume changes in a rat model of childhood attention-deficit/hyperactivity disorder. Psychiatry Research 179, 338–341.
Hubel, D.H., and Wiesel, T.N. (1968). Receptive fields and functional architecture of monkey striate cortex. J. Physiol. (Lond.) 195, 215–243.
Huot, P., and Parent, A. (2007). Dopaminergic neurons intrinsic to the striatum. Journal of Neurochemistry 101, 1441–1447.
ibanez-Sandoval, O., Xenias, H.S., Koós, T., and Tepper, J.M. (2013). Dopamine-dependent plateau potentials and subthreshold oscillations in striatal TH interneurons (Program No. 648.06. Neuroscience 2013 Abstracts[San Diego, CA]: Society for Neuroscience, 2013. Online).
Ibanez-Sandoval, O., Tecuapetla, F., Unal, B., Shah, F., Koos, T., and Tepper, J.M. (2010). Electrophysiological and morphological characteristics and synaptic connectivity of tyrosine hydroxylase-expressing neurons in adult mouse striatum. The Journal of Neuroscience : the Official Journal of the Society for Neuroscience 30, 6999–7016.
Ibanez-Sandoval, O., Tecuapetla, F., Unal, B., Shah, F., Koos, T., and Tepper, J.M. (2011). A novel functionally distinct subtype of striatal neuropeptide Y interneuron. The Journal of Neuroscience : the Official Journal of the Society for Neuroscience 31, 16757–16769.
Isoda, M., and Hikosaka, O. (2008). Role for subthalamic nucleus neurons in switching from automatic to controlled eye movement. The Journal of Neuroscience : the Official Journal of the Society for Neuroscience 28, 7209–7218.
Izzo, P.N., Graybiel, A.M., and Bolam, J.P. (1987). Characterization of substance P- and [Met] enkephalin-immunoreactive neurons in the caudate nucleus of cat and ferret by a single section Golgi procedure. Nsc 20, 577–587.
Jacobowitz, D.M., and Winsky, L. (1991). Immunocytochemical localization of calretinin in the forebrain of the rat. The Journal of Comparative Neurology 304, 198–218.
Jaeger, D., Kita, H., and Wilson, C.J. (1994). Surround inhibition among projection neurons is weak or nonexistent in the rat neostriatum | Journal of Neurophysiology. Journal of Neurophysiology 72, 2555–2558.
Jakab, R.L., and Goldman-Rakic, P. (1996). Presynaptic and postsynaptic subcellular localization of substance P receptor immunoreactivity in the neostriatum of the rat and rhesus monkey (Macaca mulatta). The Journal of Comparative Neurology 369, 125–136.
Jones, E.G., and Leavitt, R.Y. (1974). Retrograde axonal transport and the demonstration of non-specific projections to the cerebral cortex and striatum from thalamic intralaminar nuclei in the rat, cat and monkey. The Journal of Comparative Neurology 154, 349–377.
Jones, E.G., Coulter, J.D., Burton, H., and Porter, R. (1977). Cells of origin and terminal distru-

bution of corticostriatal fibers arising in the sensory-motor cortex of monkeys. The Journal of Comparative Neurology 173, 53–80.
Jones, S., Sudweeks, S., and Yakel, J.L. (1999). Nicotinic receptors in the brain: correlating physiology with function. Trends in Neurosciences 22, 555–561.
Joshua, M., Adler, A., Mitelman, R., Vaadia, E., and Bergman, H. (2008). Midbrain dopaminergic neurons and striatal cholinergic interneurons encode the difference between reward and aversive events at different epochs of probabilistic classical conditioning trials. The Journal of Neuroscience : the Official Journal of the Society for Neuroscience 28, 11673–11684.
Kaneko, T., Shigemoto, R., Nakanishi, S., and Mizuno, N. (1993). Substance P receptor-immunoreactive neurons in the rat neostriatum are segregated into somatostatinergic and cholinergic aspiny neurons. Brain Research 631, 297–303.
Karagiannis, A., Gallopin, T., Dávid, C., Battaglia, D., Geoffroy, H., Rossier, J., Hillman, E.M.C., Staiger, J.F., and Cauli, B. (2009). Classification of NPY-Expressing Neocortical Interneurons. Journal of Neuroscience 29, 3642–3659.
Karayannis, T., Elfant, D., Huerta-Ocampo, I., Teki, S., Scott, R.S., Rusakov, D.A., Jones, M.V., and Capogna, M. (2010). Slow GABA Transient and Receptor Desensitization Shape Synaptic Responses Evoked by Hippocampal Neurogliaform Cells. Journal of Neuroscience 30, 9898–9909.
Kasanetz, F., Riquelme, L.A., and Murer, M.G. (2002). Disruption of the two-state membrane potential of striatal neurones during cortical desynchronisation in anaesthetised rats. The Journal of Physiology 543, 577–589.
Katz, B., and Miledi, R. (1967). A study of synaptic transmission in the absence of nerve impulses. The Journal of Physiology 192, 407–436.
Katz, B., and Miledi, R. (1968). Role of Calcium in Neuromuscular Facilitation. J. Physiol. (Lond.) 195, 481–&.
Katz, B., and Miledi, R. (1970). Further study of the role of calcium in synaptic transmission. The Journal of Physiology 207, 789–801.
Kauffman, S. (2012). Answering descartes: beyond Turing. IN COOPER, SB & HODGES, a.(Eds.) the Once and Future Turing: Computing the World.
Kawaguchi, Y. (1993). Physiological, morphological, and histochemical characterization of three classes of interneurons in rat neostriatum. Journal of Neuroscience 13, 4908–4923.
Kawaguchi, Y. (1997). GABAergic cell subtypes and their synaptic connections in rat frontal cortex. Cerebral Cortex 7, 476–486.
Kawaguchi, Y., Wilson, C.J., and Emson, P.C. (1990). Projection subtypes of rat neostriatal matrix cells revealed by intracellular injection of biocytin. The Journal of Neuroscience : the Official Journal of the Society for Neuroscience 10, 3421–3438.
Kemp, J.M., and Powell, T.P. (1970). Cortico-Striate Projection in Monkey. Brain 93, 525–&.
Kimmel, C.B., Powell, S.L., and Metcalfe, W.K. (1982). Brain neurons which project to the spinal cord in young larvae of the zebrafish. J. Comp. Neurol. 205, 112–127.
Kimura, M., Rajkowski, J., and Evarts, E. (1984). Tonically Discharging Putamen Neurons Exhibit Set-Dependent Responses. Proceedings of the National Academy of Sciences of the United States of America-Biological Sciences 81, 4998–5001.
Kincaid, A.E., Zheng, T., and Wilson, C.J. (1998). Connectivity and convergence of single corticostriatal axons. Journal of Neuroscience 18, 4722–4731.
Kincaid, A.E., and Wilson, C.J. (1996). Corticostriatal innervation of the patch and matrix in the rat neostriatum. The Journal of Comparative Neurology 374, 578–592.
Kita, H., and Armstrong, W. (1991). A biotin-containing compound N-(2-aminoethyl)biotinamide for intracellular labeling and neuronal tracing studies: comparison with biocytin. Journal of Neuroscience Methods 37, 141–150.

Kita, H., and Kitai, S.T. (1988). Glutamate-Decarboxylase Immunoreactive Neurons in Rat Neostriatum - Their Morphological Types and Populations. Brain Research 447, 346–352.
Kita, H., and Kitai, S.T. (1994). The Morphology of Globus-Pallidus Projection Neurons in the Rat - an Intracellular Staining Study. Brain Research 636, 308–319.
Kita, H., Kita, T., and Kitai, S.T. (1985). Active membrane properties of rat neostriatal neurons in an in vitro slice preparation. Exp Brain Res 60, 54–62.
Kita, H., Kosaka, T., and Heizmann, C.W. (1990). Parvalbumin-immunoreactive neurons in the rat neostriatum: a light and electron microscopic study. Brain Research 536, 1–15.
Kita, T., Kita, H., and Kitai, S.T. (1984). Passive electrical membrane properties of rat neostriatal neurons in an in vitro slice preparation. Brain Research 300, 129–139.
Kitai, S.T., and Wilson, C.J. (1982). Kitai: Intracellular labeling of neurons in mammalian brain - Google Scholar. Cytochemical Methods in ….
Klaus, A., Planert, H., Hjorth, J.J.J., Berke, J.D., Silberberg, G., and Kotaleski, J.H. (2011). Striatal fast-spiking interneurons: from firing patterns to postsynaptic impact. Frontiers in Systems Neuroscience 5, 57.
Klausberger, T., Magill, P.J., Márton, L.F., Roberts, J.D.B., Cobden, P.M., Buzsáki, G., and Somogyi, P. (2003). Brain-state- and cell-type-specific firing of hippocampal interneurons in vivo. Nature 421, 844–848.
Knook, H.L. (1965). Knook: The Fibre Connections of the Forebrain, 477 pp - Google Scholar. Assen: Thesis.
Koob, G.F., and Volkow, N.D. (2010). Neurocircuitry of addiction. Neuropsychopharmacology 35, 217–238.
Koos, T., and Tepper, J.M. (2002). Dual cholinergic control of fast-spiking interneurons in the neostriatum. The Journal of Neuroscience : the Official Journal of the Society for Neuroscience 22, 529–535.
Koos, T., Tepper, J.M., and Wilson, C.J. (2004). Comparison of IPSCs evoked by spiny and fast-spiking neurons in the neostriatum. The Journal of Neuroscience : the Official Journal of the Society for Neuroscience 24, 7916–7922.
Koós, T., and Tepper, J.M. (1999). Inhibitory control of neostriatal projection neurons by GABAergic interneurons. Nature Neuroscience 2, 467–472.
Kravitz, A.V., Freeze, B.S., Parker, P.R.L., Kay, K., Thwin, M.T., Deisseroth, K., and Kreitzer, A.C. (2010). Regulation of parkinsonian motor behaviours by optogenetic control of basal ganglia circuitry. Nature 466, 622–626.
Kress, G.J., Yamawaki, N., Wokosin, D.L., Wickersham, I.R., Shepherd, G.M.G., and Surmeier, D.J. (2013). Convergent cortical innervation of striatal projection neurons. Nature Neuroscience 16, 665–667.
Kubo, T., Fukuda, K., Mikami, A., Maeda, A., Takahashi, H., Mishina, M., Haga, K., Ichiyama, A., Kangawa, K., Kojima, M., et al. (1986). Cloning, Sequencing and Expression of Complementary-Dna Encoding the Muscarinic Acetylcholine-Receptor. Nature 323, 411–416.
Kubota, Y., and Kawaguchi, Y. (2000). Dependence of GABAergic synaptic areas on the interneuron type and target size. The Journal of Neuroscience : the Official Journal of the Society for Neuroscience 20, 375–386.
Kubota, Y., Mikawa, S., and Kawaguchi, Y. (1993). Neostriatal GABAergic interneurones contain NOS, calretinin or parvalbumin. Neuroreport 5, 205–208.
Kunzle, H. (1975). Bilateral Projections From Precentral Motor Cortex to Putamen and Other Parts of Basal Ganglia - Autoradiographic Study in Macaca-Fascicularis. Brain Research 88, 195–209.
Kunzle, H. (1977). Projections from the primary somatosensory cortex to basal ganglia and thalamus in the monkey. Exp Brain Res 30, 481–492.

Lapper, S.R., and Bolam, J.P. (1992). Input from the frontal cortex and the parafascicular nucleus to cholinergic interneurons in the dorsal striatum of the rat. Nsc 51, 533–545.
Lavoie, B., and Parent, A. (1990). Immunohistochemical study of the serotoninergic innervation of the basal ganglia in the squirrel monkey. The Journal of Comparative Neurology 299, 1–16.
Leblois, A., Boraud, T., Meissner, W., Bergman, H., and Hansel, D. (2006). Competition between feedback loops underlies normal and pathological dynamics in the basal ganglia. The Journal of Neuroscience : the Official Journal of the Society for Neuroscience 26, 3567–3583.
Lee, K., Dixon, A.K., Freeman, T.C., and Richardson, P.J. (1998). Identification of an ATP-sensitive potassium channel current in rat striatal cholinergic interneurones. J. Physiol. (Lond.) 510, 441–453.
Lee, S., Hjerling-Leffler, J., Zagha, E., Fishell, G., and Rudy, B. (2010). The Largest Group of Superficial Neocortical GABAergic Interneurons Expresses Ionotropic Serotonin Receptors. Journal of Neuroscience 30, 16796–16808.
Lemoine, C., Tison, F., and Bloch, B. (1990). D2-Dopamine Receptor Gene-Expression by Cholinergic Neurons in the Rat Striatum. Neuroscience Letters 117, 248–252.
Liu, J.C., DeFazio, R.A., Espinosa-Jeffrey, A., Cepeda, C., de Vellis, J., and Levine, M.S. (2004). Calcium modulates dopamine potentiation of N-methyl-D-aspartate responses: electrophysiological and imaging evidence. Journal of Neuroscience Research 76, 315–322.
Logie, C., Bagetta, V., and Bracci, E. (2013). Presynaptic control of corticostriatal synapses by endogenous GABA. The Journal of Neuroscience : the Official Journal of the Society for Neuroscience 33, 15425–15431.
Luk, K.C., and Sadikot, A.F. (2001). GABA promotes survival but not proliferation of parvalbumin-immunoreactive interneurons in rodent neostriatum: an in vivo study with stereology. Neuroscience 104, 93–103.
Luo, R., Janssen, M.J., Partridge, J.G., and Vicini, S. (2013). Direct and GABA-mediated indirect effects of nicotinic ACh receptor agonists on striatal neurones. The Journal of Physiology 591, 203–217.
Mahon, S., Vautrelle, N., Pezard, L., Slaght, S.J., Deniau, J.-M., Chouvet, G., and Charpier, S. (2006). Distinct patterns of striatal medium spiny neuron activity during the natural sleep-wake cycle. Journal of Neuroscience 26, 12587–12595.
Malach, R., and Graybiel, A.M. (1986). Mosaic Architecture of the Somatic Sensory-Recipient Sector of the Cats Striatum. Journal of Neuroscience 6, 3436–3458.
Malenka, R.C., and Kocsis, J.D. (1988). Presynaptic actions of carbachol and adenosine on corticostriatal synaptic transmission studied in vitro. Journal of Neuroscience 8, 3750–3756.
Mallet, N., Le Moine, C., Charpier, S., and Gonon, F. (2005). Feedforward Inhibition of Projection Neurons by Fast-Spiking GABA Interneurons in the Rat Striatum In Vivo. The Journal of Neuroscience : the Official Journal of the Society for Neuroscience 25, 3857–3869.
Mallet, N., Micklem, B.R., Henny, P., Brown, M.T., Williams, C., Bolam, J.P., Nakamura, K.C., and Magill, P.J. (2012). Dichotomous organization of the external globus pallidus. Neuron 74, 1075–1086.
Mallet, N., Pogosyan, A., Márton, L.F., Bolam, J.P., Brown, P., and Magill, P.J. (2008). Parkinsonian beta oscillations in the external globus pallidus and their relationship with subthalamic nucleus activity. The Journal of Neuroscience : the Official Journal of the Society for Neuroscience 28, 14245–14258.
Mancilla, J.G., Lewis, T.J., Pinto, D.J., Rinzel, J., and Connors, B.W. (2007). Synchronization of electrically coupled pairs of inhibitory interneurons in neocortex. The Journal of Neuroscience : the Official Journal of the Society for Neuroscience 27, 2058–2073.
Mansari, el, M., and Blier, P. (1997). In vivo electrophysiological characterization of 5-HT re-

ceptors in the guinea pig head of caudate nucleus and orbitofrontal cortex. Neuropharmacology 36, 577–588.
Markram, H., Toledo-Rodriguez, M., Wang, Y., Gupta, A., Silberberg, G., and Wu, C.Z. (2004). Interneurons of the neocortical inhibitory system. Nature Reviews Neuroscience 5, 793–807.
Maynard, D.M., and Walton, K.D. (1975). Effects of maintained depolarization of presynaptic neurons on inhibitory transmission in lobster neuropil. Journal of Comparative Physiology ? A 97, 215–243.
McClellan, A.D., and Grillner, S. (1984). Activation of "fictive swimming" by electrical microstimulation of brainstem locomotor regions in an in vitro preparation of the lamprey central nervous system. Brain Research 300, 357–361.
McDowell, J.J. (2010). Behavioral and neural Darwinism: selectionist function and mechanism in adaptive behavior dynamics. Behavioural Processes 84, 358–365.
Middleton, F.A., and Strick, P.L. (2000). Basal ganglia and cerebellar loops: motor and cognitive circuits. Brain Research Brain Research Reviews 31, 236–250.
Milner, P.M. (1974). A model for visual shape recognition. Psychological Review 81, 521–535.
Mink, J.W. (2001). Basal ganglia dysfunction in Tourette's syndrome: a new hypothesis. Pediatric Neurology 25, 190–198.
Morris, G., Arkadir, D., Nevet, A., Vaadia, E., and Bergman, H. (2004). Coincident but Distinct Messages of Midbrain Dopamine and Striatal Tonically Active Neurons. Neuron 43, 133–143.
Nambu, A., Tokuno, H., Hamada, I., Kita, H., Imanishi, M., Akazawa, T., Ikeuchi, Y., and Hasegawa, N. (2000). Excitatory cortical inputs to pallidal neurons via the subthalamic nucleus in the monkey. Journal of Neurophysiology 84, 289–300.
Nambu, A. (2008). Seven problems on the basal ganglia. Current Opinion in Neurobiology 1–10.
Nambu, A., Tokuno, H., and Takada, M. (2002). Functional significance of the cortico-subthalamo-pallidal "hyperdirect" pathway. Neuroscience Research 43, 111–117.
Nelson, A.B., Hammack, N., Yang, C.F., Shah, N.M., Seal, R.P., and Kreitzer, A.C. (2014). Striatal Cholinergic Interneurons Drive GABA Release from Dopamine Terminals. Neuron.
Neve, K.A., and Neve, R.L. (1997). Molecular Biology of Dopamine Receptors. In The Dopamine Receptors
, (Totowa, NJ: Humana Press), pp. 27–76.
Neve, K.A., Seamans, J.K., and Trantham-Davidson, H. (2004). Dopamine Receptor Signaling. Journal of Receptors ….
Nisenbaum, E.S., Berger, T.W., and Grace, A.A. (1993). Depression of glutamatergic and GABAergic synaptic responses in striatal spiny neurons by stimulation of presynaptic GABAB receptors. Synapse 14, 221–242.
Olson, S. (2004). Neurobiology. Making sense of Tourette's. Science (New York, NY) 305, 1390–1392.
Oorschot, D. (2013). The percentage of interneurons in the dorsal striatum of the rat, cat, monkey and human: a critique of the evidence. Basal Ganglia.
Oorschot, D.E. (1996). Total number of neurons in the neostriatal, pallidal, subthalamic, and substantia nigral nuclei of the rat basal ganglia: a stereological study using the cavalieri and optical disector methods. The Journal of Comparative Neurology 366, 580–599.
Oorschot, D.E., Zhang, R., and Wickens, J.R. (1999). Absolute number and three-dimensional spatial distribution of rat neostriatal large interneurons: a first and second order stereological study. Proc Xth Int Congr Stereol.
Oswald, M.J., Oorschot, D.E., Schulz, J.M., Lipski, J., and Reynolds, J.N.J. (2009). IH current generates the afterhyperpolarisation following activation of subthreshold cortical synaptic inputs to striatal cholinergic interneurons. The Journal of Physiology 587, 5879–5897.

Pakhotin, P., and Bracci, E. (2007). Cholinergic interneurons control the excitatory input to the striatum. The Journal of Neuroscience : the Official Journal of the Society for Neuroscience 27, 391–400.
Park, M.R., Lighthall, J.W., and Kitai, S.T. (1980). Recurrent Inhibition in the Rat Neostriatum. Brain Research 194, 359–369.
Penney, J.B., and Young, A.B. (1986). Striatal inhomogeneities and basal ganglia function. Movement Disorders : Official Journal of the Movement Disorder Society 1, 3–15.
Peralta, E.G., Ashkenazi, A., Winslow, J.W., Smith, D.H., Ramachandran, J., and Capon, D.J. (1987). Distinct Primary Structures, Ligand-Binding Properties and Tissue-Specific Expression of 4 Human Muscarinic Acetylcholine-Receptors. Embo J. 6, 3923–3929.
Phelps, P.E., and Vaughn, J.E. (1986). Immunocytochemical Localization of Choline-Acetyltransferase in Rat Ventral Striatum - a Light and Electron-Microscopic Study. J. Neurocytol. 15, 595–617.
Phelps, P.E., Houser, C.R., and Vaughn, J.E. (1985). Immunocytochemical Localization of Choline-Acetyltransferase Within the Rat Neostriatum - a Correlated Light and Electron-Microscopic Study of Cholinergic Neurons and Synapses. J. Comp. Neurol. 238, 286–307.
Pickel, V.M., Sumal, K.K., Beckley, S.C., Miller, R.J., and Reis, D.J. (1980). Immunocytochemical localization of enkephalin in the neostriatum of rat brain: A light and electron microscopic study. The Journal of Comparative Neurology 189, 721–740.
Planert, H., Berger, T.K., and Silberberg, G. (2013). Membrane properties of striatal direct and indirect pathway neurons in mouse and rat slices and their modulation by dopamine. PLoS ONE 8, e57054.
Plenz, D., Wickens, J., and Kitai, S.T. (1996). Basal ganglia control of sequential activityin the cerebral cortex: a model. Computational Neuroscience.
Povysheva, N.V., Zaitsev, A.V., Kroner, S., Krimer, O.A., Rotaru, D.C., Gonzalez-Burgos, G., Lewis, D.A., and Krimer, L.S. (2007). Electrophysiological differences between neurogliaform cells from monkey and rat prefrontal cortex. Journal of Neurophysiology 97, 1030–1039.
Quinn, W.G., Harris, W.A., and Benzer, S. (1974). Conditioned behavior in Drosophila melanogaster. Proceedings of the National Academy of Sciences of the United States of America 71, 708–712.
Raz, A., Feingold, A., Zelanskaya, V., Vaadia, E., and Bergman, H. (1996). Neuronal synchronization of tonically active neurons in the striatum of normal and parkinsonian primates. Journal of Neurophysiology 76, 2083–2088.
Reig, R., and Silberberg, G. (2012). Bilateral and multisensory integration in striatal microcircuits (Program No. 380.11. 2012 Neuroscience Meeting Planner. New Orleans, LA: Society for Neuroscience, 2012. Online).
Reiner, A., and Anderson, K.D. (1990). The patterns of neurotransmitter and neuropeptide cooccurrence among striatal projection neurons: conclusions based on recent findings. Brain Research Brain Research Reviews 15, 251–265.
Revonsuo, A., and Newman, J. (1999). Binding and consciousness. Conscious Cogn 8, 123–127.
Ribak, C.E., Vaughn, J.E., and Roberts, E. (1979). The GABA neurons and their axon terminals in rat corpus striatum as demonstrated by GAD immunocytochemistry. The Journal of Comparative Neurology 187, 261–283.
Ritter, J.K., Gehlert, D.R., Gibb, J.W., Wamsley, J.K., and Hanson, G.R. (1985). Neuronal localization of substance P receptors in rat neostriatum. European Journal of Pharmacology 109, 431–432.
Rudy, B., Fishell, G., Lee, S., and Hjerling-Leffler, J. (2011). Three Groups of Interneurons Account for Nearly 100% of Neocortical GABAergic Neurons. Dev Neurobiol 71, 45–61.
Rymar, V.V., Sasseville, R., Luk, K.C., and Sadikot, A.F. (2004). Neurogenesis and stereological

morphometry of calretinin-immunoreactive GABAergic interneurons of the neostriatum. The Journal of Comparative Neurology 469, 325–339.
Sakmann, B., and Neher, E. (1984). Patch clamp techniques for studying ionic channels in excitable membranes. Annual Review of Physiology 46, 455–472.
Sancesario, G., Pisani, A., D'Angelo, V., Calabresi, P., and Bernardi, G. (1998). Morphological and functional study of dwarf neurons in the rat striatum. European Journal of Neuroscience 10, 3575–3583.
Sanchez-Vives, M.V., and McCormick, D.A. (2000). Cellular and network mechanisms of rhythmic recurrent activity in neocortex. Nature Neuroscience 3, 1027–1034.
Sato, F., Lavallée, P., Lévesque, M., and Parent, A. (2000). Single-axon tracing study of neurons of the external segment of the globus pallidus in primate. The Journal of Comparative Neurology 417, 17–31.
Schultz, W. (2002). Getting formal with dopamine and reward. Neuron 36, 241–263.
Shadlen, M.N., and Movshon, J.A. (1999). Synchrony unbound: A critical evaluation of the temporal binding hypothesis. Neuron 24, 67–77.
Sharott, A., Doig, N. M., Mallet, N. & Magill, P. J. (2012) Relationships between the firing of identified striatal interneurons and spontaneous and driven cortical activities in vivo. The Journal of neuroscience : the official journal of the Society for Neuroscience 32, 13221–13236.
Shimahara, T., and Tauc, L. (1975). Heterosynaptic facilitation in the giant cell of Aplysia. The Journal of Physiology 247, 321–341.
Shu, S.Y., and Peterson, G.M. (1988). Anterograde and retrograde axonal transport of Phaseolus vulgaris leucoagglutinin (PHA-L) from the globus pallidus to the striatum of the rat. Journal of Neuroscience Methods 25, 175–180.
Shu, Y., Hasenstaub, A., Duque, A., Yu, Y., and McCormick, D.A. (2006). Modulation of intracortical synaptic potentials by presynaptic somatic membrane potential. Nature 441, 761–765.
Smith, Y., and Parent, A. (1986). Neuropeptide Y-Immunoreactive Neurons in the Striatum of Cat and Monkey - Morphological-Characteristics, Intrinsic Organization and Colocalization with Somatostatin. Brain Research 372, 241–252.
Smith, Y., Bevan, M.D., Shink, E., and Bolam, J.P. (1998). Microcircuitry of the direct and indirect pathways of the basal ganglia. Neuroscience 86, 353–387.
Smythies, J.R., Platon (1994). Smythies (1994) The walls of Plato's cave: The science and philosophy of (brain, consciousness, and perception).
Somogyi, P., Bolam, J.P., and Smith, A.D. (1981). Monosynaptic cortical input and local axon collaterals of identified striatonigral neurons. A light and electron microscopic study using the golgi-peroxidase transport-degeneration procedure. The Journal of Comparative Neurology 195, 567–584.
Staines, W.A., and Fibiger, H.C. (1984). Collateral projections of neurons of the rat globus pallidus to the striatum and substantia nigra. Exp Brain Res 56, 217–220.
Staines, W.A., Atmadja, S., and Fibiger, H.C. (1981). Demonstration of a pallidostriatal pathway by retrograde transport of HRP-labeled lectin. Brain Research 206, 446–450.
Steinbusch, H.W.M. (1981). Distribution of Serotonin-Immunoreactivity in the Central Nervous-System of the Rat - Cell-Bodies and Terminals. Nsc 6, 557–618.
Stent, G.S., Kristan, W.B., Friesen, W.O., Ort, C.A., Poon, M., and Calabrese, R.L. (1978). Neuronal generation of the leech swimming movement. Science 200, 1348–1357.
Stephenson-Jones, M., Ericsson, J., Robertson, B., and Grillner, S. (2012). Evolution of the basal ganglia: dual-output pathways conserved throughout vertebrate phylogeny. The Journal of Comparative Neurology 520, 2957–2973.
Stephenson-Jones, M., Samuelsson, E., Ericsson, J., Robertson, B., and Grillner, S. (2011). Evolutionary conservation of the basal ganglia as a common vertebrate mechanism for action selec-

tion. Current Biology : CB 21, 1081–1091.
Steriade, M., Nunez, A., and Amzica, F. (1993). A Novel Slow (Less-Than-1 Hz) Oscillation of Neocortical Neurons in-Vivo - Depolarizing and Hyperpolarizing Components. Journal of Neuroscience 13, 3252–3265.
Steriade, M., Timofeev, I., and Grenier, F. (2001). Natural waking and sleep states: a view from inside neocortical neurons. Journal of Neurophysiology 85, 1969–1985.
Stern, E.A., Jaeger, D., and Wilson, C.J. (1998). Membrane potential synchrony of simultaneously recorded striatal spiny neurons in vivo. Nature 394, 475–478.
Stern, E.A., Kincaid, A.E., and Wilson, C.J. (1997). Spontaneous Subthreshold Membrane Potential Fluctuations and Action Potential Variability of Rat Corticostriatal and Striatal Neurons In Vivo. Journal of Neurophysiology 77, 1697–1715.
Sugita, S., Uchimura, N., Jiang, Z.G., and North, R.A. (1991). Distinct muscarinic receptors inhibit release of gamma-aminobutyric acid and excitatory amino acids in mammalian brain. Proceedings of the National Academy of Sciences of the United States of America 88, 2608–2611.
Sullivan, M.A., Chen, H., and Morikawa, H. (2008). Recurrent inhibitory network among striatal cholinergic interneurons. Journal of Neuroscience 28, 8682–8690.
Surmeier, D.J., and Graybiel, A.M. (2012). A Feud that Wasn't: Acetylcholine Evokes Dopamine Release in the Striatum. Neuron 75, 1–3.
Surmeier, D.J., Ding, J., Day, M., Wang, Z., and Shen, W. (2007). D1 and D2 dopamine-receptor modulation of striatal glutamatergic signaling in striatal medium spiny neurons. Trends in Neurosciences 30, 228–235.
Takagi, H., Somogyi, P., Somogyi, J., and Smith, A.D. (1983). Fine structural studies on a type of somatostatin-immurioreactive neuron and its synaptic connections in the rat neostriatum: A correlated light and electron microscopic study. The Journal of Comparative Neurology 214, 1–16.
Taverna, S., Canciani, B., and Pennartz, C.M.A. (2007). Membrane properties and synaptic connectivity of fast-spiking interneurons in rat ventral striatum. Brain Research 1152, 49–56.
Taverna, S., Ilijic, E., and Surmeier, D.J. (2008). Recurrent collateral connections of striatal medium spiny neurons are disrupted in models of Parkinson's disease. The Journal of Neuroscience : the Official Journal of the Society for Neuroscience 28, 5504–5512.
Tepper, J.M. (2013). Novel striatal interneuron types and microcircuits: insights from in vitro and in vivo recordings (Program No. XI. IBAGS 2013 Abstracts [Eilat, Israel]: IBAGS Online).
Tepper, J.M., and Bolam, J.P. (2004). Functional diversity and specificity of neostriatal interneurons. Current Opinion in Neurobiology 14, 685–692.
Tepper, J.M., Wilson, C.J., and Koos, T. (2008). Feedforward and feedback inhibition in neostriatal GABAergic spiny neurons. Brain Research Reviews 58, 272–281.
Threlfell, S., and Cragg, S.J. (2011). Dopamine Signaling in Dorsal Versus Ventral Striatum: The Dynamic Role of Cholinergic Interneurons. Frontiers in Systems Neuroscience 5.
Threlfell, S., Lalic, T., Platt, N.J., Jennings, K.A., Deisseroth, K., and Cragg, S.J. (2012). Striatal dopamine release is triggered by synchronized activity in cholinergic interneurons. Neuron 75, 58–64.
Timofeev, I., Grenier, F., Bazhenov, M., Sejnowski, T.J., and Steriade, M. (2000). Origin of slow cortical oscillations in deafferented cortical slabs. Cereb. Cortex 10, 1185–1199.
Tritsch, N.X., Ding, J.B., and Sabatini, B.L. (2012). Dopaminergic neurons inhibit striatal output through non-canonical release of GABA. Nature 490, 262–266.
Tsodyks, M.V., and Markram, H. (1997). The neural code between neocortical pyramidal neurons depends on neurotransmitter release probability. Proceedings of the National Academy of Sciences of the United States of America 94, 719–723.

Tunstall, M.J., Oorschot, D.E., Kean, A., and Wickens, J.R. (2002). Inhibitory interactions between spiny projection neurons in the rat striatum. Journal of Neurophysiology 88, 1263–1269.
Turner, R.S., and Desmurget, M. (2010). Basal ganglia contributions to motor control: a vigorous tutor. Current Opinion in Neurobiology 20, 704–716.
Venance, L., Glowinski, J., and Giaume, C. (2004). Electrical and chemical transmission between striatal GABAergic output neurones in rat brain slices. The Journal of Physiology 559, 215–230.
Vertes, R.P. (1991). A PHA-L analysis of ascending projections of the dorsal raphe nucleus in the rat. The Journal of Comparative Neurology 313, 643–668.
Vincent, S.R., Johansson, O., Hokfelt, T., Skirboll, L., Elde, R.P., Terenius, L., Kimmel, J., and Goldstein, M. (1983). NADPH-diaphorase: A selective histochemical marker for striatal neurons containing both somatostatin- and avian pancreatic polypeptide (APP)-like immunoreactivities. The Journal of Comparative Neurology 217, 252–263.
Vincent, S.R., Skirboll, L., Hokfelt, T., Johansson, O., Lundberg, J.M., Elde, R.P., Terenius, L., and Kimmel, J. (1982). Coexistence of somatostatin- and avian pancreatic polypeptide (APP)-like immunoreactivity in some forebrain neurons. Nsc 7, 439–446.
Vuillet, J., Goff, L.K.-L., Kachidian, P., Dusticier, G., Bosler, O., and Nieoullon, A. (1990). Striatal NPY-Containing Neurons Receive GABAergic Afferents and may also Contain GABA: An Electron Microscopic Study in the Rat. European Journal of Neuroscience 2, 672–681.
Wall, N.R., Wickersham, I.R., Cetin, A., La Parra, De, M., and Callaway, E.M. (2010). Monosynaptic circuit tracing in vivo through Cre-dependent targeting and complementation of modified rabies virus. Proceedings of the National Academy of Sciences 107, 21848–21853.
Wang, Z., Kai, L., Day, M., Ronesi, J., Yin, H.H., Ding, J., Tkatch, T., Lovinger, D.M., and Surmeier, D.J. (2006). Dopaminergic control of corticostriatal long-term synaptic depression in medium spiny neurons is mediated by cholinergic interneurons. Neuron 50, 443–452.
Ward, R.P., and Dorsa, D.M. (1996). Colocalization of serotonin receptor subtypes 5-HT2A, 5-HT2C, and 5-HT6 with neuropeptides in rat striatum. The Journal of Comparative Neurology 370, 405–414.
Watanabe, K., and Kimura, M. (1998). Dopamine receptor-mediated mechanisms involved in the expression of learned activity of primate striatal neurons. Journal of Neurophysiology 79, 2568–2580.
Webster, K.E. (1961). Cortico-striate interrelations in the albino rat. Journal of Anatomy 95, 532.
West, M.J., Ostergaard, K., Andreassen, O.A., and Finsen, B. (1996). Estimation of the number of somatostatin neurons in the striatum: an in situ hybridization study using the optical fractionator method. The Journal of Comparative Neurology 370, 11–22.
White, J.G., Southgate, E., Thomson, J.N., and Brenner, S. (1986). The structure of the nervous system of the nematode Caenorhabditis elegans. Philosophical Transactions of the Royal Society of London Series B, Biological Sciences 314, 1–340.
Wickens, J.R., Begg, A.J., and Arbuthnott, G.W. (1996). Dopamine reverses the depression of rat corticostriatal synapses which normally follows high-frequency stimulation of cortex in vitro. Nsc 70, 1–5.
Wickens, J.R., Kotter, R., and Alexander, M.E. (1995). Effects of Local Connectivity on Striatal Function - Simulation and Analysis of a Model. Synapse 20, 281–298.
Wilson, C.J. (1986). Postsynaptic potentials evoked in spiny neostriatal projection neurons by stimulation of ipsilateral and contralateral neocortex. Brain Research 367, 201–213.
Wilson, C.J. (1993). The generation of natural firing patterns in neostriatal neurons. Progress in Brain Research 99, 277–297.
Wilson, C.J., and Groves, P.M. (1980). Fine structure and synaptic connections of the common

spiny neuron of the rat neostriatum: a study employing intracellular inject of horseradish peroxidase. The Journal of Comparative Neurology 194, 599–615.
Wilson, C.J., and Kawaguchi, Y. (1996). The origins of two-state spontaneous membrane potential fluctuations of neostriatal spiny neurons. The Journal of Neuroscience : the Official Journal of the Society for Neuroscience 16, 2397–2410.
Wilson, C.J., Chang, H.T., and Kitai, S.T. (1983). Disfacilitation and long-lasting inhibition of neostriatal neurons in the rat. Exp Brain Res 51, 227–235.
Wilson, C.J., Chang, H.T., and Kitai, S.T. (1990). Firing Patterns and Synaptic Potentials of Identified Giant Aspiny Interneurons in the Rat Neostriatum. The Journal of Comparative Neurology 302, 508–519.
Wilson, C.J. (2007). GABAergic inhibition in the neostriatum. Progress in Brain Research 160, 91–110.
Yung, K.K.L., Smith, A.D., Levey, A.I., and Bolam, J.P. (1996). Synaptic Connections Between Spiny Neurons of the Direct and Indirect Pathways in the Neostriatum of the Rat: Evidence from Dopamine Receptor and Neuropeptide Immunostaining. European Journal of Neuroscience 8, 861–869.
Zhu, J., Jiang, M., Yang, M., Hou, H., and Shu, Y. (2011). Membrane potential-dependent modulation of recurrent inhibition in rat neocortex. PLoS Biology 9, e1001032.
Zoli, M., Torri, C., Ferrari, R., Jansson, A., Zini, I., Fuxe, K., and Agnati, L.F. (1998). The emergence of the volume transmission concept. Brain Research Brain Research Reviews 26, 136–147.

[redacted]

I

Manuscript

Novel striatal GABAergic interneuron populations labeled in the 5HT3aEGFP mouse

A. B. Muñoz-Manchado1*, C. Foldi1*, S. Szydlowski2*, L. Sjulson3,4, M. Farries5, C. Wilson5, G. Silberberg2, J. Hjerling-Leffler1§

Histological and morphological studies indicate that approximately 5% of striatal neurons are cholinergic or GABAergic interneurons. However, the number of striatal neurons expressing known interneuron markers is too small to account for the entire interneuron population. We therefore studied the 5HT3aEGFP mouse, in which we found that a large number of striatal GABAergic interneurons are labeled. Roughly 20% of 5HT3aEGFP-positive cells co-express PV and exhibit fast-spiking electrophysiological properties. However, the majority of labeled neurons do not overlap with known molecular interneuron markers. Intrinsic electrical properties reveal at least two distinct novel subtypes; a late-spiking NPY-negative neurogliaform (NGF) interneuron, and a large heterogeneous population with several features resembling low threshold-spiking (LTS) interneurons but that do not express SST, NPY or nNOS. Although the EGFP-positive NGF and LTS-like interneurons have electrophysiological properties similar to previously described populations, they are pharmacologically distinct. In direct contrast to previously described NPY+ LTS and NGF cells, LTS-like 5HT3aEGFP cells show robust responses to nicotine administration while the 5HT3aEGFP NGF cell type shows little or no response. By constructing a molecular map of the overlap between these novel populations and existing interneuron populations, we are able to reconcile the morphological and molecular estimates of striatal interneuron numbers.

The striatum is comprised of a large majority of projection neurons (medium-sized spiny neurons - MSNs), and a small, yet diverse minority of interneurons, most of which are inhibitory GABAergic interneurons (gINs) (Kawaguchi et al., 1995). Efforts to quantify and characterize striatal interneuron diversity began with anatomical studies assessing the relative size of the gIN population. Since striatal gINs express higher levels of the GABA-producing enzyme Gad67 compared to MSNs (Kita 1993), earlier studies have used high Gad67 expression to determine the size of the gIN population to be 4-8% of neurons in striatum (Kita and Kitai 1988; Lindefors et al. 1989). . The gINs also have a higher uptake of surrounding GABA, and by injecting tritiated GABA into the striatum it was shown that gINs have a nuclear envelope with characteristic indentations (Bolam et al. 1983; Iversen and Schon 1973) that are also found in aspiny choline acetyltransferase (ChAT)-expressing cholinergic interneurons (Phelps et al. 1985). Prior anatomical work based on these nuclear indentations estimates the size of the interneuron population in the rodent striatum to be approximately 5% of all neurons (Graveland and DiFiglia 1985).

Telencephalic gINs are highly heterogeneous, but major groups can be distinguished based on the expression of histochemical markers. In the rodent striatum, parvalbumin (PV)-expressing cells are fast-spiking (with short half-width action potentials) basket cells, while the somatostatin (SST)-expressing cells are low threshold spiking (LTS) cells with an extended axonal arborization. Most SST cells also express neuropeptide-Y (NPY) and neuronal nitric oxide synthase (nNOS)(Vuillet et al. 1990). A third group of interneurons expresses calretinin (CR), although there seem to be a clear species difference with far fewer CR cells observed in the mouse as compared to the rat. This list of gIN-subtypes has recently been expanded with a number of new subtypes including an NPY-expressing (SST-negative) neurogliaform

1, Department of Medical Biochemistry and Biophysics, Karolinska Institutet, Stockholm, Sweden
2, Department of Neuroscience, Karolinska Institutet, Stockholm, Sweden
3, Department of Psychiatry, NYU Langone School of Medicine, New York, USA
4, NYU Neuroscience Institute, Dept of Neuroscience and Physiology, NYU Langone School of Medicine, New York, USA
5, Dept. of Biology, University of Texas at San Antonio, San Antonio, USA
* these authors contributed equally.
§ Correspondence should be addressed to Jens Hjerling-Leffler, Dept. of Medical Biochemistry and Biophysics, Karolinska Institutet, Scheelesv 1, 17177 Stockholm, Sweden. Phone: 46 8 524 869 74, Fax: 46 8 341 960 E-mail: jens.hjerling-leffler@ki.se

(NGF) cell and a heterogeneous group expressing tyrosine hydroxylase (TH) (Ibanez-Sandoval et al. 2010; 2011; Tepper et al. 2010).

The two largest subpopulations are PV- and SST-expressing, and their relative contributions to striatal neuronal numbers are approximately 0.5 and 0.8% respectively (Oorschot 2013). Together, the number of cells belonging to the molecularly defined classes of interneurons in the striatum accounts for a total of 2.2-3.7% (cholinergic interneurons: 0.4-1.5% and gINs: 1.8-2.2%) (Gerfen and Wilson 1996; Luk and Sadikot 2001; Rymar et al. 2004; Tepper et al. 2010). In recent years a number of genetic strategies to target striatal interneuron populations have been developed that do not rely on the aforementioned markers, but rather on genetic programs necessary for development or indicative of their developmental origin. However, these mouse lines either 1) label only cells derived from the medial ganglionic eminence (MGE) and pre-optic area (POA): the PV-, SST-, CR-, and/or ChAT-expressing cells (Lhx6cre/egfp, Nkx2-1cre), or 2) also label a significant number of MSNs derived from the lateral ganglionic eminence (LGE) (Dlx1/2CreER, Dlx1-venusfl, Gad1cre/egfp). This has so far has precluded an overarching analysis of interneuron numbers (Fragkouli et al. 2009; Gittis et al. 2010; Rubin et al. 2010; Xu et al. 2008).

In the mouse cortex nearly all gINs fall into one of three non-overlapping populations that express either PV, SST or the ionotropic serotonin receptor 5HT3a (Lee et al. 2010; Rudy et al. 2011). The 5HT3a-expressing neurons are derived from the caudal ganglionic eminence (CGE) and respond robustly to activation of nicotinic acetylcholine receptors (nAChR). In the striatum, there is evidence for nAChR-dependent GABAergic signaling that so far cannot be mapped onto any of the known MGE-derived subtypes (Sullivan et al. 2008), providing further evidence that there remain undescribed gIN subtypes in the striatum.

In this study we describe two novel sub-populations of striatal gINs labeled in the 5HT3aEGFP mouse line. These sub-populations are molecularly and pharmacologically distinct from previously described subtypes. Furthermore, by constructing a comprehensive map of the size and overlap of molecularly defined dorsal striatal interneuron populations we show that the addition of these two sub-populations nearly doubles the size of the identified gIN population, to match the 5% estimated by morphological and histological studies.

METHODS

Transgenic mice

We used the transgenic mouse 5HT3aEGFP on a CD-1 background to characterize the EGFP expressing cells in striatum. In this mouse line EGFP is expressed under the control of the Htr3a promoter (GENSAT project, Rockefeller University, NY). To construct the striatal interneuron map we also utilized the wild-type CD-1 mouse strain. For nicotine response recordings we used Lhx6EGFP mice as controls (GENSAT project, Rockefeller University, NY). We used the B6.FVB-Tg(NPY-hrGFP)1Lowl/J strain (Jackson Laboratory, CA) mouse to confirm our immunostainings for NPY. Experimental animals included mice of both sexes. All experimental procedures performed on animals followed the guidelines and recommendations of local animal protection legislation and were approved by the local committees for ethical experiments on laboratory animals (Stockholms Norra Djurförsöksetiska nämnd, Sweden, and The University of Texas at San Antonio IACUC).

Tissue preparation for immunofluorescence and in situ hybridization.

Brains from P21-P28 5HT3aEGFP or wild-type mice were dissected after transcardiac perfusion with 10 ml of PBS and 25 ml 4% PFA in PBS consecutively, followed by 1 or 4 h (immuno and in situ respectively) postfixation with 4% PFA at 4°C. Tissue was cryoprotected using a 15% followed by 30% sucrose/PBS solution overnight at 4°C. Brains were embedded in OCT cryomount (Histolab Products AB), frozen on dry ice, and sectioned at 20 µm using a cryostat (1850UV, Leica Biosystems). From each brain coronal sections were obtained for the study of the dorsolateral striatum (Bregma AP +1.42 to -0.34; Franklin and Paxinos, 2008) and divided in 10 series (kept at -20°C).

Immunohistochemistry.

Sections were washed in PBS and incubated in a blocking solution (10% normal goat serum, 2.5% BSA, 0.5 M NaCl, and 0.3% Tween 20 in PBS) for 1 h at room temperature. They were then incubated in primary antibodies in dilution buffer (2.5% BSA, 0.5 M NaCl, and 0.3% Tween 20 in PBS) overnight at 4°C, washed in PBS four times for 10 min each and 1 h of secondary antibody incubation at room temperature, followed by 4 washes in PBS for 5 min each. Nuclear counterstaining was performed with 100 ng/ml 4,6-diamidino-2-phenylindole (DAPI) solution in water for 10 min. Primary antibodies were used at the following concentrations: chicken anti-green fluorescent protein (1:2000, Abcam), mouse anti-parvalbumin (1:1000; Sigma-Aldrich), rat anti-somatostatin (1:500; Millipore Bioscience Research Reagents), rabbit anti-neuropeptide Y (1:2000; Diasorin), rabbit anti-calretinin (1:1000; Swant), mouse anti-reelin (1:500; MBL), rat anti-COUP-TF interacting protein 2 (1:500, Abcam), sheep anti-neuronal nitric oxide synthase (nNOS) (Herbison et al. 1996) (1:10000), rabbit anti tyrosine hydroxylase (1:1000, Pel-Freez), rabbit anti vasoactive intestinal polypeptide (1:500, Incstar). Secondary antibodies conjugated with Cy3, and Cy5 (1:200; Jackson ImmunoResearch) or Alexa Fluor dyes 488, 594 and 647 (1:1000; Invitrogen) were used to visualize the signals. TSA Plus Cyanine 3/Fluorescein System (PerkinElmer) was used to amplify the signal with the nNOS antibody according to the manufacturer's instructions. Fluorescent images for cell counting were taken using a Zeiss LSM 700 confocal microscope.

Double in situ hybridization.

In situ hybridization with a digoxigenin full-length cDNA probe of Gad67 was performed as previously described (Lee et al. 2010), followed by immunohistochemistry against EGFP in 5HT3aEGFP mice (see previous section). Images were obtained by confocal microscopy using Zeiss LSM 700 microscope.

6-OHDA lesion.

5HT3aEGFP mice received unilateral injection of 6-hydroxydopamine (6-OHDA) (Sigma-Aldrich) in the substantia nigra (SNc). Mice were anesthetized in an induction chamber under 1.5-2% isoflurane using O2 as carrier gas. Following shaving and cleaning of the surgical area, the animal was placed in a stereotaxic frame (Kopf Instruments) and anaesthesia was maintained under 1.5-2% isoflurane in O2. Bregma was exposed via incision of the skin, and a small burr hole was created using a dental drill to which the lesion cannula was lowered to reach the SNc using

these stereotaxic coordinates: AP -3.0, ML -1.2, DV -4.5 mm. The nose bar was set at 0.0 mm. The 6-OHDA was administered at a concentration of 3 µg/µl dissolved in 0.9% sterile saline with 0.2 mg/ml ascorbic acid, injecting 1 µl/mouse at a rate of 0.3 µl/min with a 30-gauge steel cannula connected via polyethylene tubing to a 10 ul Hamilton syringe mounted on a micro-drive pump.

Electrophysiological recordings

Whole-cell patch-clamp electrophysiological recordings were obtained from EGFP-expressing cells in acute brain slices prepared from P16–P34 animals. Animals were anesthetized deeply with isoflurane, decapitated and the brain was quickly removed and transferred to ice-cold artificial cerebrospinal fluid (aCSF) of the following composition (mM): 125 NaCl, 2.5 KCl, NaHCO3, 1.25 NaH2PO4, 1 MgCl2, 2 CaCl2 and 20 glucose. The brain was then fixed to a stage and 250-300 µm slices were cut on a vibratome (Vibratome 1000, Leica). Slices were then individually transferred into an incubation chamber containing oxygenated aCSF at room temperature for a minimum period of 1 h before recordings. Alternatively the slices were incubated at 35°C for 30-60 min and then transferred to room temperature (22-25°C). During recording, slices were continually perfused with oxygenated aCSF of the same composition and kept at room temperature or 34±0.5°C. Patch electrodes were made from borosilicate glass (resistance 5–10MΩ; Hilgenberg, GmbH) and filled with a solution containing (in mM): 128 K-gluconate, 4 NaCl, 0.3 Mg-GTP, 5 Na-ATP, 10 HEPES, 1 glucose, and 5 mg/ml biocytin (Sigma) or 105 K-gluconate, 30 KCl, 10 Na-Phosphocreatine, 10 HEPES, 4 Mg-ATP, 0.3 Na-GTP and 5 mg/ml biocytin (Sigma). All recordings were performed in current-clamp mode, using EPC10 (HEKA) or Multiclamp 700B (Molecular devices) amplifiers and analyzed off-line in Clampfit version 10.2 and IGOR Pro (Wavemetrics). Perforated patch clamp recordings (Figure 4) were obtained using pipettes containing (mM) 140 K-methylsulfate, 10 HEPES, 0.2 EGTA, 7.5 NaCl, 2 Mg-ATP, and 0.2 Na-GTP. Gramicidin-D was added from a stock solution of 0.5 mg/mL in DMSO to achieve a final concentration of 0.5 - 1 µg/mL in the pipette solution. At the end of these experiments, the membrane was ruptured to fill the recorded cell with biocytin.

For pharmacological stimulation, 100 µM nicotine ditartrate (Tocris Bioscience) was applied directly onto the soma of the recorded cell by puffing (30 ms, using a Picospritzer-III device; Parker Hannifin) through a second patch pipette located 10 - 30 µm away from the soma. Extracellular solution contained the glutamatergic AMPA/kainate and NMDA receptor antagonists (CNQX and AP-V; Sigma-Aldrich) and a GABA-A antagonist (gabazine; Sigma) was also applied to ensure that responses to nicotine were direct and not mediated by polysynaptic transmission. All blockers were used at a final concentration of 10 µM. Following recordings, slices were fixated in 4% paraformaldehyde and then cryoprotected in a 30% sucrose solution in phosphate-buffered saline (PBS), frozen, and resectioned to 50 µm thickness with a sledge microtome. The sections were rinsed in PBS and incubated in Alexa 594-conjugated streptavidin (1:200 in PBS with 0.1% triton X-100) for at least 2 hours. The sections were then rinsed 5 times in PBS (at least 15 minutes per rinse), mounted on slides using the Fluoromount-G medium (Southern Biotech) and coverslipped. Labeled cells were subsequently imaged by confocal or two-photon microscopy.

Measurement of intrinsic properties.

Depolarizing and hyperpolarizing current steps were used to extract the following electrical properties of recorded neurons (see also table 2): The resting membrane potential (RMP) was measured momentarily after membrane rupture; input resistance (Rin) was obtained by the steady-state voltage response to a hyperpolarizing current step injection; membrane time constant (Taum) was extracted by performing an exponential fit to the decay phase of a voltage response to a negative current step; H-current mediated sag was measured as the voltage difference between the peak hyperpolarization and the steady-state response to a long (1 s) current step. The action potential (AP) threshold was obtained from the first action potential discharge during a ramp current injection (from 0 pA to ~2 times threshold current, over 3 s). The additional following parameters were measured from the same protocol: AP amplitude; AP width at half amplitude; after-hyperpolarization (AHP) latency (the time from spike threshold to lowest point of the AHP).

Statistical analyses of intrinsic properties.

All data were analyzed for statistical significance using the SPSS (v.17) software package (IBM, Chicago). We utilized informal cut-offs to categorize the population heterogeneity and conducted several rounds of supervised clustering based on key measures of intrinsic properties to classify cells into subgroups with similar physiological profiles. Principle components analysis (PCA) with varimax rotation was used to extract groups of measurements based on their linear correlation and stepwise regression analysis was used to determine which components predicted subgroup classification. All data were then analyzed for between-group statistical significance using multivariate analyses of variance (ANOVA) to examine overall differences between the groups. Post hoc independent-samples t-tests with Bonferroni's correction for multiple comparisons were then conducted to examine differences between individual subgroups. then conducted to examine differences between individual subgroups.

RESULTS

5HT3aEGFP labels a large striatal GABAergic population that does not include MSNs

Using a transgenic mouse line that expresses EGFP under the 5HT3A promoter we observed labeled cells throughout the striatum (Figure 1a). All EGFP+ cells were GABAergic (100%, n=4 animals), as shown by in situ hybridization for Gad1 combined with immunohistochemistry against EGFP (Figure 1b). While 6.84 ±1.58% (n=7 animals) of EGFP+ cells was labeled by the MSN-marker COUP-TF interacting protein 2 (Ctip2) (Arlotta et al. 2008), double immunofluorescence revealed no overlap with DARPP-32, another MSN marker, in EGFP expressing cells (Figure 1b,c). Furthermore, the EGFP/Ctip2 double positive neurons never exhibited spiny dendrites (see Supplementary Figure 4) arguing that Ctip2 is not specific to MSNs (n=15 cells), furthermore we have never observed a spiny Ctip2-negative EGFP+ cells. In addition, we could not detect EGFP+ axons in the globus , nor did we observe retrogradely-labeled EGFP+ cells after injection of fluorescently labeled beads into the substantia nigra (n=3 not shown).

In order to assess the relative size of the EGFP+ population, we counted the number of EGFP-expressing cells per microscopic field in the dorsolateral striatum and compared this to the number of MSNs (Ctip2+/EGFP-) in the same area. The 5HT3aEGFP population was 3.74 ±0.64% (n=7 animals) of the size of the MSN population.

Quantitative assessment of molecular marker expression in striatal GABAergic interneuron population

With the aim of creating a comprehensive map of the novel, as well as known interneuron populations in the dorsolateral striatum we used double and triple labeling against known striatal GABAergic interneuron markers and quantified the overlap with 5HT3aEGFP cells. Because we had already quantified the proportion of EGFP+ cells relative to MSNs, we counted PV-, TH-, CR-, SST-, nNOS- and NPY-positive cells relative to EGFP+ cells to determine the size of each population (summarized in table 1). We saw very little overlap with the markers SST, nNOS, NPY and CR (figure 2b, for single fluorescent channels see supplementary figure 1). However, 19.78 ± 0.26% of the EGFP+ population expressed PV (n=3 animals) (Figure 2a). In order to refine our molecular interneuron map, we also studied the size and overlap between the SST, NPY and nNOS populations (Figure 2b). Another previously described population of GABAergic interneurons express TH but at levels too low to be detected by immunohistochemistry. These neurons are however detectable in the THEGFP mouse or by reducing the surrounding levels of TH in striatum via a 6-OHDA lesion in the substantia nigra (SNc) (Darmopil et al. 2008; Ibanez-Sandoval et al. 2010; Jollivet et al. 2004). In order to elucidate if the EGFP+ population in this study overlaps with the TH population we performed unilateral 6-OHDA lesions in the SNc of 5HT3aEGFP mice. One week after injection we quantified our lesions by immunohistochemistry for TH in the striatum and SNc (supplementary Figure 2) and performed double immunohistochemistry against TH and EGFP in the striatum. The number of EGFP positive cells per field of view did not differ between lesioned and non-lesioned hemipsheres (68.60 ± 0.99 vs. 68.20 ± 1.18, n=5 animals, p=0.96), but the number of detectable TH-immunoreactive cells increased significantly on the lesioned side (9.44 ± 0.47 vs. 2.80 ± 0.48 (n=5), p=0.004, two-tailed student's t-test). A small fraction of EGFP-positive cells in the dopamine depleted striatum were also TH-immunoreactive (2.48% ±0.51). We did not quantify the mutual overlap between TH, CR and PV with any other marker than EGFP since these markers have been shown to be non-overlapping (Ibanez-Sandoval et al. 2010; Tepper et al. 2010). We used this molecular characterization of striatal interneuron populations to create a diagram in which the proportion of cells expressing each marker and overlap between markers are represented as area (Figure 2b). In order to reconcile the previously described morphological data with our molecular map, and to determine how large the gIN populations were, we also calculated the size of the population identified by all interneuron markers combined as compared to numbers of MSNs (Ctip2+/EGFP- cells). We found that all of the stained gIN populations collectively combined comprised 4.46% of all neurons in the dorsolateral striatum. Given that the 0.4-1.5% of cholinergic neurons was excluded from this analysis, this result is in close range to the 5% of interneurons in the striatum as identified by nuclear morphology (Graveland and DiFiglia 1985).

EGFP-positive cells have heterogeneous electrophysiological properties

In order to address the diversity in the population labeled in the 5HT3aEGFP mouse we obtained current clamp recordings of intrinsic properties of 129 EGFP+ neurons. Whole-cell or perforated patch (to reveal spontaneous activity) recordings showed that the EGFP+ population was highly heterogeneous both with regards to intrinsic firing properties and morphology. Quantification of intrinsic properties is summarized. in table 2. Based on the intrinsic electrical properties of recorded neurons (See Methods and further description below) we defined three subtypes in this population, which we named 5HT3aEGFP Types I-III. Three different intra-cellular solutions were used in these experiments but there was no significant effect on intrinsic properties within subtypes and the results were therefore pooled. While Type I and Type II 5HT3aEGFP interneurons were largely homogeneous and reminiscent of previously described cell types, Type III demonstrated substantial variability. None of the recorded EGFP+ neurons had firing properties resembling MSNs or cholinergic interneurons. Representative examples of the intrinsic properties of

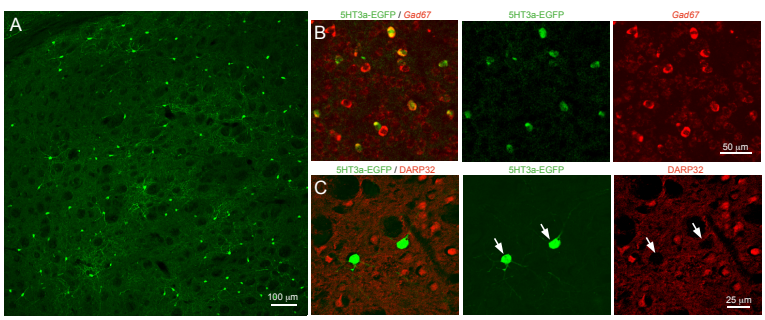

Figure 1. 5HT3AEGFP mouse labels a population of striatal GABAergic interneurons. A, Immunofluorescence for EGFP show the dorsolateral striatal 5HT3AEGFP expressing population. B, Double immunohistochemistry for EGFP and in situ hybridization for Gad67 respectively. Note that all 5HT3AEGFP cells are also Gad67 positive. C. Double immunohistochemical staining for medium spiny neuron (MSN) marker DARPP32 and EGFP show that cells labeled in the 5HT3aEGFP mouse are not MSN cells. Scale bars are 100, 50 and 25 µm.

Table 1. Overlap and size of molecular markers for striatal GABAergic interneurons

Marker	Proportion of total GABAergic interneuron population (%)	% of 5HT3a^{EGFP} population expressing marker	% of marker population expressing EGFP
PV	13.68	19.8 ±0.3	46.98 ±0.24
nNOS	16.93	0	0
SST	15.23	0.11 ±0.11	0.38 ±0.38
NPY	16.27	1.67 ±0.48	4.63 ±1.11
TH	2.58	2.48 ±0.51	26.45 ±1.02
CR	2.06	1.51 ±0.27	24.64 ±1.22
5HT3a^{EGFP}	33.24	----	100

each subtype are shown in figure 3A1-3.

We further analyzed the intrinsic membrane properties of recorded EGFP+ cells for between-subtype differences. Overall, multivariate ANOVA demonstrated main effects of subtype on AHP amplitude ($F_{2,55}=16.53$, $p<0.001$) and latency ($F_{2,55}=4.64$, $p=0.02$), resting membrane potential (Vrest; $F_{2,55}=9.09$, $p<0.001$), IH (sag; $F_{2,55}=11.03$, $p<0.001$), membrane time constant (tau; $F_{2,55}=12.75$, $p<0.001$), rebound depolarization ($F_{2,55}=8.40$, $p<0.001$) and input resistance (IR: $F_{2,55}=10.50$, $p<0.001$). To dissect differences between the three subtypes, one-way ANOVA with Bonferroni's correction for multiple comparisons was performed for each parameter.

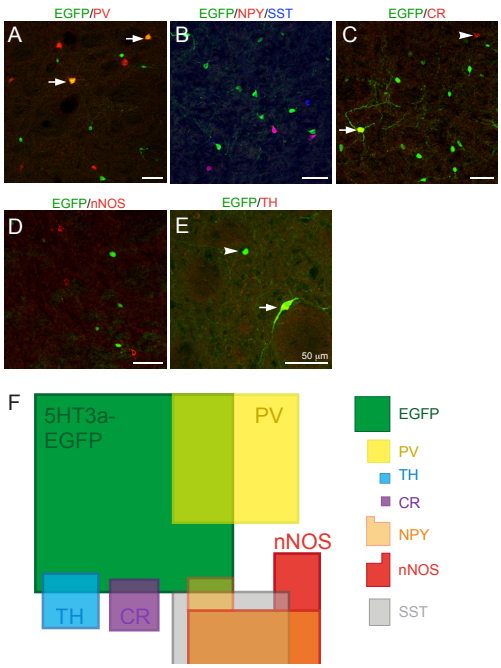

Figure 2. A majority of striatal 5HT3aEGFP cells do not overlap with known interneuron markers.
A-E. Double and triple immunohistochemical staining of the dorsolateral striatal 5HT3AEGFP population for EGFP and (A) parvalbumin (PV), (B) neuropeptide-Y and somatostatin (NPY/SST), (C) calretinin (CR), (D) neuronal nitric oxide synthase (nNOS) and (E) tyrosine hydroxylase (TH; in a 6-OHDA lesioned striatum). Arrows and arrowheads mark double positive neurons and single positive neurons respectively, scale bars are 50 µm. F. A schematic of the populations expressing known striatal interneuron markers including those labeled in the 5HT3aEGFP mouse. The area of each box, including all overlaps, are proportional to the size found in our study. (See table 1 for detailed description). On the right side is placed the legend showing the relative size, color and shape of the described cell populations in the map.

All but three comparisons were significantly different between groups; AP threshold was similar in all three groups, AHP latency was the same for Type II and Type III cells and the AP amplitude of Type I and Type III cells were not statistically different. The results of post hoc statistical analyses are described in supplementary table 1.

Type I cells (32%, n=41 cells) exhibited properties typical of fast-spiking (FS) interneurons, including short action potential half-width, low input resistance, deep after-hyperpolarization, a high maximum firing rate, and non-accommodating, often stuttering, firing (figure 3A1). These cells were indistinguishable from FS cells labeled in the Lhx6EGFP mouse line (Cobos et al. 2006) and in dual recordings of 5HT3aEGFP+ FS-cells we found a pair that was electrically coupled to each other suggesting that these are indeed typical PV-expressing FS-cells (Gittis et al. 2010; Koos and Tepper 1999) (Supplementary Figure 3). Type II cells (16%; n=20 cells) exhibited delayed firing at and above threshold with a ramp leading up to the first AP. They also had slightly larger AP half widths with a slower, more rounded AHP and an accommodating firing pattern (figure 3A2). Type II cells exhibited significantly longer AHP latencies compared to Type I cells (Figure 3B5), and the firing pattern was reminiscent of striatal NPY-expressing NGF cells (English et al. 2012; Ibanez-Sandoval et al. 2011) and cortical 5HT3a-expressing late-spiking LS1 cells, which also have NGF-like morphologies (Lee et al. 2010). Type III cells were the most frequently observed subgroup of 5HT3aEGFP cells, constituting 53% of the total striatal EGFP+ population

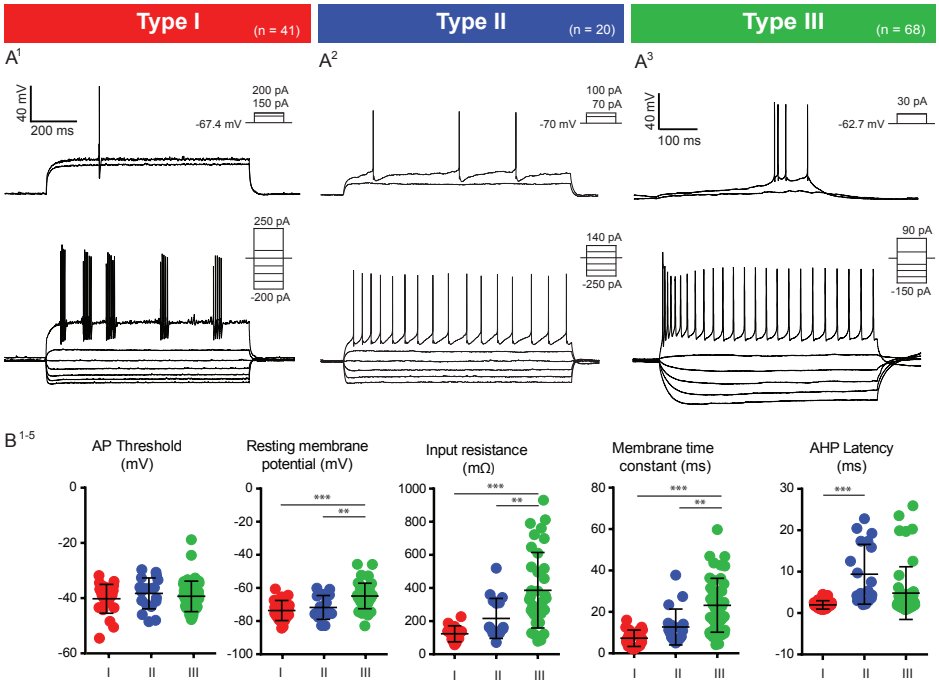

Figure 3. Electrophysiological profiles of 5HT3aEGFP cells.
Three distinct subtypes were discovered within the 5HT3aEGFP population. Type 1 cells exhibited properties typical of fast-spiking (FS) cells, with short action potential (AP) half-widths and fast and deep after-hyperpolarizations (A1). Type II cells were very similar to the previously described late-spiking neurogliaform (LS-NGF) cells, both in terms of physiology and morphology (A2). Type III cells (A3) formed the largest sub-group, and was also the most heterogeneous, exhibiting a range of specific features not seen in the other two groups. Multivariate ANOVA and post hoc multiple comparisons demonstrated a number of measured parameters were able to differentiate the three subgroups successfully. While the threshold for AP activation did not differ between groups (B1), Type III cells had significantly different resting membrane potentials, membrane time constants and input resistances, compared to both Type I and II cells (B2,3,4). The features that best distinguished Type I and Type II cells were related to the speed of firing, e.g. Type II cells exhibited longer AHP latencies than did Type I cells (B5).

Table 2. Intrinsic properties for interneurons labeled by 5HT3A^{EGFP}. Mean ± S.E.M. for Type I, II and III cells.

Parameters measured	Type I	Type II	Type III
AP Threshold (mV)	-40.23 ±1.04	-38.29 ±1.29	-39.34 ±0.81
AP half-width (ms)	0.60 ±0.1	0.97 ±0.09	0.89 ±0.08
AP Amplitude (mV)	53.59 ±2.96	58.22 ±3.45	62.77 ±1.69
AHP amplitude (mV)	20.47 ±1.96	16.26 ±1.37	11.57 ±0.68
AHP latency (ms)	1.51 ±0.20	9.37 ±1.65	4.82 ±0.93
V rest (mV)	-73.64 ±1.85	-71.76 ±1.80	-64.84 ±1.21
Sag (mV ratio change)	0.92 ±0.33	0.53 ±0.09	2.97 ±0.39
Rebound depol. (mV)	-0.47 ±0.22	-0.34 ±0.19	-1.89 ±0.32
Input resistance (mΩ)	123.86 ±12.87	215.95 ±29.29	386.51 ±38.01
Time constant (τ)	6.57 ±1.33	12.69 ±2.05	23.19 ±1.96
Spontaneous activity (%)	0	25.0	31.6
Rebound LTS spike (%)	0	0	23.5
Sub-threshold oscillat. (%)	31.6	72.0	13.0

(n=68/129 cells). The Type III subgroup was a diverse non-FS/non-NGF population with some LTS-like properties (Figure 3A3). For example, a proportion of Type III cells exhibited an initial burst of action potential at threshold (21%) as often seen in the typical SST/NPY pLTS cells, while some Type III cells exhibited an LTS after hyperpolarization (24%), and 32% of Type III cells (n=6/19 cells) demonstrated spontaneous activity during perforated patch, with a frequency of 11.2 ±1.2 Hz. The resting membrane potential, input resistance and membrane time constant were all significantly higher in Type III cells compared to the other two sub-groups (Figure 3B1,3,4). cholinergic interneurons. Representative examples of the intrinsic properties of each subtype are shown in figure 3A1-3. We further analyzed the intrinsic membrane properties of recorded EGFP+ cells for between-subtype differences. Overall, multivariate ANOVA demonstrated main effects of subtype on AHP amplitude ($F_{2,55}=16.53$, $p<0.001$) and latency ($F_{2,55}=4.64$, $p=0.02$), resting membrane potential (Vrest; $F_{2,55}=9.09$, $p<0.001$), IH (sag; $F_{2,55}=11.03$, $p<0.001$), membrane time constant (tau; $F_{2,55}=12.75$, $p<0.001$), rebound depolarization ($F_{2,55}=8.40$, $p<0.001$) and input resistance (IR: $F_{2,55}=10.50$, $p<0.001$). To dissect differences between the 3 subtypes, one-way ANOVA with Bonferroni's correction for multiple comparisons were performed for each parameter. All but 3 comparisons were significantly different between groups; AP threshold was similar in all three groups, AHP latency was the same for Type II and Type III cells and the AP amplitude of Type I and Type III cells were not statistically different. The results of post hoc statistical analyses are described in supplementary table 1.

Heterogeneity of 5HT3aEGFP cells is reflected in the morphologies.

During some of the electrophysiological recordings we included biocytin or neurobiotin in the gramicidin-containing intracellular solution to recover examples of cell morphologies from each of the three subtypes (Figure 4). None of the EGFP cells examined demonstrated spiny dendrites, characteristic of MSN cells (Supplementary Figure 4). Although small sample sizes precluded statistical analysis, the subtypes showed clear differences in morphology. The EGFP+ Type I cells (n=6) had medium-sized somas and compact dendritic and axonal branching, much like typical PV-FS basket cells. Likewise, the EGFP+ Type II cells (n=2) showed the dense and extensive dendritic branching close to the soma similar to the previously described NPY-NGF cells (Ibanez-Sandoval et al. 2011). EGFP+ Type III morphologies (n=5) were characterized by a wide stretched dendritic tree with 2-3 primary dendrites arranged in a longitudinal manner. To determine soma size in these cells, we measured the vertical axis of cells with a clear nucleus on confocal images of 5HT3aEGFP sections immunostained for EGFP with DAPI as nuclear counterstain (230 neurons from 3 animals) (Figure 4D). This analysis revealed that a majority of cells are indeed medium sized (8-13 µm)

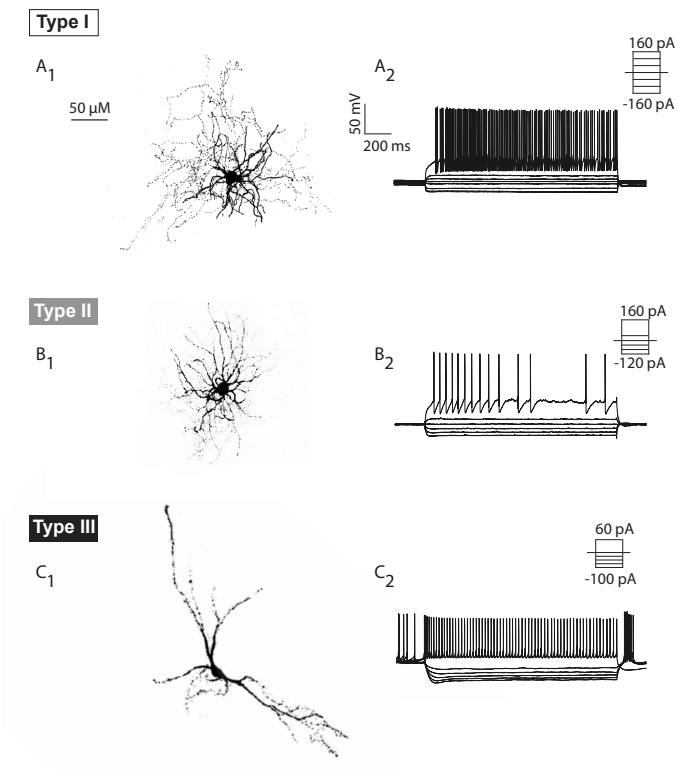

Figure 4. Morphology of the 5HT3aEGFP interneuron subtypes.
Examples of different morphologies of 5HT3aEGFP gINs (A1-C1) and their corresponding electrophysiological recordings (A2-C2). (A) Type I interneurons had medium-sized somas and compact dendritic and axonal branching (A1) and exhibited typical fast-spiking properties (A2). (B) A late-spiking NGF cell (Type II) exhibiting a typical neurogliaform morphology with dense and extensive dendritic branching close to the soma (B1). This cells exhibited some characteristics similar to fast-spiking cells but had a larger input-resistance and pronounced intra-spike interval adaptation (B2). (C) An example of a Type III cell with spontaneous activity and a pronounced sag, which exhibited a morphology with 2-3 main dendrites and a longitudinally stretched out dendritic tree.

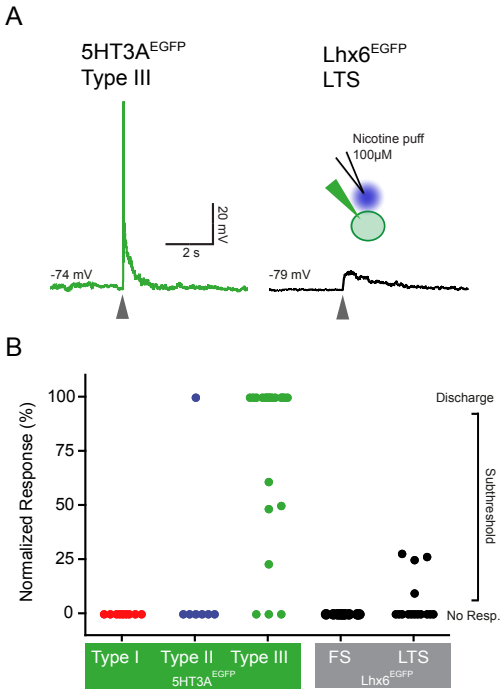

Figure 5. Type III 5HT3aEGFP interneurons are robustly activated by nicotine.
(A). Representative traces of responses to puffing with 100 μM Nicotine ditartate on a Type I 5HT3aEGFP cell (left) and a Lhx-6EGFP LTS cell (right). (B) graph representing the normalized response to nicotine puffing in the different cell types labeled in 5HT3aEGFP and Lhx6EGFP mice. Peak of responses were scaled between resting membrane potential (0%) and threshold. (100%), meaning that any cell that fired in response to puffing was 100%. Note that a majority of 5HT3aEGFP Type III cells responded strongly while only scattered responses was seen in some other cell types.

but that there is considerable diversity. This diversity probably reflects a heterogeneity of cell types but may also stem from randomly oriented elongated Type III cells.

5HT3a-cells are molecularly and pharmacologically distinct

We probed the pharmacological response of the three different 5HT3a-EGFP subtypes to the cholinergic agonist nicotine. None of the Type I cells (0/13) and only 25% (2/8) Type II cells responded with a depolarization when puffed with 100 uM nicotine. Conversely, a majority of the Type III cells (86%, n=18/21) responded with a robust depolarization often causing firing of multiple action potentials following a brief (30 ms) pulse of nicotine. As a comparison we also applied nicotine to PV-expressing FS cells and NPY/SST expressing LTS-like cells in slices from Lhx6EGFP mice (Gittis et al. 2010). We observed one very small response in an FS-cell and only 27% (4/15) in the LTS-like cells (Figure 5). The magnitude of responses in Lhx6EGFP LTS-cells was significantly lower with no cell reaching discharge threshold while 14/18 5HT3aEGFP Type III cells responded with action potential discharge (Figure 5 b).

DISCUSSION

The 5HT3aEGFP population reconciles the disparate estimates of interneuron numbers in the striatum

Here we present evidence for two novel populations of GABAergic interneurons in the dorsolateral striatum. The total number of gINs labeled in the 5HT3aEGFP mouse is almost as large as the cumulative sum of all previously described populations and brings the total number of molecularly defined GABAergic interneurons up to that originally proposed by morphological studies (Graveland and DiFiglia 1985). In addition to the three larger classical molecular subtype divisions in the striatum (NPY/SST/nNOS, PV and ChAT), and the more recently discovered TH (Tepper et al. 2010) and NPY-NGF populations, the present study proposes at least two novel distinct striatal subtypes, namely the NPY-negative LS-NGF cell type (Type II) and the SST/NPY/nNOS-negative LTS-like cell type (Type III). The size of the PV-, CR- and TH-negative 5HT3aEGFP cell population maps precisely onto the missing proportion of interneurons that was described by assessment of nuclear morphology but remained unaccounted for by known markers (Luk and Sadikot 2001; Rymar et al. 2004; Tepper et al. 2010). Therefore, it appears likely that the field is now close to identifying the full spectrum of striatal interneuron subtypes.

Striatal gINs exhibit substantial molecular and electrophysiological heterogeneity

We demonstrate that an unexpectedly large variety of likely non-overlapping interneuron subtypes exists in the striatum. The striatal cells labeled by the 5HT3aEGFP were heterogeneous and exhibited three distinct electrophysiological and morphological profiles that were similar to previously reported populations. However, their molecular and pharmacological profiles showed that they were, with the exception of PV-cells, largely non-overlapping with the known populations. The PV-expressing EGFP+ cells appeared in all respects to be classical FS cells and did not differ significantly in electrophysiological and/or molecular parameters from previously described FS interneurons (Gittis et al. 2010; Koos and Tepper 1999). We also describe a novel LS-NGF cell-type that did not express the classical marker NPY and did not reliably respond to the application of nicotine. This is in stark contrast to the previously described NPY-NGF cell that inhibits MSN cells upon cholinergic activation of nicotinic acetylcholine receptors (nAChRs) (English et al. 2012; Ibanez-Sandoval et al. 2011). Likewise, while the Type III cell described in this study were electrophysiologically and morphologically similar to the classical NPY/SST/nNOS LTS-cells, they differ in the expression of all three markers as well as demonstrating strikingly more pronounced responses to activation of nAChRs. Differences in marker expression could may vary over time since NPY is up-regulated in striatal non-NPY-expressing neurons upon injections of methamphetamine (possibly by activation of

D1 receptors) (Horner et al. 2006). The differences in response to activation of nAChRs however would suggest that these two populations of NGF cells partake in distinct striatal sub circuits. We did see a modest overlap between EGFP and the markers TH, CR and NPY (in total 5.66% of EGFP+ cells) and it is likely that these cells were electrophysiologically classified within in the type II group. This small overlap may explain the infrequent response to nicotine observed in type II EGFP cells. While the sheer number of non-MSN cells labeled in the 5HT3aEGFP mouse raises the question of how these cells have escaped detection, it is clear that upon examining recordings at first pass, most of these cells could be classified as typical FS, LTS or NGF cells. It is only by combining marker expression with pharmacological and physiological characterization that we were able to detect the difference.

Developmental origin of striatal 5HT3aEGFP cells

Inhibitory telencephalic structures such as the striatum and the central nucleus of the amygdala have been assumed to be populated by gINs derived solely from the MGE or the POA (Fishell and Rudy 2011). Transplantation studies have previously suggested a CGE-contribution to the striatum but in the form of MSNs (Nery et al. 2002) though contributions from LGE cells migrating through CGE could not be ruled out.. Since all 5HT3a-expressing gINs in the cortex and the hippocampus are CGE-derived, the findings of this paper challenge the hypothesis that the CGE exclusively contributes gINs to excitatory telencephalic structures (Lee et al. 2010; Tricoire et al. 2011). Whether striatal 5HT3aEGFP cells originate from the CGE remains to be shown directly. Since no effective genetic fate mapping strategy exists to label striatal CGE-derived cells exclusively, a deductive fate mapping strategy could be employed using Lhx6cre or Nkx2-1cre to label MGE-derived cells and assess the overlap with 5HT3aEGFP.

Putative function of 5HT3aEGFP cells in striatal cholinergic tone.

During the last several years we have seen a drastic increase in our knowledge of intra-striatal connectivity (English et al. 2012; Szydlowski et al. 2013). However, the network basis for many observed phenomena remains unclear, including the burst-pause response and synchronization of cholinergic cells. There is electrophysiological evidence of an unknown GABAergic source providing feedback and lateral inhibition between ChAT cells via activation of nicotinic acetylcholine receptors (nAChRs) (Sullivan et al. 2008), and synchronous firing of ChAT cells is sufficient to cause DA-release (Threlfell et al. 2012). Interestingly, pharmacological stimulation of striatal 5HT3a-receptors is enough to cause DA-release in slice experiments (Blandina et al. 1989). It is thus possible that this novel nAChR-expressing 5HT3aEGFP population is involved in the synchronization of ChAT cells.

Understanding the cellular diversity is a prerequisite for understanding the intricate wiring scheme of any brain structure. Until now, cellular diversity within the striatum was thought to be much to be smaller than in other telencephalic structures, such as the well-studied neocortex and hippocampus. The data presented in this paper demonstrates a larger heterogeneity in striatal interneuron types than previously thought and also raises the intriguing possibility that striatal interneuron classes may be more closely homologous to cortical interneuron classes than previously thought. Further investigation along these lines will which will undoubtedly facilitate our understanding of integration and processing of information of signals in the basal ganglia.

ACKNOWLEDGEMENTS

The authors would like to thank Stephan Nilsson for technical help and Tomas Hökfelt for providing antibodies. This work was supported by Swedish Medical Research Council, StratNeuro, Jeanssons Foundation, Hedlunds Foundation and Magn Bergvalls Foundation, ERC starting grant (to GS), and by NIH grant NS072197 (to CJW). Confocal microscopy at UTSA was supported by NIH grant G12MD007591. The authors declare no competing financial interests. Correspondence should be addressed to Jens Hjerling-Leffler, Dept. of Medical Biochemistry and Biophysics, Karolinska Institutet, Scheelesv 1, 17177 Stockholm, Sweden. Phone: 46 8 524 869 74, Fax: 46 8 341 960 E-mail: jens.hjerling-leffler@ki.se

REFERENCES

Andersen E, Dafny N. 1982. Dorsal raphe nucleus modulates sensory evoked responses in caudate and septum. The International journal of neuroscience 17(3):151-5.

Arlotta P, Molyneaux BJ, Jabaudon D, Yoshida Y, Macklis JD. 2008. Ctip2 controls the differentiation of medium spiny neurons and the establishment of the cellular architecture of the striatum. J Neurosci 28(3):622-32.

Blandina P, Goldfarb J, Craddock-Royal B, Green JP. 1989. Release of endogenous dopamine by stimulation of 5-hydroxytryptamine3 receptors in rat striatum. The Journal of pharmacology and experimental therapeutics 251(3):803-9.

Bolam JP, Clarke DJ, Smith AD, Somogyi P. 1983. A type of aspiny neuron in the rat neostriatum accumulates [3H]gamma-aminobutyric acid: combination of Golgi-staining, autoradiography, and electron microscopy. The Journal of comparative neurology 213(2):121-34.

Cobos I, Long JE, Thwin MT, Rubenstein JL. 2006. Cellular patterns of transcription factor expression in developing cortical interneurons. Cereb Cortex 16 Suppl 1:i82-8.

Connor JD. 1968. Caudate unit responses to nigral stimuli: evidence for a possible nigro-neostriatal pathway. Science 160(3830):899-900.

Darmopil S, Muneton-Gomez VC, de Ceballos ML, Bernson M, Moratalla R. 2008. Tyrosine hydroxylase cells appearing in the mouse striatum after dopamine denervation are likely to be projection neurones regulated by L-DOPA. Eur J Neurosci 27(3):580-92.

Dougherty JJ, Nichols RA. 2009. Cross-regulation between colocalized nicotinic acetylcholine and 5-HT3 serotonin receptors on presynaptic nerve terminals. Acta Pharmacol Sin 30(6):788-94.

English DF, Ibanez-Sandoval O, Stark E, Tecuapetla F, Buzsaki G, Deisseroth K, Tepper JM, Koos T. 2012. GABAergic circuits mediate the reinforcement-related signals of striatal cholinergic interneurons. Nat Neurosci 15(1):123-30.

Fishell G, Rudy B. 2011. Mechanisms of inhibition within the telencephalon: "where the wild things are". Annu Rev Neurosci 34:535-67.

Fragkouli A, van Wijk NV, Lopes R, Kessaris N, Pachnis V. 2009. LIM homeodomain transcription factor-dependent specification of bipotential MGE progenitors into cholinergic and GABAergic striatal interneurons. Development 136(22):3841-51.

Gerfen CR, Wilson CJ. 1996. Chapter II The basal ganglia. In: L.W. Swanson ABñ, H√ñkfelt T, editors. Handbook of Chemical Neuroanatomy. Elsevier. p. 371-468.

Gittis AH, Nelson AB, Thwin MT, Palop JJ, Kreitzer AC. 2010. Distinct roles of GABAergic interneurons in the regulation of striatal output pathways. J Neurosci 30(6):2223-34.

Graveland GA, DiFiglia M. 1985. The frequency and distribution of medium-sized neurons with indented nuclei in the primate and rodent neostriatum. Brain Res 327(1-2):307-11.

Guzman MS, De Jaeger X, Raulic S, Souza IA, Li AX, Schmid S, Menon RS, Gainetdinov RR, Caron MG, Bartha R et al. . 2011. Elimination of the vesicular acetylcholine transporter in the striatum reveals regulation of behaviour by cholinergic-glutamatergic co-transmission. PLoS Biol 9(11):e1001194.
Haber SN. 2003. The primate basal ganglia: parallel and integrative networks. J Chem Neuroanat 26(4):317-30.
Horner KA, Westwood SC, Hanson GR, Keefe KA. 2006. Multiple high doses of methamphetamine increase the number of preproneuropeptide Y mRNA-expressing neurons in the striatum of rat via a dopamine D1 receptor-dependent mechanism. The Journal of pharmacology and experimental therapeutics 319(1):414-21.
Ibanez-Sandoval O, Tecuapetla F, Unal B, Shah F, Koos T, Tepper JM. 2010. Electrophysiological and morphological characteristics and synaptic connectivity of tyrosine hydroxylase-expressing neurons in adult mouse striatum. J Neurosci 30(20):6999-7016.
Ibanez-Sandoval O, Tecuapetla F, Unal B, Shah F, Koos T, Tepper JM. 2011. A novel functionally distinct subtype of striatal neuropeptide Y interneuron. J Neurosci 31(46):16757-69.
Iversen LL, Schon FE. 1973. The use of autoradiographic techniques for the identification and mapping of transmitter-specific neurons in the CNS. In: Mandell AJ, editor. New Concepts in Neurotransmitter Regulation. New York: Plenum Press. p. 153-193.
Jollivet C, Montero-Menei CN, Venier-Julienne MC, Sapin A, Benoit JP, Menei P. 2004. Striatal tyrosine hydroxylase immunoreactive neurons are induced by L-dihydroxyphenylalanine and nerve growth factor treatment in 6-hydroxydopamine lesioned rats. Neurosci Lett 362(2):79-82.
Kita H. 1993. GABAergic circuits of the striatum. Prog Brain Res 99:51-72.
Kita H, Kitai ST. 1988. Glutamate decarboxylase immunoreactive neurons in rat neostriatum: their morphological types and populations. Brain Res 447(2):346-52.
Koos T, Tepper JM. 1999. Inhibitory control of neostriatal projection neurons by GABAergic interneurons. Nat Neurosci 2(5):467-72.
Lee S, Hjerling-Leffler J, Zagha E, Fishell G, Rudy B. 2010. The largest group of superficial neocortical GABAergic interneurons expresses ionotropic serotonin receptors. J Neurosci 30(50):16796-808.
Lindefors N, Brene S, Herrera-Marschitz M, Persson H. 1989. Region specific regulation of glutamic acid decarboxylase mRNA expression by dopamine neurons in rat brain. Exp Brain Res 77(3):611-20.
Luk KC, Sadikot AF. 2001. GABA promotes survival but not proliferation of parvalbumin-immunoreactive interneurons in rodent neostriatum: an in vivo study with stereology. Neuroscience 104(1):93-103.
Mallet N, Micklem BR, Henny P, Brown MT, Williams C, Bolam JP, Nakamura KC, Magill PJ. 2012. Dichotomous organization of the external globus pallidus. Neuron 74(6):1075-86.
Nery S, Fishell G, Corbin JG. 2002. The caudal ganglionic eminence is a source of distinct cortical and subcortical cell populations. Nat Neurosci 5(12):1279-87.
Oorschot DE. 2013. The percentage of interneurons in the dorsal striatum of the rat, cat, monkey and human: A critique of the evidence. Basal Ganglia 3(1):19-24.
Phelps PE, Houser CR, Vaughn JE. 1985. Immunocytochemical localization of choline acetyltransferase within the rat neostriatum: a correlated light and electron microscopic study of cholinergic neurons and synapses. The Journal of comparative neurology 238(3):286-307.
Rubin AN, Alfonsi F, Humphreys MP, Choi CK, Rocha SF, Kessaris N. 2010. The germinal zones of the basal ganglia but not the septum generate GABAergic interneurons for the cortex. J Neurosci 30(36):12050-62.
Rudy B, Fishell G, Lee S, Hjerling-Leffler J. 2011. Three groups of interneurons account for nearly 100% of neocortical GABAergic neurons. Dev Neurobiol 71(1):45-61.
Rymar VV, Sasseville R, Luk KC, Sadikot AF. 2004. Neurogenesis and stereological morphometry of calretinin-immunoreactive GABAergic interneurons of the neostriatum. J Comp Neurol 469(3):325-39.
Sullivan MA, Chen H, Morikawa H. 2008. Recurrent inhibitory network among striatal cholinergic interneurons. J Neurosci 28(35):8682-90.
Szydlowski SN, Pollak Dorocic I, Planert H, Carlen M, Meletis K, Silberberg G. 2013. Target selectivity of feedforward inhibition by striatal fast-spiking interneurons. J Neurosci 33(4):1678-83.
Tepper JM, Tecuapetla F, Koos T, Ibanez-Sandoval O. 2010. Heterogeneity and diversity of striatal GABAergic interneurons. Frontiers in neuroanatomy 4:150.
Threlfell S, Lalic T, Platt NJ, Jennings KA, Deisseroth K, Cragg SJ. 2012. Striatal dopamine release is triggered by synchronized activity in cholinergic interneurons. Neuron 75(1):58-64.
Tricoire L, Pelkey KA, Erkkila BE, Jeffries BW, Yuan X, McBain CJ. 2011. A blueprint for the spatiotemporal origins of mouse hippocampal interneuron diversity. J Neurosci 31(30):10948-70.
Tunstall MJ, Oorschot DE, Kean A, Wickens JR. 2002. Inhibitory interactions between spiny projection neurons in the rat striatum. J Neurophysiol 88(3):1263-9.
Wilson CJ, Groves PM. 1980. Fine structure and synaptic connections of the common spiny neuron of the rat neostriatum: a study employing intracellular inject of horseradish peroxidase. J Comp Neurol 194(3):599-615.
Xu Q, Tam M, Anderson SA. 2008. Fate mapping Nkx2.1-lineage cells in the mouse telencephalon. The Journal of comparative neurology 506(1):16-29.

Supplementary material

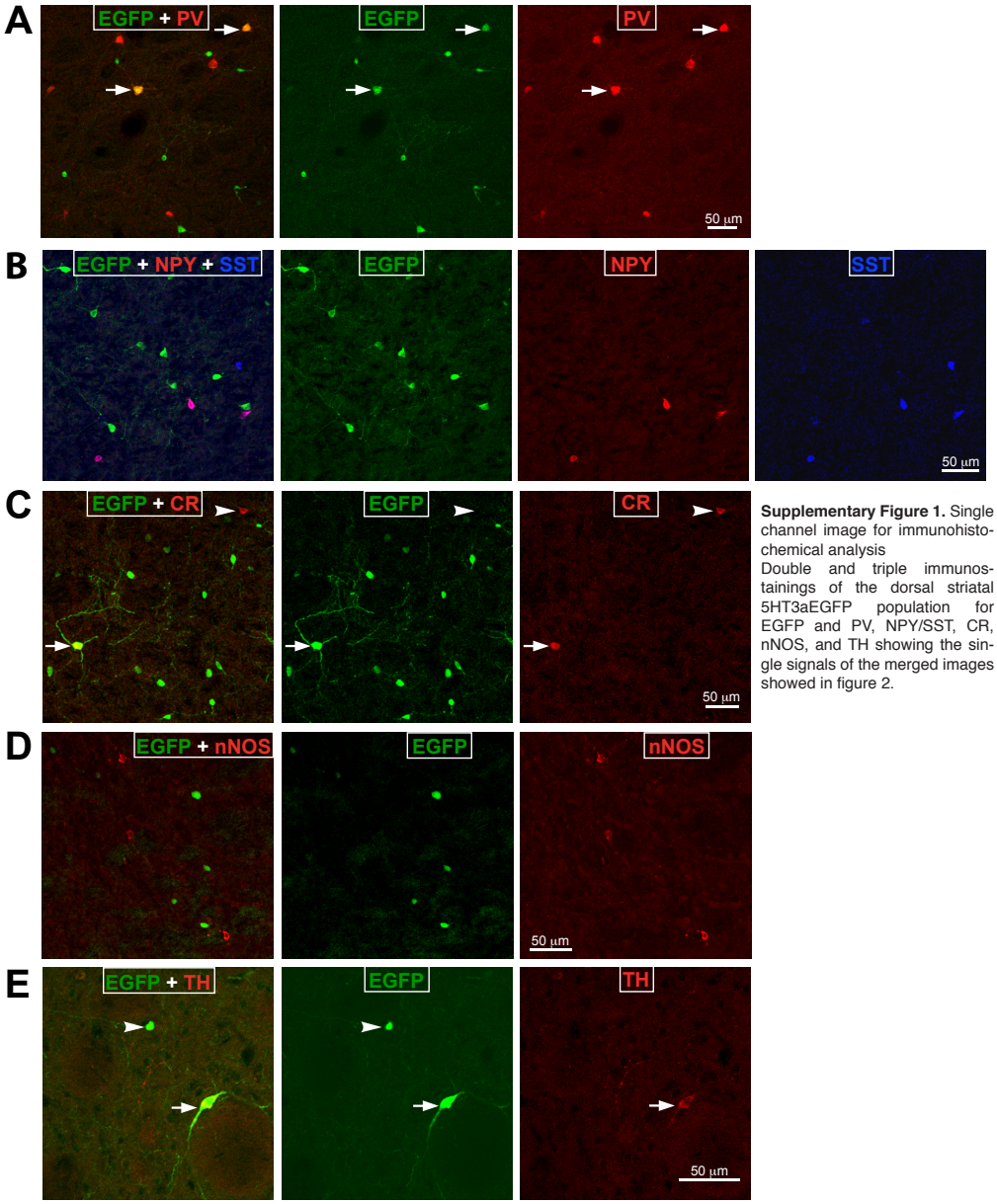

Supplementary Figure 1. Single channel image for immunohistochemical analysis
Double and triple immunostainings of the dorsal striatal 5HT3aEGFP population for EGFP and PV, NPY/SST, CR, nNOS, and TH showing the single signals of the merged images showed in figure 2.

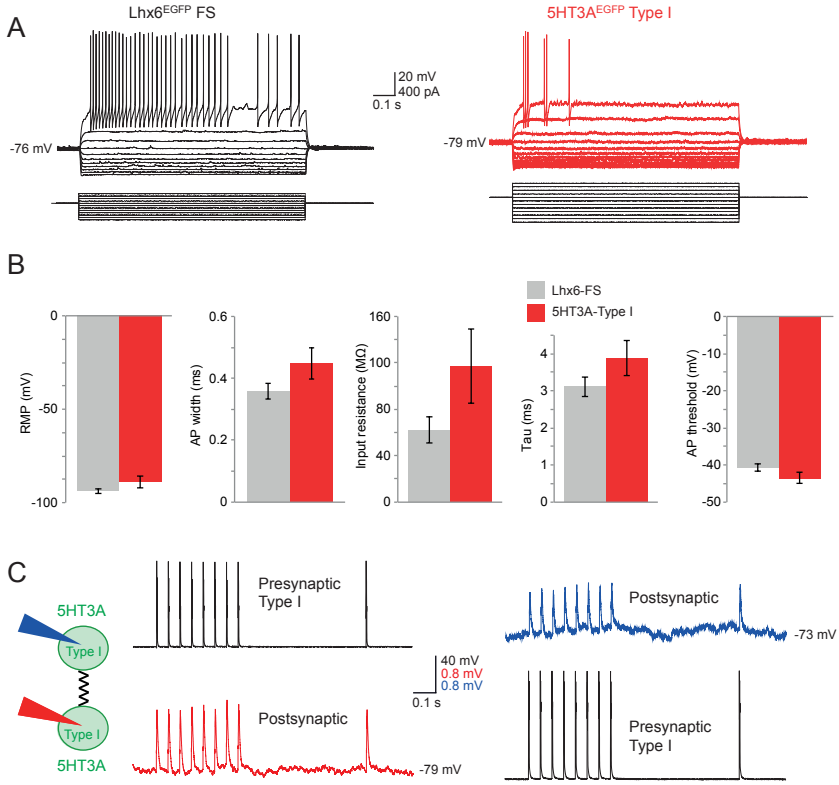

Supplementary Figure 2. 5HT3aEGFP-FS cells are likely to be normal FS cells.The largest subgroup of cells labeled with 5HT3aEGFP exhibit physiological profiles that resemble typical striatal FS cells (A and B), with high rates of action potential generation, fast spike timing and deep and fast after-hyperpolarizations. No statistical differences in intrinsic membrane properties could be detected when comparing 5HT3aEGFP FS cells to Lhx6EGFP FS cells (C). In addition, dual patch recordings of pairs of 5HT3a-EGFP-FS cells demonstrate that they are electrically coupled, much like typical FS cells (D) by which stimulation of one cell in the pair produces a depolarizing response in the other cell and vice versa.

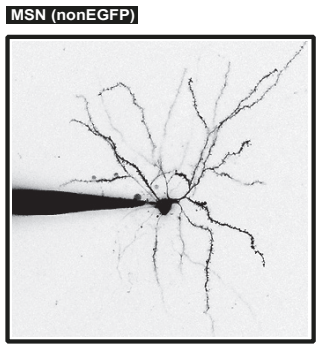

Supplementary Figure 3. An example of an MSN morphology, which was never observed within the EGFP-positive population.

II

Behavioral/Systems/Cognitive

Dynamics of Synaptic Transmission between Fast-Spiking Interneurons and Striatal Projection Neurons of the Direct and Indirect Pathways

Henrike Planert,[1,3] Susanne N. Szydlowski,[1,3] J. J. Johannes Hjorth,[2,3] Sten Grillner,[1,3]* and Gilad Silberberg[1,3]*

[1]Department of Neuroscience, Karolinska Institute, 171 77 Stockholm, Sweden, [2]Computational Biology, Royal Institute of Technology, 106 91 Stockholm, Sweden, and [3]Stockholm Brain Institute, Karolinska Institutet, 171 77 Stockholm, Sweden

The intrastriatal microcircuit is a predominantly inhibitory GABAergic network comprised of a majority of projection neurons [medium spiny neurons (MSNs)] and a minority of interneurons. The connectivity within this microcircuit is divided into two main categories: lateral connectivity between MSNs, and inhibition mediated by interneurons, in particular fast spiking (FS) cells. To understand the operation of striatum, it is essential to have a good description of the dynamic properties of these respective pathways and how they affect different types of striatal projection neurons.

We recorded from neuronal pairs, triplets, and quadruplets in slices of rat and mouse striatum and analyzed the dynamics of synaptic transmission between MSNs and FS cells. Retrograde fluorescent labeling and transgenic EGFP (enhanced green fluorescent protein) mice were used to distinguish between MSNs of the direct (striatonigral) and indirect (striatopallidal) pathways. Presynaptic neurons were stimulated with trains of action potentials, and activity-dependent depression and facilitation of synaptic efficacy was recorded from postsynaptic neurons. We found that FS cells provide a strong and homogeneously depressing inhibition of both striatonigral and striatopallidal MSN types. Moreover, individual FS cells are connected to MSNs of both types. In contrast, both MSN types receive sparse and variable, depressing and facilitating synaptic transmission from nearby MSNs. The connection probability was higher for pairs with presynaptic striatopallidal MSNs; however, the variability in synaptic dynamics did not depend on the types of interconnected MSNs. The differences between the two inhibitory pathways were clear in both species and at different developmental stages. Our findings show that the two intrastriatal inhibitory pathways have fundamentally different dynamic properties that are, however, similarly applied to both direct and indirect striatal projections.

Introduction

The striatum plays a major role in motor learning and in determining the pattern of behavior that is selected at any given time in all vertebrates (Graybiel et al., 1994; Barnes et al., 2005; Grillner et al., 2005; McHaffie et al., 2005). It receives converging glutamatergic input from cortex and thalamus, dopaminergic projections from substantia nigra pars compacta, as well as selective GABAergic input from the external pallidum (Bevan et al., 1998), all of which interact with the primarily GABAergic intrinsic striatal microcircuitry.

The striatal microcircuit consists mostly of GABAergic neurons, of which medium spiny neurons (MSNs), the projection neurons, constitute the vast majority (Wilson and Groves, 1980; Graveland and DiFiglia, 1985). Synaptic connectivity between MSNs has long been predicted from their morphology (Wilson and Groves, 1980) and in recent years was confirmed at the electrophysiological level (Czubayko and Plenz, 2002; Tunstall et al., 2002; Koós et al., 2004; Venance et al., 2004; Tecuapetla et al., 2007, 2009; Taverna et al., 2008). Synaptic connectivity between MSNs is sparse (Czubayko and Plenz, 2002; Tunstall et al., 2002; Koós et al., 2004; Venance et al., 2004; Taverna et al., 2008) and formed mainly on dendritic shafts and spines (Wilson and Groves, 1980; Somogyi et al., 1981). MSNs also receive strong GABAergic input from the different types of interneurons, with input from fast spiking (FS) cells mainly targeted to the soma and perisomatic regions (Kita et al., 1990; Bennett and Bolam, 1994; Koós and Tepper, 1999; Taverna et al., 2007).

The connectivity between MSNs of the direct (striatonigral) and indirect (striatopallidal) pathways was recently reported (Taverna et al., 2008), showing a higher prevalence of connections formed by striatopallidal neurons onto target MSNs than those formed by striatonigral MSNs. MSNs of the two pathways also differ in the long-term synaptic plasticity of glutamatergic inputs and their dopaminergic modulation (Surmeier et al., 2007; Day et al., 2008). However, the short-term plasticity of afferent excitatory inputs does not differ significantly between direct- and

Received Oct. 15, 2009; revised Dec. 17, 2009; accepted Jan. 18, 2010.

This work was supported by the European Commission Coordination Action Network of European Neuroscience Institutes Contract LSHM-CT-2005-19063, the Human Frontier Science Program, the Swedish Science Research Council (VR-M), the Swedish Parkinson's Disease Foundation (Parkinsonfonden), and the European Union Seventh Framework Programme (Cortex and Select and Act). We thank Brita Robertson and Thomas Berger for help with the morphological staining and retrograde labeling.

*S.G. and G.S. contributed equally to this work.

Correspondence should be addressed to either Sten Grillner or Gilad Silberberg at the above address. E-mail: sten.grillner@ki.se or gilad.silberberg@ki.se.

DOI:10.1523/JNEUROSCI.5139-09.2010

 0270-6474/10/303499-09$15.00/0

indirect-pathway MSNs (Ding et al., 2008). In the striatum, GABAergic connectivity between MSNs is assumed to have a different functional role than the GABAergic synapses from interneurons onto MSNs (Koós and Tepper, 1999; Koós et al., 2004; Gustafson et al., 2006; Tecuapetla et al., 2007), with the latter suggested to mediate feedforward inhibition after cortical activation (Mallet et al., 2005). To understand the function of these respective intrastriatal synaptic pathways, it is necessary to determine their dynamic properties and how they differ across cell types. In this study, we analyzed the dynamic properties of synapses between identified neuronal pairs in the rodent striatum, in particular the lateral connections between striatonigral and striatopallidal MSNs, and the synaptic connections they receive from FS interneurons. These results have been partly reported in abstract form (Planert et al., 2008).

Materials and Methods

Slice preparation and recordings. All experiments were performed according to the guidelines of the Stockholm municipal committee for animal experiments. Parasagittal and coronal slices were obtained from rats and mice (postnatal days 14–18 and 21–36, respectively). To distinguish between striatonigral and striatopallidal MSNs, we used transgenic BAC mice expressing enhanced green fluorescent protein (EGFP) in D_1 MSNs (Wang et al., 2006b). Slices were cut in ice-cold extracellular solution, kept at 35°C for 30 min, and then moved to room temperature before recordings. Whole-cell patch recordings were obtained from striatal neurons at a temperature of 35 ± 0.5°C. Neurons were visualized using infrared–differential interference contrast (IR-DIC) microscopy (Zeiss FS Axioskop). Recorded neurons were selected visually and up to four neighboring neurons with lateral somatic distances <100 μm were simultaneously recorded (see Fig. 1*A*,*B*). In experiments in which striatonigral MSNs were labeled, we used a mercury lamp (HBO 100; Zeiss) mounted on the same microscope and a fluorescent filter cube (green or red, depending on the use of GFP or fluorescent beads) to determine the subtype of MSNs, and then switched to IR-DIC to perform whole-cell recordings. Classification of nonlabeled MSNs and interneurons was performed during electrophysiological recordings and, when performed, verified by morphological staining. The extracellular solution (both for cutting and recording) contained the following (in mM): 125 NaCl, 25 glucose, 25 $NaHCO_3$, 2.5 KCl, 2 $CaCl_2$, 1.25 NaH_2PO_4, 1 $MgCl_2$. Recordings were amplified using Axoclamp 2B or MultiClamp 700B amplifiers (Molecular Devices), filtered at 2 kHz, digitized (5–20 kHz) using ITC-18 (InstruTECH), and acquired using Igor Pro (Wavemetrics). Patch pipettes were pulled with a Flaming/Brown micropipette puller P-97 (Sutter Instrument) and had an initial resistance of 5–10 MΩ, containing the following (in mM): 110 K-gluconate, 10 KCl, 10 HEPES, 4 Mg-ATP, 0.3 GTP, 10 phosphocreatine, and in a subset of neurons 0.4–0.5% biocytin. A subset of experiments in retrogradely labeled rat slices was performed with higher internal chloride concentrations, with either 20 mM K-gluconate and 100 mM KCl, or 105 mM K-gluconate and 30 mM KCl. The latter concentrations were used for all experiments in mice. Liquid junction potential (~10 mV) was not corrected for in any of the recordings. Recordings were performed both in current- and voltage-clamp mode, with access resistance compensated throughout the experiments. Recordings were discarded when access resistance increased beyond 35 MΩ.

Retrograde labeling. Striatonigral neurons were labeled by stereotactic injection of fluorescent latex microspheres (Lumafluor) into the substantia nigra pars reticulata of juvenile rats (postnatal day 12). The beads are transported retrogradely by the axons that terminate at the site of injection. The injection procedure has been described in detail previously (Le Bé et al., 2007). In short, rats were anesthetized with an intraperitoneal injection of a mixture of Fentanyl (Fentanyl; B. Braun Melsungen) and medetomidine (Domitor; Orion Pharma), diluted in 0.9% saline and administered at a final dose of 300 μg/kg. The smooth surface of the skull was pierced with a 20 gauge Microlance syringe (BD Biosciences), and red microspheres were injected with a Hamilton syringe at a volume of 0.4 μl over 1 min. Stereotactic coordinates were as follows: 2.2 mm lateral from midline, 1.1 mm anterior to lambda, and 6.9 mm below the skull surface. To allow diffusion of the solution from the injection site, the syringe was left at the place of injection for at least 5 min. Bupivacain (Marcain; 2.5 mg/ml; AstraZeneca) was used as local anesthetic before the wound was closed with chirurgical glue (Histoacryl; Aesculap). The analgesic karprofen (Rimadyl; Pfizer) was administered subcutaneously at 5 mg/kg, and the rats were awakened with intraperitoneal injections of a mixture of atipamezole (Antisedan; Orion Pharma; 1 mg/kg) and naloxone (0.1 mg/kg), diluted in 0.9% saline. After surgery, the pups were returned to their mother's cage. Slices were visualized under fluorescent microscopy, and only slices in which the striatum was clearly labeled were used for electrophysiological recordings.

Stimulation protocols and analysis. Recorded neurons were subject to various stimulation protocols to determine the synaptic and intrinsic electrical properties. Synaptic connections were identified and characterized by stimulation of a presynaptic cell with a train (10, 20, 40, or 70 Hz) of eight strong and brief current pulses (0.5–2 nA; 3 ms), followed by a so-called recovery test pulse between 500 and 600 ms after the train, all reliably eliciting action potentials (APs). Postsynaptic neurons were held near −80 mV to ensure depolarizing responses to GABAergic synapses. For analysis of synaptic properties, the average postsynaptic trace of >20 sweeps was examined for the existence of synaptic responses. Synaptic responses were obtained in current-clamp and voltage-clamp modes, and in both cases exhibited similar dynamic properties.

Parameters describing the dynamics of recorded synapses included the synaptic utilization parameter (U) (equivalent to the average release probability) and the time constants of recovery from depression (D) and facilitation (F). These parameters were extracted using the model for synaptic dynamics as previously described (Markram et al., 1998; Tsodyks et al., 1998). Amplitudes of postsynaptic responses are calculated from postsynaptic responses to presynaptic depolarizing pulses. To extract correct amplitudes of postsynaptic responses lying on the decay phase of previous responses, the synaptic decay was fitted by an exponential curve and subtracted. The amplitude of the postsynaptic response, PSP_n, is a product of the fraction of available resources, R_n, and a facilitating utilization factor, u_n, scaled by the absolute synaptic efficacy, A_{se}, as follows:

$$PSP_n = A_{se} R_n u_n. \quad (1)$$

The utilization factor is increased by each AP and decays back toward U in the time between APs, t_{ISI}. This process is described by utilization of the synaptic efficiency in the first AP ($u_0 = U$), and the recovery time constant from facilitation, F, as follows:

$$u_{n+1} = u_n \exp\left(-\frac{t_{ISI}}{F}\right) + U\left(1 - u_n \exp\left(-\frac{t_{ISI}}{F}\right)\right). \quad (2)$$

Each AP uses the fraction u_n from the synaptic resources, R_n, which then recovers to a value of 1 at rate of D as follows:

$$R_{n+1} = R_n(1 - u_n) \exp\left(\frac{-t_{ISI}}{D}\right) + 1 - \exp\left(\frac{-t_{ISI}}{D}\right). \quad (3)$$

The model parameters describing each of the analyzed connections were extracted from the average synaptic responses.

Morphological staining. Slices in which recorded cells were biocytin filled were fixed in 0.1 M phosphate buffer (PB) containing 4% paraformaldehyde overnight before the staining procedure. Slices stained for light microscopy were first incubated with 0.6% H_2O_2 in methanol, rinsed in 0.01 M PBS, and thereafter incubated with the ABC elite kit (Vector Laboratories) for 3 h. The ABC complex was diluted with 0.3% Triton X-100 in 0.1 M PB. After rinsing with 0.01 M PBS, the slices were incubated with DAB (The ImmPACT DAB kit; Vector Laboratories) for 4–10 min. Slices were then mounted on gelatin-coated slides, dehydrated, cleared in xylene, and coverslipped with DPX (dibutylphthalate polystyrene xylene) (Sigma-Aldrich). Slices used for fluorescent microscopy were incubated overnight with streptavidin-Cy2 (1:1000;

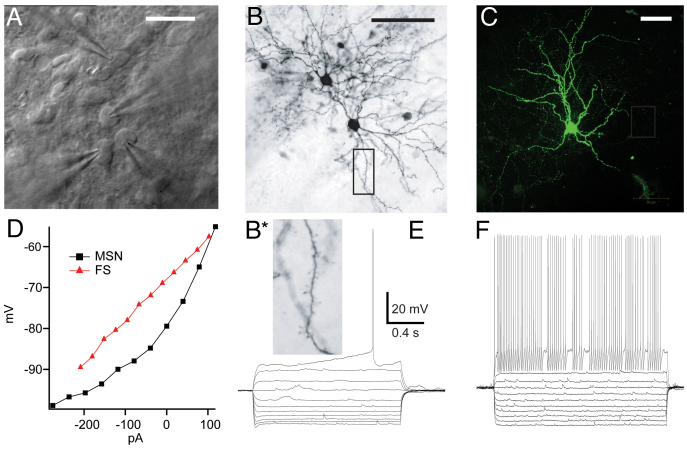

Figure 1. Patch recordings from MSN and FS striatal neurons. ***A***, Infrared microscopy image of a multineuron patch experiment. ***B***, Biocytin-filled pair of MSNs (rat; 18 d of age) stained for light microscopy. The enlarged image (***B****) shows dendritic spines characteristic of MSNs. ***C***, FS interneuron, biocytin loaded and stained for fluorescent microscopy with aspiny beaded dendrites (rat; 15 d of age). ***D***, Example of the current–voltage relationship obtained from an MSN (black squares) and FS cell (red triangles). Note the rectification in the MSN, apparent from the change in curve slope. ***E***, Response of an MSN to increasing step current injections showing the rectification in hyperpolarized steps, as well as characteristic ramp and delay preceding the action potential. ***F***, A typical response of an FS cell to the same stimulation protocol as in ***E***, showing high discharge rate, nonaccommodating discharge pattern, and the fast and deep afterhyperpolarization. Scale bars, 25 μm.

Jackson ImmunoResearch Laboratories) diluted in 0.1 M PB containing 1% Triton X-100. In between all experimental procedures, slices were washed with 0.01 M PBS. Finally, they were placed on slides, let to dry, and thereafter mounted with glycerol containing 2.5% diazabicyclooctane (Sigma-Aldrich) and stored at −20°C.

Results

Classification of recorded neurons

We recorded simultaneously from pairs, triplets, and quadruplets of neighboring (within 100 μm lateral somatic distance) striatal neurons (Fig. 1*A–C*). The first set of experiments was performed in rat striatal slices, in which neurons were not fluorescently labeled; therefore, differentiation could be done only between MSNs and interneurons. To differentiate between direct- and indirect-pathway MSNs, we then used two complementary methods, fluorescent retrograde labeling in rats and slices from BAC transgenic EGFP mice. Classification of MSNs or FS cells was done according to their electrical properties and, when performed, morphological staining. MSNs and FS cells were unambiguously distinguished from each other by their voltage responses to depolarizing and hyperpolarizing current steps (Kawaguchi et al., 1995; Koós and Tepper, 1999; Taverna et al., 2007). The majority of recorded neurons were MSNs, characterized by a hyperpolarized resting membrane potential, strong inward rectification (Fig. 1*D*,*E*), depolarizing ramp response for near-threshold current steps, typical discharge response (Fig. 1*E*), and spiny dendrites (Fig. 1*B*). FS cells were characterized by their nonaccommodating or "stuttering" (Gupta et al., 2000) discharge patterns (Fig. 1*F*), high discharge rate, fast and deep afterhyperpolarization, narrow APs, and aspiny dendrites (Fig. 1*C*).

Synaptic connections onto MSNs in rat striatum

Synaptic connectivity was examined for all recorded neuron pairs by evoking APs in presynaptic neurons by brief current injections (see Materials and Methods) and recording the responses in the other simultaneously recorded neurons. Synaptic responses in postsynaptic MSNs were measured at a membrane potential near −80 mV, both in current and voltage clamp. Synaptic responses were recorded within the first 30 min after achieving a whole-cell recording, and in most cases no apparent rundown was observed within that time frame. In rat slices, connectivity between MSNs was sparse (20%; $n = 40$ of 202 of tested MSN pairs) compared with connections from FS cells to MSNs (74%; $n = 29$ of 39). Apart from a single case of very weak electrical coupling (coupling coefficient, <0.3%), all connections formed onto MSNs were unidirectional. Synaptic strength differed between the two types of connections, measured as the amplitude of the first synaptic response (PSP) in the train (Fig. 2). FS→MSN connections were more than three times larger than MSN→MSN ones, with an average amplitude of 1.52 mV (±2.37; ranging from 0.1 to 7.7 mV; $n = 31$) compared with 0.45 mV (±0.27; range, 0.07–1.21 mV; $n = 23$; $p = 0.02$, Student's t test) (Fig. 2*C*, Table 1). To assess differences in release probability between the two pathways, we performed a paired-pulse analysis, in which the amplitude ratio of the second and first responses in the train was calculated for a 50 ms interval. Both pathways displayed on average paired-pulse depression; however, in MSN→MSN connections, the range of paired-pulse ratios was much larger than in FS→MSN connections (0.88 ± 0.54; range, 0.28–2.6; compared with 0.64 ± 0.20, ranging 0.25–0.90, respectively) (Fig. 2*D*, Table 1). Paired-pulse facilitation was observed in seven MSN→MSN connections (see example in Fig. 2*A*, middle trace) but never in FS→MSN connections.

Differential synaptic dynamics

The variability observed in the paired-pulse properties of MSN→MSN connections suggested that, in these synapses, facilitation and depression take place simultaneously and underlie the observed dynamics. To extract these properties, we used a phenomenological model for synaptic dynamics that captures a wide range of synaptic activity dependence (Markram et al., 1998; Tsodyks et al., 1998) and is relatively simple to apply to experimental data (see Materials and Methods). The commonly used protocol for this analysis is an AP train followed by a recovery test pulse (see Materials and Methods) (Fig. 3). Interestingly, the recovery test pulse revealed a large difference between the two pathways, in which connections between MSNs displayed strong facilitation (>50% increase) compared with the depression observed in FS→MSN synapses (Fig. 3*C*,*D*). The facilitation ratio between the recovery response and the first PSP in MSN→MSN connections was 1.51 (±1.1; ranging between 0.58 and 5.37). Recovery response facilitation was observed in most (22 of 31) of these connections, in sharp contrast to the FS→MSN connections, which displayed depression in all cases (amplitude ratio, 0.63 ± 0.2; range, 0.24–0.95; $n = 23$). The facilitation of the recovery test response was present at different train frequencies (Fig. 3*A*)

and at both current- and voltage-clamp recording configurations (Fig. 3*B*). We then used the measured synaptic amplitudes to extract the model parameters quantifying the synaptic dynamics (see Materials and Methods), in particular the time constants for facilitation (F) and depression (D). The relationship between these two time constants determines whether a synapse is depressing ($D > F$), facilitating ($F > D$), or is governed by both processes ($D \approx F$). The respective time constants were extracted for all analyzed synapses and showed clear separation between the two types of synapses (Fig. 3*E*). Whereas FS→MSN synapses were purely depressing, with a very short F (53 ± 53 ms, ranging from 1 to 160 ms), a much longer D (902 ± 954 ms; range, 238–4332 ms), and a small F/D ratio of 0.16, MSN→MSN synapses had a clear facilitatory component alongside depression, as evident from their respective time constants (F, 859 ± 1009 ms; D, 222 ± 189 ms) and the high F/D ratio of 4.76 (Fig. 3*F*). The dynamics of the different connections was similar when recorded in voltage- or current-clamp modes, with apparent depression in FS–MSN connections, and a facilitatory component in MSN–MSN connections (Fig. 3*B*). MSN–MSN connections differed only slightly between the two recording configurations, with a decrease in the recovery test response (RTR) facilitation ratio in current traces (1.08 ± 0.28; 0.99 ± 0.32; $n = 6$). Our data show that MSN–MSN connections are sparser, smaller, and more diverse than connections from FS to MSNs. One possible explanation for this diversity is the division of MSNs into two differently projecting subpopulations, namely, the striatonigral and striatopallidal MSNs.

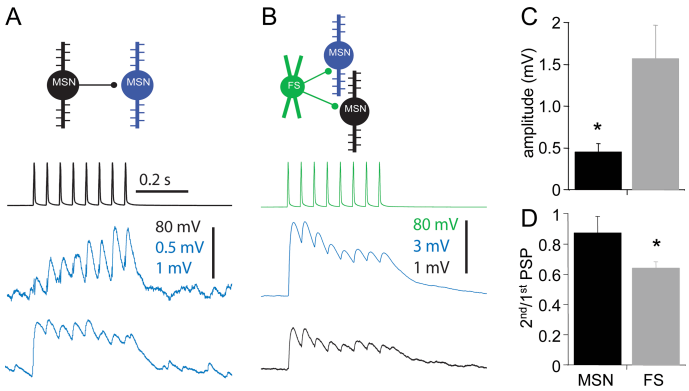

Figure 2. Synaptic connections formed by MSNs and FS cells onto MSNs. ***A***, Two examples of synaptic connectivity between MSNs. The presynaptic MSN was stimulated with a 20 Hz train of action potentials (top trace; black) and postsynaptic responses (bottom traces; blue) were recorded in postsynaptic MSNs. The middle trace shows a facilitating synaptic response, whereas the bottom one is of a depressing synapse, recorded from a different MSN. ***B***, Synaptic connectivity from FS to MSN. An example of divergent connection from an FS interneuron (green) onto two target MSNs (blue and black). ***C***, Synaptic amplitude of the two types of synapses, measured at the first synaptic response in the train (MSN–MSN connections in black, $n = 31$; FS–MSN in gray, $n = 23$). The difference was significant, with $p = 0.02$, Student's t test. ***D***, Paired-pulse depression in the respective pathways, as calculated from the amplitudes of the first and second responses ($p = 0.03$, t test). The average paired-pulse ratio of MSN–MSN pairs was larger because of the occurrence of depressing and facilitating synapses, which were absent in FS–MSN connections. $^*p < 0.05$, Student's t test. Error bars indicate SEM.

To identify MSNs according to their projection type, we used two alternative methods, retrograde labeling of striatonigral MSNs with fluorescent beads and transgenic EGFP mice (see Materials and Methods) (Fig. 4). In retrogradely labeled rat slices, we simultaneously recorded from labeled (dMSN, for putative direct-pathway MSNs) and nearby nonlabeled (iMSN, for putative indirect-pathway MSNs) neurons (Fig. 4*A–C*). Retrogradely labeled neurons were all MSNs, as verified by their electrical properties. In retrogradely labeled slices, we recorded from a total of 83 pairs, 8 of which had synaptic connections (6 connections between MSNs and 2 from FS to MSNs). Both MSN types also received synaptic connections from presynaptic iMSNs (iMSN→iMSN, 2 of 14; iMSN→dMSN, 3 of 10), and 1 connection was found between dMSNs (dMSN→dMSN, 1 of 13). From the six MSN–MSN connections, four had facilitation of the test response, and two were depressing connections (average amplitude ratio, 110 ± 45%; $n = 6$). Labeled and nonlabeled MSNs received synapses from FS cells (one of one FS→dMSN and one of one FS→iMSN connected pairs), both of which were depressing connections, with a clear decrease in the amplitude of the recovery test response (67 and 77% of first PSP, respectively).

Connectivity of identified MSNs in mouse striatum

As an additional independent method for identifying MSN subpopulations, we used transgenic mice expressing EGFP in dMSNs (Wang et al., 2006b). We recorded from labeled and nonlabeled neighboring neurons in slices of D_1-EGFP mice (see Materials and Methods) (Fig. 4*D–F*) and found synaptic interactions in 23 of 294 MSN–MSN tested connections (Fig. 5). From these MSN–MSN connections, a majority (74%; 17 of 23) was from presynaptic iMSNs and 6 connections (26%) had a presynaptic dMSN (for synaptic properties, see Table 1). The connections from dMSNs did not have significantly different amplitudes than those from iMSNs (0.28 and 0.39 mV, respectively; $p = 0.55$, t test). These connections displayed recovery test facilitation (110 ± 47%; ranging from 62 to 170%; $n = 6$), with two (of three) facilitating dMSN→iMSN connections and one facilitating dMSN→dMSN connection (the three others were depressing synapses).

iMSNs formed connections onto dMSNs (13%; $n = 10$ of 80 pairs) and iMSNs (23%; $n = 7$ of 31 pairs), both of which had depressing and facilitating synapses (Fig. 5*A*). The connections from iMSNs onto the two types of target cells were not significantly different in their amplitude (0.27 ± 0.09 and 0.45 ± 0.44 mV, respectively; $p = 0.17$, t test), paired-pulse ratio (of 111 ± 59 and 95 ± 48%; $p = 0.67$), recovery test facilitation (151 ± 64 and 139 ± 69%; $p = 0.98$) (Fig. 5*D*), as well as the utilization factor (U) (0.36 ± 0.18 and 0.34 ± 0.19; $p = 0.82$). In these connections, with presynaptic iMSNs, the type of postsynaptic MSNs did not determine the dynamics of the synaptic connection, as we saw in two cases in which a dMSN received both a depressing and a facilitating connection from two different iMSNs (Fig. 5*A*). In two separate cases, the same presynaptic iMSN contacted a dMSN and an iMSN with facilitating synapses, showing that the individual presynaptic MSN, but not the MSN type, determined the synaptic dynamics of the connection (see example in Fig. 5*A*).

Homogenous inhibition of both MSN subpopulations by FS cells

As in rat striatum, FS→MSN connectivity recorded in mice had higher prevalence than MSN→MSN connectivity (78%,

Table 1. Properties of synaptic connections between MSNs and FS cells

	Connection probability (%; *n*/*N* pairs)	Amplitude (mV)	Paired-pulse ratio (2nd/1st response)	Recovery test ratio (RTR/1st response)	Depression time constant (*D*) (ms)	Facilitation time constant (*F*) (ms)	Synaptic utilization factor (*U*)
Rat							
MSN–MSN	20%; 40/202	0.45 ± 0.27	0.88 ± 0.54	1.51 ± 1.10	222 ± 189	859 ± 1009	0.42 ± 0.21
FS–MSN	74%; 29/39	1.52 ± 2.37	0.64 ± 0.20	0.63 ± 0.2	902 ± 954	53 ± 53	0.29 ± 0.19
GFP mice							
D1–D1	7%; 3/43	0.24 ± 0.15	0.91 ± 0.63	1.23 ± 0.50	192 ± 114	1266 ± 1427	0.39 ± 0.22
D1–D2	4.5%; 3/66	0.33 ± 0.15	0.84 ± 0.30	1.16 ± 0.29	96 ± 9	313 ± 363	0.46 ± 0.24
D2–D1	13%; 10/80	0.27 ± 0.09	1.1 ± 0.6	1.51 ± 0.64	365 ± 471	570 ± 783	0.36 ± 0.18
D2–D2	23%; 7/31	0.45 ± 0.44	0.95 ± 0.48	1.39 ± 0.69	149 ± 90	1462 ± 1800	0.34 ± 0.19
FS–D1	89%; 8/9	4.8 ± 4.9	0.62 ± 0.12	0.72 ± 0.08	740 ± 350	3.1 ± 2.4	0.24 ± 0.07
FS–D2	67%; 6/9	3.1 ± 4.1	0.66 ± 0.14	0.63 ± 0.19	850 ± 500	4.5 ± 2.7	0.23 ± 0.07

The table presents a summary of the properties of synaptic connections formed between MSNs and FS cells. Data are presented as mean ± SD.

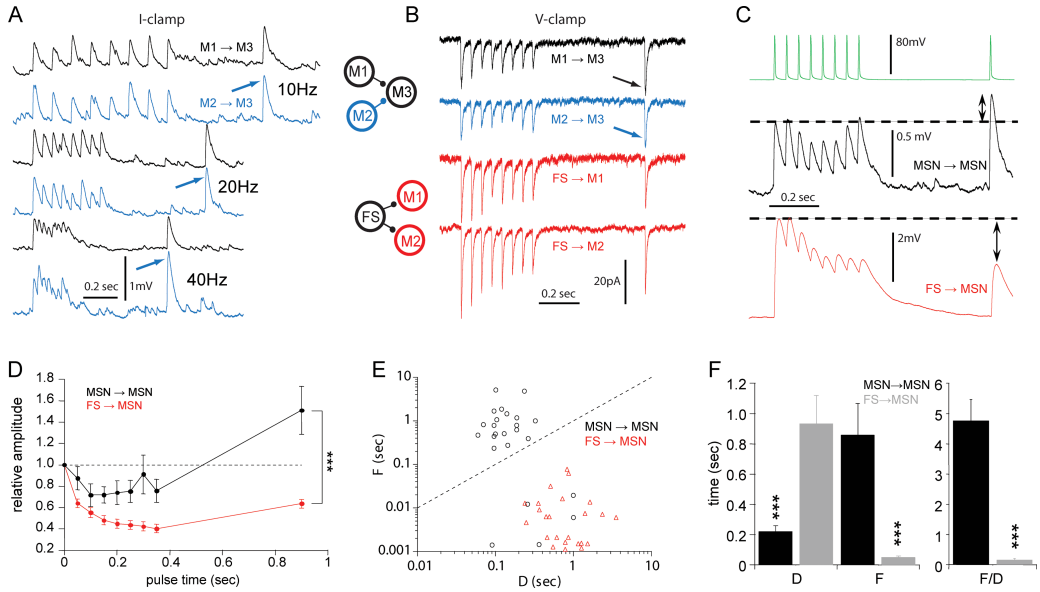

Figure 3. Differential synaptic dynamics of feedback and feedforward connections. ***A***, An example of converging MSN–MSN connectivity. A postsynaptic MSN (M3) received direct connections from two neighboring MSNs (M1 and M2). The connection was tested in different train frequencies (10, 20, 40 Hz trains of 8 action potentials), showing frequency-dependent depression and facilitation. Note the increase in amplitude of the recovery test response (denoted by blue arrows), revealing the underlying facilitatory component. ***B***, Examples of divergent synaptic connectivity from FS to two neighboring MSNs as recorded in voltage clamp (red traces, bottom). Note the depression of the recovery test response after 0.55 s after a 20 Hz train. The top traces are of the same connections as in ***A***, acquired in voltage-clamp mode. ***C***, MSNs receive different types of input from neighboring MSNs and FS cells. Two examples of synaptic responses to 20 Hz trains (green) and a recovery response are depicted. Note the facilitation of the recovery response in the MSN⟶MSN connection (black) compared with the depression of the FS⟶MSN response (red). ***D***, Average responses of all analyzed connections normalized to the amplitude of the first PSP (FS–MSN connections in red, $n = 23$; MSN–MSN in black, $n = 31$). ***E***, Facilitation and depression time constants of all analyzed connections are plotted against each other in a logarithmic plot. The dashed line represents the $F = D$ curve, showing that all FS⟶MSN, but not all MSN⟶MSN connections, were depressing. ***F***, The synaptic dynamics of the two connection types are significantly different, as seen by the values of the time constants for facilitation (*F*) and depression (*D*), and the ratio (right bar graph). ***$p < 0.001$, Student's *t* test. Error bars indicate SEM.

14 of 18; compared with 10%, 23 of 227), larger amplitude (4.21 ± 3.9 mV; 0.41 ± 0.35 mV; $p < 0.001$, Student's *t* test), and displayed only depressing dynamics. The high connection probability, combined with the homogeneity in dynamic properties, suggested that both direct- and indirect-pathway MSNs are similarly inhibited by FS interneurons. Indeed, both iMSNs (67%; $n = 6$ of 9) and dMSNs (89%; $n = 8$ of 9) received inhibitory connections from FS cells with very similar dynamic properties. Moreover, in two experiments, we found individual FS cells forming divergent connections on both MSN types (one example depicted in Fig. 6*A*), further suggesting unspecific inhibition mediated by FS cells. The synaptic properties of FS⟶dMSN and FS⟶iMSN were not significantly different in terms of their amplitudes (4.8 ± 4.9, $n = 8$; and 3.1 ± 4.1, $n = 6$), paired-pulse depression (62 ± 12 and 66 ± 14%), recovery test response (72 ± 8 and 63 ± 19%), and dynamic model parameters (*U*, 0.24 ± 0.07 and 0.23 ± 0.07; *D*, 0.74 ± 0.35 and 0.85 ± 0.5 s; *F*, 3.1 ± 2.4 and 4.5 ± 2.7 ms) (Fig. 6*B*,*C*, Table 1). These data show that both MSN subpopulations receive ubiquitous and homogeneous inhibition from FS cells, which is, moreover, mediated by the same pool of presynaptic interneurons.

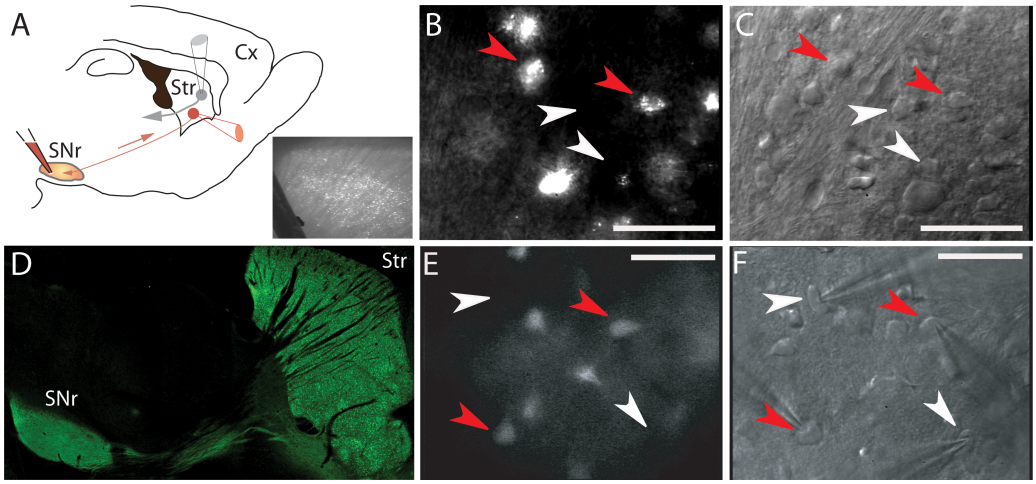

Figure 4. Fluorescent identification of direct-pathway MSNs. ***A***, Retrograde labeling of rat striatonigral MSNs by injection of fluorescent beads into the substantia nigra pars reticulata. The beads are transported by the axons to the cell bodies and can then be visualized under fluorescence microscopy. ***B***, Individual striatal neurons after retrograde labeling. The red arrows designate retrogradely labeled striatonigral MSNs, and the white arrows show the position of unlabeled neurons, which are MSNs or interneurons. ***C***, The same neurons as in ***B*** under infrared microscopy. ***D***, Confocal image of the striatum and substantia nigra pars reticulata of a BAC transgenic D_1-EGFP mouse (image by courtesy of Emmanuel Valjent and Gilberto Fisone, Karolinska Institute, Stockholm, Sweden). ***E***, Individual striatal neurons in slices of EGFP mouse. The labeled neurons are visible under epifluorescence microscopy and can be selected for recording. ***F***, The same neurons as in ***E***, under IR microscopy. The red arrows designate the fluorescent neurons selected to be recorded under IR optics. Scale bars, 50 μm. SNr, Substantia nigra pars reticulata; Str, striatum; Cx, cortex.

Discussion

In this study, we showed fundamental differences in the dynamic properties of two inhibitory pathways within the striatal microcircuitry. Inhibition by FS cells is robust, homogenous, and exerted by the same FS cells onto both striatonigral and striatopallidal projection neurons. In contrast, MSN–MSN connectivity is sparser, weaker, and exhibits diverse activity-dependent synaptic dynamics. The connectivity prevalence between MSNs depended on the type of presynaptic MSN; however, the dynamic properties were not determined by the type of interconnected MSNs. The differences between the FS→MSN and MSN→MSN connectivity are clear in both species and throughout different developmental stages, suggesting that they indeed constitute a basic organizational principle in the striatal microcircuitry.

Robust feedforward inhibition from FS cells onto MSNs

Inhibition mediated by FS cells onto MSNs had very different dynamics than that observed between MSNs. FS→MSN synaptic connections mediated large, depressing responses with negligible facilitation, which were strikingly homogenous across different target cells. We show that both neighboring direct- and indirect-pathway MSNs are inhibited by FS cells, with similar amplitudes and dynamics. It is still not clear whether and to what degree FS cells have preferences for any of the MSN projection types; however, as exemplified in our data, the same FS cells target MSNs of both projection types (Fig. 6*A*). FS cells therefore may not selectively inhibit one striatal projection or the other, but rather efficiently and similarly inhibit a large fraction of their neighboring MSNs of both types. The depressing nature of the FS→MSN synapse makes it tuned to faithfully transmit the onset of FS activity, enabling FS cells to mediate potent synchronized inhibition after cortical excitation (Mallet et al., 2005; but see Berke, 2008). The role of such inhibition by FS cells may be in preventing target MSNs from discharge after excitatory input, but it may also be effective in synchronizing the output of target MSNs without necessarily silencing them completely, but rather by delaying discharge (Koós and Tepper, 1999). Our results suggest that both types of inhibition are very different in terms of their respective dynamics regardless of the postsynaptic MSN type. This was also shown to be the case for glutamatergic input to MSNs, in which the dynamics of thalamic input was very different from that of cortical input, for both striatopallidal and striatonigral MSNs (Ding et al., 2008).

FS→MSN connectivity was severalfold more prevalent than MSN–MSN connectivity, in accord with previous reports (Koós and Tepper, 1999; Koós et al., 2004; Gustafson et al., 2006; Taverna et al., 2007; Tecuapetla et al., 2007). This big difference in connectivity can be partly attributed to the electrotonic attenuation of synaptic responses at distal dendrites compared with the little attenuation of perisomatic inputs from FS cells (Tepper et al., 2008). However, even in experiments in which high intracellular chloride concentrations were used to improve the detection of GABAergic inputs (Koós et al., 2004; Taverna et al., 2008; Tecuapetla et al., 2009), feedback connectivity was sparse. Interestingly, a similar connectivity pattern is found in the neocortical microcircuit, in which projection neurons (pyramidal cells) also constitute the vast majority of neurons and are sparsely interconnected (Markram et al., 1997), whereas connectivity from GABAergic FS interneurons onto pyramidal cells is severalfold higher (Holmgren et al., 2003). This suggests that FS cells in the respective microcircuits, in addition to their similar intrinsic properties (Kawaguchi, 1995; Kawaguchi et al., 1995), share similar network properties and function in mediating feedforward inhibition to their respective principal targets.

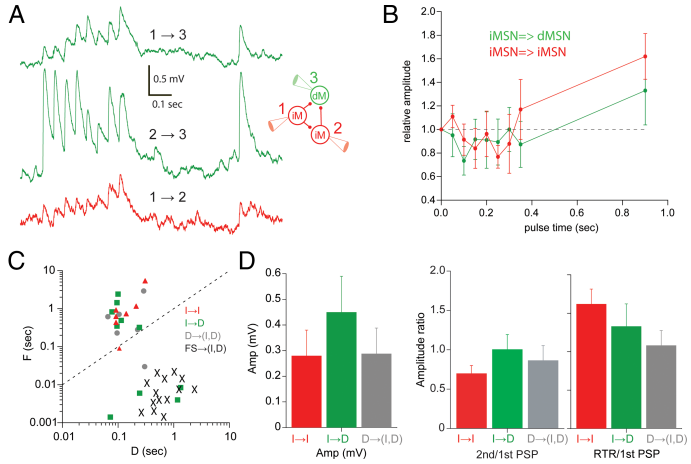

Figure 5. Synaptic connections between EGFP-identified MSNs. ***A***, A network of neighboring MSNs in ventral striatum displaying divergent and convergent synaptic connections. Cell 3 is a direct-pathway MSN (dM) receiving convergent input from two indirect MSNs (iM) with different dynamic properties. Note the facilitation in the 1⟶3 connection (top trace) compared with the depressing connection received by cell 3, and the facilitating connections onto both targets of cell 1. ***B***, Average amplitudes, normalized to the amplitude of the first PSP, for connections from iMSNs onto dMSNs (in green; $n = 10$) and iMSNs (in red; $n = 7$). Note the facilitation of the recovery test response, which is absent in FS⟶MSN connections (Figs. 3, 6). ***C***, Facilitation and depression time constants of connections between identified MSNs are plotted against each other in a logarithmic plot. iMSN⟶iMSN connections are marked with red triangles, iMSN⟶dMSN in green squares, presynaptic dMSN connections in gray circles, and FS⟶MSN connections in black "X." ***D***, Synaptic properties of connections from presynaptic iMSNs did not significantly differ according to the postsynaptic MSN type and were not significantly different from connections between MSNs in which presynaptic neurons were dMSNs. Error bars indicate SEM.

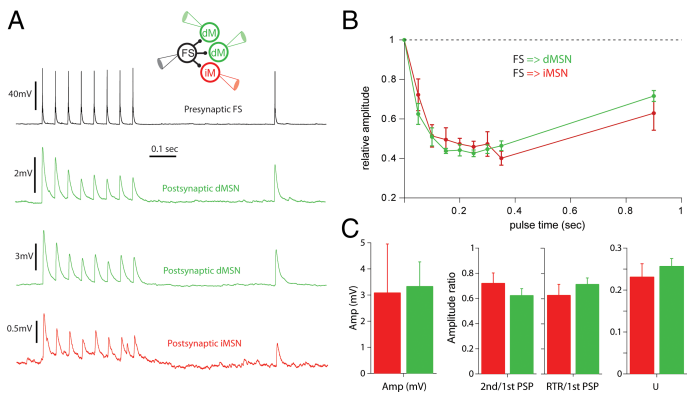

Figure 6. Synaptic connections from FS cells onto both types of MSNs. ***A***, An example of a divergent connection from a single FS cell onto three target MSNs of different projection types. Note the similarity in the dynamics of the responses on the different MSN types. ***B***, Average amplitudes normalized to the amplitude of the first PSP, for connections from FS onto iMSNs (in red; $n = 6$) and dMSNs (in green; $n = 9$). ***C***, Synaptic properties of connected FS cells did not differ significantly according to the postsynaptic MSN type. Both ***B*** and ***C*** show the high degree in homogeneity in the FS⟶MSN pathway onto both projection types of MSNs. Error bars indicate SEM.

Connectivity between MSNs of different types

Synaptic connections between MSNs of both types displayed a large diversity in terms of the dynamic properties, with cases of depression, facilitation, and mixed responses in which synaptic depression was followed by facilitation of the recovery test response (Fig. 3*A*). This was in sharp contrast to the homogenous dynamics of FS⟶MSN connections. This variability in dynamics was, surprisingly, not accounted for by the projection identity of the presynaptic and postsynaptic neurons, since all four possible combinations (presynaptic and postsynaptic iMSN/dMSN) had cases of facilitating as well as depressing synapses (Fig. 5). One aspect of MSN–MSN connectivity that did, however, depend on the presynaptic MSN subtype was the prevalence of connectivity. As reported recently (Taverna et al., 2008), we also observed a nonrandom organization of MSN interconnectivity, in which synapses formed by iMSNs seemed to be more common than those formed by presynaptic dMSNs. The reasons for this difference are still not clear but may be related to properties of the axonal arborization and the dendritic targeting preferences of the respective types. The fact that these differences were observed both in rats as well as D_1-EGFP mice suggests that it is not an artifact attributable to the particular transgenic mouse used. Whereas the projection type of connected MSNs did not determine the synaptic dynamics, individual presynaptic neurons induced similar response dynamics in their targets, as seen in divergent connections, both from presynaptic MSNs and FS cells (Figs. 5, 6). Interestingly, this is not the typical scenario in other microcircuits, in which the same presynaptic neuron may induce drastically different synaptic responses in different types of postsynaptic targets (Thomson et al., 1993; Markram et al., 1998; Reyes et al., 1998).

Variability in the dynamics of MSN–MSN synaptic transmission

Unlike the very dominant facilitation observed at certain types of cortical synapses (Thomson et al., 1993), the facilitation in MSN⟶MSN connections was commonly masked by a simultaneously occurring depressing component. The interplay between these processes is likely to cause the variability we observed in MSN⟶MSN connectivity and may also underlie previous reports of both facilitation and depression mediated by presynaptic MSNs (Czubayko and Plenz, 2002; Venance et al., 2004; Rav-Acha et al., 2005; Gustafson et al., 2006). One possible explanation for the observed variability is the postsynaptic dendritic location of MSN–MSN synapses (Wilson and Groves, 1980; Somogyi et al., 1981; Tepper et al., 2008). Unlike FS–MSN synapses, which target a closer and more confined perisomatic region, synapses between MSNs target dendrites with variable thickness and at various electrotonic distances from the soma and dendritic branching points.

The dendritic locus of MSN–MSN inhibition enables it to affect the nonlinear processes of dendritic integration as well as the plasticity of nearby excitatory inputs, which also target MSN dendrites (Plenz, 2003; Carter et al., 2007; Wilson, 2007; Tepper et al., 2008). In addition to these functional properties, the dendritic location also shapes the apparent dynamics of the synaptic responses (Banitt et al., 2005). Synaptic activation causes a local conductance increase as well as reduction of the synaptic driving force, both of which induce a depressing component in synaptic responses. This "apparent depression" strongly depends on the location of the synaptic contact and is likely to contribute to the variability we observed in synaptic dynamics.

Similar recovery test facilitation was observed in other neural microcircuits in the prefrontal cortex (Wang et al., 2006a) and in the hippocampus (Hefft and Jonas, 2005). As in the MSN–MSN connections we observed, responses typically displayed depression during the burst of action potentials, but facilitated after a pause of several hundreds of milliseconds. This facilitation was observed both in current- and voltage-clamp modes, and was also observed when postsynaptic neurons were recorded in a cesium-based pipette solution, suggesting that it is mainly dictated by presynaptic processes. The biophysical mechanisms underlying the observed synaptic dynamics were not explored in this study; however, it is predicted that protocols affecting the release process such as changing extracellular calcium concentrations or loading the presynaptic neurons with CsCl (Hull et al., 2009) would significantly alter the dynamics of these connections. Presynaptic calcium channels are subject to multiple modulatory processes that may underlie the various forms of synaptic facilitation (for review, see Catterall and Few, 2008).

The variability in synaptic dynamics in MSN–MSN connections was not explained by the type of connected neurons but it may reflect intrinsic variability in both presynaptic and postsynaptic elements. In our study, we did not record neuronal positions with respect to the patch and matrix striatal compartments, which may also contribute to the observed variability in dynamics, as recently suggested for synaptic strength (Tecuapetla et al., 2009).

Summary

Our study shows that MSN→MSN and FS→MSN inhibitory pathways in the striatum have fundamentally different functional properties, with highly homogenously depressing, reliable inhibition from FS onto both projection pathways, and sparse and variable interconnectivity among MSNs of both direct and indirect projection systems. These results suggest that the functional role of inhibition from FS cells might be not in separating the activity of the two striatal projections, but rather in shaping striatal output for both.

References

Banitt Y, Martin KA, Segev I (2005) Depressed responses of facilitatory synapses. J Neurophysiol 94:865–870.

Barnes TD, Kubota Y, Hu D, Jin DZ, Graybiel AM (2005) Activity of striatal neurons reflects dynamic encoding and recoding of procedural memories. Nature 437:1158–1161.

Bennett BD, Bolam JP (1994) Synaptic input and output of parvalbumin-immunoreactive neurons in the neostriatum of the rat. Neuroscience 62:707–719.

Berke JD (2008) Uncoordinated firing rate changes of striatal fast-spiking interneurons during behavioral task performance. J Neurosci 28:10075–10080.

Bevan MD, Booth PA, Eaton SA, Bolam JP (1998) Selective innervation of neostriatal interneurons by a subclass of neuron in the globus pallidus of the rat. J Neurosci 18:9438–9452.

Carter AG, Soler-Llavina GJ, Sabatini BL (2007) Timing and location of synaptic inputs determine modes of subthreshold integration in striatal medium spiny neurons. J Neurosci 27:8967–8977.

Catterall WA, Few AP (2008) Calcium channel regulation and presynaptic plasticity. Neuron 59:882–901.

Czubayko U, Plenz D (2002) Fast synaptic transmission between striatal spiny projection neurons. Proc Natl Acad Sci U S A 99:15764–15769.

Day M, Wokosin D, Plotkin JL, Tian X, Surmeier DJ (2008) Differential excitability and modulation of striatal medium spiny neuron dendrites. J Neurosci 28:11603–11614.

Ding J, Peterson JD, Surmeier DJ (2008) Corticostriatal and thalamostriatal synapses have distinctive properties. J Neurosci 28:6483–6492.

Graveland GA, DiFiglia M (1985) The frequency and distribution of medium-sized neurons with indented nuclei in the primate and rodent neostriatum. Brain Res 327:307–311.

Graybiel AM, Aosaki T, Flaherty AW, Kimura M (1994) The basal ganglia and adaptive motor control. Science 265:1826–1831.

Grillner S, Hellgren J, Ménard A, Saitoh K, Wikström MA (2005) Mechanisms for selection of basic motor programs—roles for the striatum and pallidum. Trends Neurosci 28:364–370.

Gupta A, Wang Y, Markram H (2000) Organizing principles for a diversity of GABAergic interneurons and synapses in the neocortex. Science 287:273–278.

Gustafson N, Gireesh-Dharmaraj E, Czubayko U, Blackwell KT, Plenz D (2006) A comparative voltage and current-clamp analysis of feedback and feedforward synaptic transmission in the striatal microcircuit in vitro. J Neurophysiol 95:737–752.

Hefft S, Jonas P (2005) Asynchronous GABA release generates long-lasting inhibition at a hippocampal interneuron-principal neuron synapse. Nat Neurosci 8:1319–1328.

Holmgren C, Harkany T, Svennenfors B, Zilberter Y (2003) Pyramidal cell communication within local networks in layer 2/3 of rat neocortex. J Physiol 551:139–153.

Hull C, Adesnik H, Scanziani M (2009) Neocortical disynaptic inhibition requires somatodendritic integration in interneurons. J Neurosci 29:8991–8995.

Kawaguchi Y (1995) Physiological subgroups of nonpyramidal cells with specific morphological characteristics in layer II/III of rat frontal cortex. J Neurosci 15:2638–2655.

Kawaguchi Y, Wilson CJ, Augood SJ, Emson PC (1995) Striatal interneurones: chemical, physiological and morphological characterization. Trends Neurosci 18:527–535.

Kita H, Kosaka T, Heizmann CW (1990) Parvalbumin-immunoreactive neurons in the rat neostriatum: a light and electron microscopic study. Brain Res 536:1–15.

Koós T, Tepper JM (1999) Inhibitory control of neostriatal projection neurons by GABAergic interneurons. Nat Neurosci 2:467–472.

Koós T, Tepper JM, Wilson CJ (2004) Comparison of IPSCs evoked by spiny and fast-spiking neurons in the neostriatum. J Neurosci 24:7916–7922.

Le Bé JV, Silberberg G, Wang Y, Markram H (2007) Morphological, electrophysiological, and synaptic properties of corticocallosal pyramidal cells in the neonatal rat neocortex. Cereb Cortex 17:2204–2213.

Mallet N, Le Moine C, Charpier S, Gonon F (2005) Feedforward inhibition of projection neurons by fast-spiking GABA interneurons in the rat striatum *in vivo*. J Neurosci 25:3857–3869.

Markram H, Lübke J, Frotscher M, Roth A, Sakmann B (1997) Physiology and anatomy of synaptic connections between thick tufted pyramidal neurones in the developing rat neocortex. J Physiol 500:409–440.

Markram H, Wang Y, Tsodyks M (1998) Differential signaling via the same axon of neocortical pyramidal neurons. Proc Natl Acad Sci U S A 95:5323–5328.

McHaffie JG, Stanford TR, Stein BE, Coizet V, Redgrave P (2005) Subcortical loops through the basal ganglia. Trends Neurosci 28:401–407.

Planert H, Grillner S, Robertson B, Silberberg G (2008) Intrinsic properties and synaptic connectivity of different subtypes of the striatal medium spiny neuron. Soc Neurosci Abstr 34:670.8.

Plenz D (2003) When inhibition goes incognito: feedback interaction between spiny projection neurons in striatal function. Trends Neurosci 26:436–443.

Rav-Acha M, Sagiv N, Segev I, Bergman H, Yarom Y (2005) Dynamic and spatial features of the inhibitory pallidal GABAergic synapses. Neuroscience 135:791–802.

Reyes A, Lujan R, Rozov A, Burnashev N, Somogyi P, Sakmann B (1998) Target-cell-specific facilitation and depression in neocortical circuits. Nat Neurosci 1:279–285.

Somogyi P, Bolam JP, Smith AD (1981) Monosynaptic cortical input and local axon collaterals of identified striatonigral neurons. A light and electron microscopic study using the Golgi-peroxidase transport-degeneration procedure. J Comp Neurol 195:567–584.

Surmeier DJ, Ding J, Day M, Wang Z, Shen W (2007) D1 and D2 dopamine-receptor modulation of striatal glutamatergic signaling in striatal medium spiny neurons. Trends Neurosci 30:228–235.

Taverna S, Canciani B, Pennartz CM (2007) Membrane properties and synaptic connectivity of fast-spiking interneurons in rat ventral striatum. Brain Res 1152:49–56.

Taverna S, Ilijic E, Surmeier DJ (2008) Recurrent collateral connections of striatal medium spiny neurons are disrupted in models of Parkinson's disease. J Neurosci 28:5504–5512.

Tecuapetla F, Carrillo-Reid L, Bargas J, Galarraga E (2007) Dopaminergic modulation of short-term synaptic plasticity at striatal inhibitory synapses. Proc Natl Acad Sci U S A 104:10258–10263.

Tecuapetla F, Koós T, Tepper JM, Kabbani N, Yeckel MF (2009) Differential dopaminergic modulation of neostriatal synaptic connections of striatopallidal axon collaterals. J Neurosci 29:8977–8990.

Tepper JM, Wilson CJ, Koós T (2008) Feedforward and feedback inhibition in neostriatal GABAergic spiny neurons. Brain Res Rev 58:272–281.

Thomson AM, Deuchars J, West DC (1993) Single axon excitatory postsynaptic potentials in neocortical interneurons exhibit pronounced paired pulse facilitation. Neuroscience 54:347–360.

Tsodyks M, Pawelzik K, Markram H (1998) Neural networks with dynamic synapses. Neural Comput 10:821–835.

Tunstall MJ, Oorschot DE, Kean A, Wickens JR (2002) Inhibitory interactions between spiny projection neurons in the rat striatum. J Neurophysiol 88:1263–1269.

Venance L, Glowinski J, Giaume C (2004) Electrical and chemical transmission between striatal GABAergic output neurones in rat brain slices. J Physiol 559:215–230.

Wang Y, Markram H, Goodman PH, Berger TK, Ma J, Goldman-Rakic PS (2006a) Heterogeneity in the pyramidal network of the medial prefrontal cortex. Nat Neurosci 9:534–542.

Wang Z, Kai L, Day M, Ronesi J, Yin HH, Ding J, Tkatch T, Lovinger DM, Surmeier DJ (2006b) Dopaminergic control of corticostriatal long-term synaptic depression in medium spiny neurons is mediated by cholinergic interneurons. Neuron 50:443–452.

Wilson CJ (2007) GABAergic inhibition in the neostriatum. Prog Brain Res 160:91–110.

Wilson CJ, Groves PM (1980) Fine structure and synaptic connections of the common spiny neuron of the rat neostriatum: a study employing intracellular inject of horseradish peroxidase. J Comp Neurol 194:599–615.

III

Systems/Circuits

Target Selectivity of Feedforward Inhibition by Striatal Fast-Spiking Interneurons

Susanne N. Szydlowski,* Iskra Pollak Dorocic,* Henrike Planert,* Marie Carlén, Konstantinos Meletis, and Gilad Silberberg

Department of Neuroscience, Karolinska Institutet, Stockholm 17177, Sweden

The striatal microcircuitry consists of a vast majority of projection neurons, the medium spiny neurons (MSNs), and a small yet diverse population of interneurons. To understand how activity is orchestrated within the striatum, it is essential to unravel the functional connectivity between the different neuronal types. Fast-spiking (FS) interneurons provide feedforward inhibition to both direct and indirect pathway MSNs and are important in sculpting their output to downstream basal ganglia nuclei. FS interneurons are also interconnected with each other via electrical and chemical synapses; however, whether and how they inhibit other striatal interneuron types remains unknown. In this study we combined multineuron whole-cell recordings with optogenetics to determine the target selectivity of feedforward inhibition by striatal FS interneurons. Using transgenic and viral approaches we directed expression of channelrhodopsin 2 (ChR2) to FS interneurons to study their connectivity within the mouse striatal microcircuit. Optogenetic stimulation of ChR2-expressing FS interneurons generated strong and reliable $GABA_A$-dependent synaptic inputs in MSNs. In sharp contrast, simultaneously recorded neighboring cholinergic interneurons did not receive any synaptic inputs from photostimulated FS cells, and a minority of low-threshold spiking (LTS) interneurons responded weakly. We further tested the synaptic connectivity between FS and LTS interneurons using paired recordings, which showed only sparse connectivity. Our results show that striatal FS interneurons form a feedforward inhibitory circuit that is target selective, inhibiting projection neurons while avoiding cholinergic interneurons and sparsely contacting LTS interneurons, thus supporting independent modulation of MSN activity by the different types of striatal interneurons.

Introduction

Striatal and neocortical circuits share a common structural principle: a major projecting neuronal population interlaced with a small yet diverse interneuron population (Kawaguchi et al., 1995; Markram et al., 2004). One important and functionally distinct interneuron type, the fast-spiking (FS) interneuron, provides robust perisomatic inhibition to projection neurons in both striatal (Kita et al., 1990; Bennett and Bolam, 1994; Koós and Tepper, 1999; Gittis et al., 2010; Planert et al., 2010) and cortical (Somogyi et al., 1998; Gupta et al., 2000; Tamás et al., 2000) microcircuits. In the neocortex, recent studies have shown a seemingly unselective synaptic connectivity between FS interneurons and a vast majority of neighboring neocortical neurons of all types (Staiger et al., 1997; Gibson et al., 1999; Deans et al., 2001; Cruikshank et al., 2010; Gittis et al., 2010; Packer and Yuste, 2011; Avermann et al., 2012). Similarly, both direct and indirect pathway striatal medium spiny neurons (MSNs) receive synaptic inputs from nearby FS interneurons (Gittis et al., 2010; Planert et al., 2010). FS interneurons are also interconnected by electrical and GABAergic synapses (Koós and Tepper, 1999; Gittis et al., 2010). In the neocortex, a high degree of reciprocal connectivity was described between neighboring FS and low-threshold spiking (LTS) interneurons using paired recordings (Gibson et al., 1999; Deans et al., 2001; Ma et al., 2012). Whether striatal FS interneurons target other interneuron types such as cholinergic and LTS interneurons has not been established.

Striatal cholinergic interneurons are involved in various forms of corticostriatal synaptic plasticity (Wang et al., 2006; Pisani et al., 2007) and provide the cholinergic modulation of striatal neurons and synapses (Koós and Tepper, 2002; Pakhotin and Bracci, 2007; Shen et al., 2007). As seen *in vivo*, they are highly synchronized (Raz et al., 1996), suggesting that they may be driven by common inhibitory input from GABAergic striatal interneurons (Sullivan et al., 2008). Paired recordings revealed no synaptic connectivity between different types of striatal interneurons (Gittis et al., 2010); however, optogenetic activation of cholinergic interneurons resulted in polysynaptic inhibition of MSNs and weaker responses in FS interneurons (English et al., 2012). Morphological reconstructions of parvalbumin-positive (PV+) and ChAT+ interneurons in rat striatum indicated only unidirectional connectivity from cholinergic to PV+ interneurons (Chang and Kita, 1992) although PV+ synapses were reported to target cholinergic interneurons in primates (Gonzales et al., 2012). Whether and to what extent target selectivity exists

Received July 26, 2012; revised Nov. 24, 2012; accepted Dec. 5, 2012.

Author contributions: M.C., K.M., and G.S. designed research; S.N.S., I.P.D., H.P., and G.S. performed research; S.N.S., I.P.D., H.P., M.C., K.M., and G.S. analyzed data; S.N.S., H.P., K.M., and G.S. wrote the paper.

This study has been supported by National Alliance for Research on Schizophrenia and Depression Young Investigator grants (M.C. and K.M.), a Marie Curie European reintegration grant (K.M.), Knut och Alice Wallenberg Foundation (M.C. and K.M.), Hjärnfonden (M.C and K.M.), StratNeuro (G.S. and K.M.), and ERC starting grant (G.S.). We thank Karl Deisseroth for the ChR2-mCherry vector and Silvia Arber for the transgenic PV-Cre mice. We thank Abdel El Manira and Paul Bolam for comments on this manuscript.

*S.N.S., I.P.D., and H.P. contributed equally to this work.

Correspondence should be addressed to either of the following at the above address: Gilad Silberberg or Konstantinos Meletis. E-mail: gilad.silberberg@ki.se or dinos.meletis@ki.se.

DOI:10.1523/JNEUROSCI.3572-12.2013

 0270-6474/13/331678-06$15.00/0

between different classes of striatal interneurons has not been unequivocally established, largely due to the limitation of available techniques.

In this study we aimed to resolve the question of target selectivity of striatal FS interneurons by using optogenetic techniques enabling us to selectively stimulate FS interneurons while simultaneously recording from several neighboring neurons of different types.

Materials and Methods

Animals. All experiments were performed according to the Guidelines of the Stockholm municipal committee for animal experiments. PV-Cre mice (Hippenmeyer et al., 2005) of either sex ($n = 49$) were virus injected and used for slice recordings and immunohistochemical analysis 10–18 d after injections. To assess the direct connectivity between interneurons, we also used Lhx6-GFP BAC (bacterial artificial chromosome) transgenic mice ($n = 14$) in which FS and LTS interneurons express GFP.

Virus injections. Animals were anesthetized with isoflurane and placed in a stereotaxic frame (Harvard Apparatus). A small craniotomy was made 0.5 mm anterior to bregma and 2.0 mm lateral to the midline. Between 0.8 and 1.5 μl of virus (pAAV-Ef1a-DIO-hChR2(H134R)-mCherry-WPRE-pA) was injected by a micropipette at two ventral coordinates, −2.5 and −2.0 mm, at 0.1 μl min^{-1} by Quintessential Stereotaxic Injector (Stoelting) The pipette was held in place for 5 min after the injection before being slowly retracted from the brain. Postinjection analgesics were given (0.03 mg/kg buprenorphine).

Slice preparation and whole-cell recordings. Mice at postnatal day 24–51 were killed and used for slice recordings. They were anesthetized with isoflurane and their brains removed in ice-cold artificial CSF containing the following (in mM): 125 NaCl, 25 glucose, 25 $NaHCO_3$, 2.5 KCl, 2 $CaCl_2$, 1.25 NaH_2PO_4, 1 $MgCl_2$. Parasagittal slices, 250 μm thick, were cut (Leica VT 1000S), then transferred to 35°C for 30–60 min and then kept at room temperature (22−24°C). Whole-cell patch recordings were obtained at 35 ± 0.5°C. Glass electrodes were pulled with a Flaming/Brown micropipette puller P-97 (Sutter Instruments) and had a resistance of 5–10 MΩ. They contained (in mM) 105 K-gluconate, 30 KCl, 10 HEPES, 10 Na-Phosphocreatine, 4 Mg-ATP, 0.3 Na-GTP, and in some experiments 0.3% Neurobiotin. Neurons were visualized with infrared differential interference contrast (IR-DIC) microscopy (Zeiss FS Axioskop) and fluorescent microscopy, using a mercury lamp (HBO 100, Zeiss) and a fluorescent filter cube mounted on the same microscope. Pairs, triplets, and quadruplets of neurons were recorded within a range of 200 μm from mCherry fluorescently labeled somata. Recordings were done in current-clamp mode with access resistance compensated throughout the experiment. Experiments with access resistance >35 MΩ were discarded. Recordings were amplified using MultiClamp 700B (Molecular Devices) and digitized by an ITC-18 (HEKA Elektronik) acquisition board. Data were acquired and analyzed using IGOR Pro (WaveMetrics). Liquid junction potential was not corrected for and is approximated to be ~10 mV. Photostimulation was generated through a 1 watt blue LED (wavelength 465 nm) mounted on the microscope oculars and delivered through the objective lens. In a few experiments the same LED was mounted under the slice as described previously (English et al., 2012), providing illumination to the entire field. Photostimulation was controlled by a LED driver (Mightex Systems) connected to the ITC-18 acquisition board, enabling control over the duration and intensity. The photostimulation diameter through the objective lens was ~400 μm with an illumination intensity of 9 mW/mm^2.

Stimulation protocols and analysis. Recorded neurons were subject to various stimulation protocols to determine the synaptic and electrical properties. Synaptic connections were characterized by stimulation of a presynaptic neuron with a train (10 or 20 Hz) of 8 brief current pulses (0.5–2 nA, 3 ms) or by blue light pulses (2 ms). Postsynaptic neurons were held between −70 and −80 mV to ensure depolarizing responses to GABAergic synapses, and traces were removed for analysis when depolarized more than −60 mV. The GABA reversal potential was approximately −30 mV and synaptic input could induce MSN action potential discharge when it was held just below threshold. Parameters describing the dynamics of recorded synapses included the synaptic utilization parameter (U, equivalent to release probability), the time constants of recovery from depression (D) and facilitation (F). These parameters were extracted using the model for synaptic dynamics (Markram et al., 1998; Tsodyks et al., 1998; Planert et al., 2010).

Immunohistochemistry. Mice were transcardially perfused with 100 mM PBS followed by 4% formaldehyde in PBS, and brains were postfixed for 18 h at 4°C. Sections of 40 μm were cut using a vibratome (Leica VT1000), and free-floating sections were incubated in blocking solution (10% donkey serum in PBS with 0.3% Triton X-100) for 1 h at 22°C and then incubated with primary antibody (parvalbumin PVG-214; Swant; 1:2000) in blocking solution overnight at 22°C. Antibody staining was revealed using species-specific fluorophore-conjugated secondary antibodies. Spread and labeling efficiency were scored for the presence of mCherry fluorescence. For quantification of colabeling of channelrhodopsin 2 (ChR2)-mCherry and parvalbumin, confocal images were acquired using confocal microscopy (Zeiss LSM 510) and individual cells were identified independently for each of the two fluorescent channels.

Results

To selectively activate striatal FS interneurons, we genetically targeted expression of ChR2 to PV+ cells. We injected an adeno-associated viral (AAV) vector, which expressed a ChR2-mCherry fusion protein in a Cre-dependent manner, into the striatum of transgenic PV-Cre mice, thereby achieving specific ChR2 expression in PV+/FS cells (Cardin et al., 2009). We targeted injections to the dorsolateral striatum and found virally transduced cells within a diameter of 300 ± 100 μm. Neurons expressing mCherry-ChR2 were PV positive (97%, Fig. 1*A*), confirming the genetic restriction of ChR2 to PV+ neurons.

We targeted whole-cell recordings to mCherry-expressing neurons using combined fluorescent and IR-DIC microscopy (Fig. 1*B*) and characterized the optogenetic activation of these neurons by delivering short pulses of blue light (see Materials and Methods). All neurons identified by fluorescence and depolarizing response to light stimulation were FS interneurons ($n = 24$ of 24), as determined by their characteristic electrophysiological properties such as non-accommodating discharge pattern, high discharge rate, narrow action potentials, and fast and deep afterhyperpolarization (Fig. 1*D*). Interneurons responded to light pulses with strong and immediate depolarization, leading in most cases ($n = 12$ of 19) to action potential discharge (Fig. 1*E*). In those cases, light pulses of 2 ms duration were usually sufficient to induce action potentials, enabling the stimulation of FS interneurons with trains of action potentials (Fig. 1*G*). Occasionally, short (2 ms) light pulses induced discharge of spike-doublets, as recorded from photostimulated FS interneurons (see example in Fig. 1*G*). Longer light pulses induced membrane depolarization throughout the illumination duration, indicating activation of ChR2 in recorded neurons.

To determine the precise connectivity between FS interneurons and other neuronal types within the striatal microcircuit, we characterized the synaptic connectivity of ChR2-expressing FS interneurons onto their neighboring neurons. We recorded from neurons in proximity to the ChR2-expressing FS interneurons (Fig. 2*A*), where the majority of nonfluorescent neurons were MSNs, as characterized by their hyperpolarized membrane potential (−77.5 ± 5.7 mV) and typical inward rectification response to hyperpolarizing and depolarizing current steps (Fig. 2*C*). Most MSNs ($n = 112$ of 163) responded to brief 2 ms light pulses with a strong and reliable synaptic response (Fig. 2*D*). In a majority of the cases where a responding MSN was recorded simultaneously with a neighboring MSN, they both responded ($n = 90$ of 106). In cases where MSNs did not receive synaptic

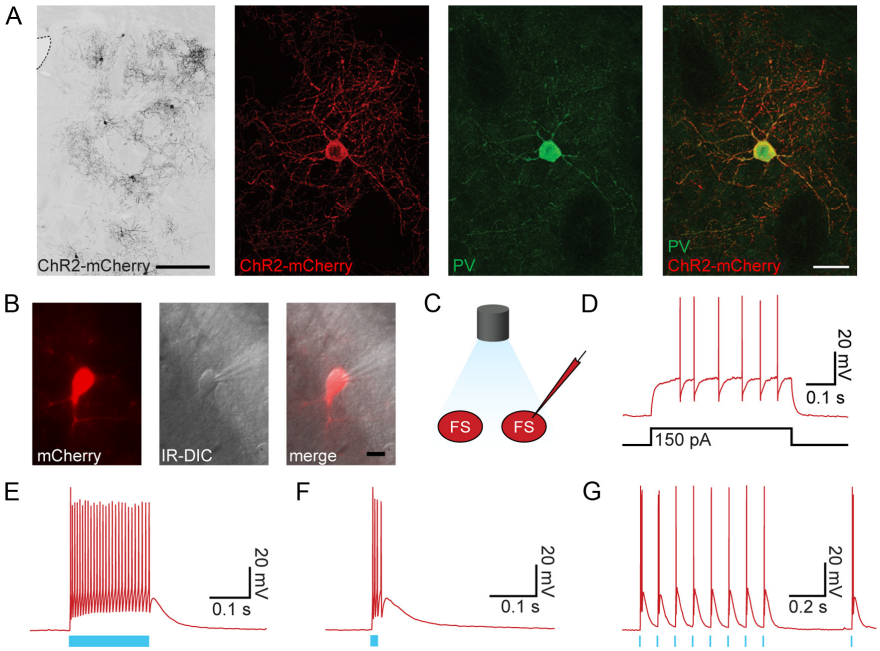

Figure 1. Optogenetic control of striatal PV-expressing FS interneurons. ***A***, Confocal images of parvalbumin-expressing striatal interneurons with ChR2-mCherry expression. Overview of fluorescent image showing ChR2 (black) expression in striatal PV+ interneurons. The lateral ventricle is delineated (left). Scale bar, 250 μm. Magnification of a ChR2-mCherry-labeled neuron (middle left). The same neuron with PV immunostaining (middle right). Merged image demonstrating colocalization (right). Scale bar, 25 μm. ***B***, A fluorescent image showing mCherry expression (left). The same interneuron visualized and recorded under IR microscopy (middle), and the merged image (right). ***C***, Illustration of the experimental set-up with optogenetic stimulation of FS interneurons and targeted whole-cell recording. ***D***, Typical electrophysiological response of an FS interneuron to a suprathreshold step current injection. ***E***, Response of the FS interneuron to photostimulation with a single 200 ms pulse. ***F***, Response of the same FS interneuron to a single 10 ms pulse. ***G***, Response of the same FS interneuron to a train of light pulses (10 Hz, 2 ms duration). Blue bars illustrate the light stimulation period.

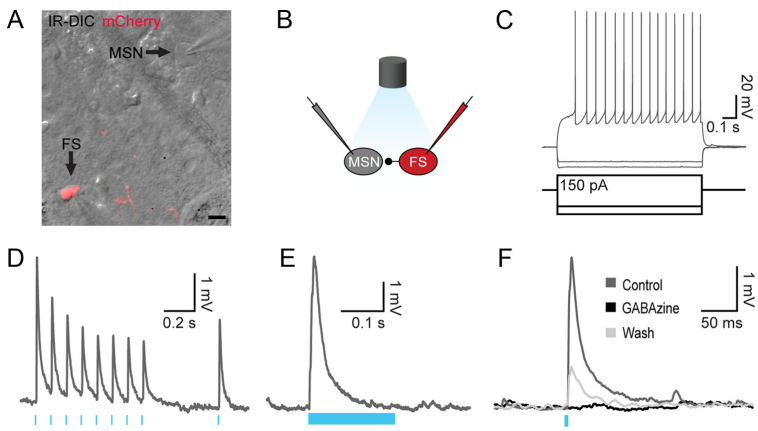

Figure 2. Light-induced feedforward inhibition from striatal PV-expressing FS interneurons onto MSNs. ***A***, Image showing IR-DIC and fluorescent red signal during dual patching of a ChR2-mCherry-expressing FS cell and a neighboring MSN. Scale bar, 10 μm. ***B***, Illustration of the experimental set-up with optogenetic stimulation and paired recording from an FS interneuron and MSN. ***C***, Example of the electrophysiological response of an MSN to step current injections. ***D***, Depressing synaptic input to a MSN following a train of blue light pulses (10 Hz, 2 ms). ***E***, Response of the same MSN to a 200 ms blue light pulse. ***F***, Postsynaptic response of an MSN to optogenetic activation (5 ms) of FS cells before, during, and after application of 10 μM gabazine. The response was abolished following gabazine application and partially recovered after washout ($n = 6$ of 6).

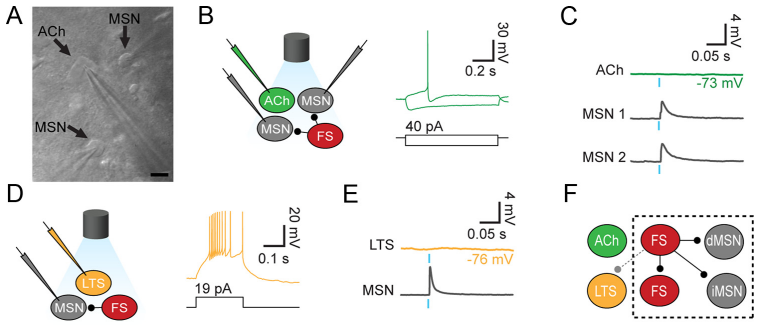

Figure 3. Target selectivity of striatal PV-expressing FS interneurons. ***A***, Simultaneous whole-cell recording of two MSNs and a cholinergic interneuron under IR-DIC microscopy. Scale bar, 10 μm. ***B***, Illustration of experimental set-up with optogenetic stimulation of FS cells and whole-cell recordings from two MSNs and a cholinergic interneuron (ACh). Typical electrophysiological response of a cholinergic interneuron to step current injections. ***C***, Photostimulation of FS cells (2 ms pulse) and responses in MSNs and cholinergic interneurons. Simultaneous whole-cell recordings from cholinergic interneuron and MSNs revealed no synaptic response in the cholinergic interneuron while the neighboring MSNs received reliable synaptic input. ***D***, Illustration of experimental set-up with optogenetic stimulation of FS cells and whole-cell recordings from MSNs and LTS interneurons. Typical response of a LTS interneuron to a step current injection. ***E***, Photostimulation of FS cells (2 ms pulse) and responses in MSNs and LTS interneurons. Simultaneous whole-cell recordings from LTS interneuron and MSNs reveal no synaptic response in the LTS interneuron while a neighboring MSN shows clear responses. ***F***, Schematic model of the identified connectivity from striatal FS interneurons targeting MSNs (direct and indirect pathway MSNs) as well as neighboring FS interneurons, with sparse connectivity to LTS interneurons and none to cholinergic interneurons.

input following light stimulation, most simultaneously recorded MSNs did not receive inputs either ($n = 36$ of 50). These results suggest that the reason for nonresponsive MSNs was inability to induce light-evoked discharge in neighboring FS interneurons, rather than the lack of synaptic FS–MSN connectivity. The recorded light-induced synaptic responses were $GABA_A$-R dependent (Fig. 2*F*, $n = 6$ of 6 blocked by 10 μM gabazine). Light-induced synaptic responses were more than four times larger than unitary direct connections recorded in FS–MSN pairs in the same slices (7.5 ± 7.4 mV, $n = 47$ vs 1.8 ± 1.4 mV $n = 14$, $p < 0.001$), suggesting that photostimulation triggered action potential discharge in several labeled FS interneurons. Stimulation with trains of light pulses (10 Hz, 2 ms, Fig. 2*D*) induced depressing synaptic responses, similar to previously reported direct connections between FS interneurons and MSNs (Planert et al., 2010; Gittis et al., 2011; Klaus et al., 2011). The dynamic properties of light-evoked synaptic responses were quantified using a model for synaptic dynamics (Markram et al., 1998; Tsodyks et al., 1998) (see Materials and Methods) and compared with direct FS–MSN connections recorded in the same animals ($n = 13$ synaptically connected pairs). Time constants for depression and facilitation in optical versus direct synaptic connections were similar ($p > 0.5$, $n = 13$ optical and $n = 11$ direct connections); however, the release probability (utilization factor, U) was higher in the light-induced responses (U = 0.59 ± 0.18 vs 0.46 ± 0.06, $p = 0.03$), apparent also in a smaller paired-pulse ratio in light-induced responses compared with direct connections (0.65 ± 0.22 vs 0.84 ± 0.19, $p = 0.03$). This apparent difference in synaptic release is likely to be caused by the doublets of action potentials observed in some cases (for example Fig. 1*G*), also described previously for the activation of ChR2 (Gunaydin et al., 2010).

To study the synaptic connectivity from FS interneurons to other types of striatal interneurons, we recorded from cholinergic and LTS interneurons during photostimulation of ChR2-expressing FS cells. To confirm the proper optogenetic light activation of FS interneurons and their synaptic transmission at the recording area, we simultaneously recorded from pairs or triplets of neurons, in which at least one MSN or FS interneuron exhibited light-induced synaptic responses or action potentials, respectively (Fig. 3). Cholinergic interneurons were identified using typical morphological and electrophysiological properties, including large soma, depolarized membrane potential (−53.0 ± 5.6 mV), voltage sag response, and pronounced discharge accommodation (Fig. 3*B*). Interestingly, cholinergic interneurons ($n = 13$) did not show any synaptic events following light activation of ChR2-expressing FS interneurons, in contrast to the simultaneous strong and reliable synaptic response recorded at nearby (<100 μm) MSNs ($n = 13$ of 13, Fig. 3*C*). We also recorded from LTS interneurons, characterized by their high input resistance (471 ± 170 MΩ), lower action potential discharge threshold (−47.3 ± 2.4 mV), depolarized membrane potential (−44 ± 5 mV), long membrane time constant (21 ± 7 ms), and accommodating discharge to a step current injection (Fig. 3*D*). Most LTS interneurons ($n = 4$ of 5) did not receive any synaptic inputs following photostimulation of FS interneurons, while the neighboring neurons recorded simultaneously all responded, suggesting that LTS interneurons are only sparsely targeted by neighboring FS cells (Fig. 3*E*). The single LTS that responded to optogenetic stimulation displayed relatively weak responses (2.1 mV), compared with large responses recorded from two neighboring MSNs (9.6 and 6.9 mV). To further assess the connectivity between FS and LTS interneurons, we recorded from pairs of FS and LTS interneurons. To facilitate interneuron recordings we used Lhx6-GFP transgenic mice in which LTS and FS interneurons are fluorescently labeled (Gittis et al., 2010). Indeed, from 12 tested FS–LTS pairs we found only two, weak (0.5 and 0.8 mV) synaptic connections, both from FS to LTS, further supporting the results obtained by optogenetic stimulation.

In summary, our work has identified that feedforward inhibition from striatal FS interneurons is highly selective, reliably targeting MSNs and FS interneurons while avoiding cholinergic interneurons and only sparsely contacting LTS interneurons (schematic in Fig. 3*F*).

Discussion

In this study we showed that feedforward inhibition exerted by striatal FS interneurons is not promiscuous but highly selective in terms of postsynaptic targets. FS interneurons contact neighboring MSNs with high probability providing strong and reliable

inhibition, while cholinergic interneurons are avoided and LTS interneurons are contacted only with low probability. Interestingly, neocortical FS interneurons display a similar targeting pattern onto pyramidal neurons (Somogyi et al., 1998; Gupta et al., 2000; Packer and Yuste, 2011), while also forming reciprocal electrical and chemical connections with each other (Galarreta and Hestrin, 1999; Gibson et al., 1999). Both striatal and neocortical projection neurons are sparsely interconnected, with a minority of neighboring neurons forming synaptic connections (Markram et al., 1997; Czubayko and Plenz, 2002; Tunstall et al., 2002; Taverna et al., 2008; Brown and Hestrin, 2009; Planert et al., 2010). In contrast, connectivity from FS interneurons onto projection neurons is robust and widespread (Koós and Tepper, 1999; Gittis et al., 2010; Gittis et al., 2011; Packer and Yuste, 2011).

Despite the similar electrophysiological properties between cortical and striatal FS and LTS interneurons (Kubota and Kawaguchi, 1994; Kawaguchi and Kubota, 1997), there are important differences in microcircuit architecture. First, unlike striatum, neocortical FS interneurons form reciprocal connections with LTS interneurons (Gibson et al., 1999; Deans et al., 2001; Cruikshank et al., 2010) and other interneuron types (Staiger et al., 1997; Gupta et al., 2000; Avermann et al., 2012). Second, the dominant reciprocal connectivity between neocortical interneurons and projection neurons (Reyes et al., 1998; Beierlein et al., 2003; Holmgren et al., 2003; Silberberg and Markram, 2007) is not found in striatum, where feedforward inhibition from FS onto MSNs is unidirectional (Koós and Tepper, 1999; Gittis et al., 2010; Planert et al., 2010; Chuhma et al., 2011). The degree of target selectivity of cortical FS interneurons within cortical microcircuits is not fully characterized and it remains to be seen whether it follows similar rules as in the striatal microcircuitry.

Our results show no functional synaptic connectivity from striatal PV+ to cholinergic interneurons. While in agreement with previous anatomical results from rat striatum (Chang and Kita, 1992), there is an apparent discrepancy with recent data from macaque monkey putamen, where PV+ terminals were shown to form symmetric synapses with dendrites of cholinergic neurons (Gonzales et al., 2012). There are a few possible explanations to this discrepancy. First, the symmetric PV+ terminals may originate from pallidostriatal axons (Kita et al., 1999; Mallet et al., 2012), which would therefore not be infected by the viral injection in the striatum. Second, the reported cholinergic neurons were targeted on distal dendrites, which may result in electrotonic attenuation in our somatic recordings. Third, the contrasting findings may indicate differences between the studied species, which would also explain the differences between the two aforementioned anatomical studies (Chang and Kita, 1992; Gonzales et al., 2012).

Functional implications

The selectivity in FS interneuron feedforward inhibition suggests independent roles for different interneuron types in sculpting striatal output. The striatum receives convergent input from various sources such as glutamatergic inputs from cortex and thalamus (Dubé et al., 1988; Thomas et al., 2000; Ding et al., 2008; Doig et al., 2010), dopaminergic inputs from the substantia nigra pars compacta, and GABAergic inputs from the globus pallidus (Bevan et al., 1998; Mallet et al., 2012). The way these inputs orchestrate striatal output depends not only on their direct projections onto MSNs but also on their connectivity onto different interneuron types. The avoidance of cholinergic interneurons suggests that their correlation in pauses and discharge (Raz et al., 1996) is not generated by FS-mediated feedforward inhibition. MSNs therefore receive independent streams of feedforward inhibition, one of which is mediated by FS interneurons (Koós and Tepper, 1999; Gage et al., 2010), another provided by cholinergic interneurons (English et al., 2012), in addition to the lateral inhibition between MSNs (Tunstall et al., 2002) and pallidal input (Mallet et al., 2012). This richness of GABAergic pathways is crucial for the differential sculpting of striatal output under a variety of conditions and brain states.

References

Avermann M, Tomm C, Mateo C, Gerstner W, Petersen CC (2012) Microcircuits of excitatory and inhibitory neurons in layer 2/3 of mouse barrel cortex. J Neurophysiol 107:3116–3134. CrossRef Medline

Beierlein M, Gibson JR, Connors BW (2003) Two dynamically distinct inhibitory networks in layer 4 of the neocortex. J Neurophysiol 90: 2987–3000. CrossRef Medline

Bennett BD, Bolam JP (1994) Synaptic input and output of parvalbumin-immunoreactive neurons in the neostriatum of the rat. Neuroscience 62:707–719. CrossRef Medline

Bevan MD, Booth PA, Eaton SA, Bolam JP (1998) Selective innervation of neostriatal interneurons by a subclass of neuron in the globus pallidus of the rat. J Neurosci 18:9438–9452. Medline

Brown SP, Hestrin S (2009) Intracortical circuits of pyramidal neurons reflect their long-range axonal targets. Nature 457:1133–1136. CrossRef Medline

Cardin JA, Carlén M, Meletis K, Knoblich U, Zhang F, Deisseroth K, Tsai LH, Moore CI (2009) Driving fast-spiking cells induces gamma rhythm and controls sensory responses. Nature 459:663–667. CrossRef Medline

Chang HT, Kita H (1992) Interneurons in the rat striatum: relationships between parvalbumin neurons and cholinergic neurons. Brain Res 574: 307–311. CrossRef Medline

Chuhma N, Tanaka KF, Hen R, Rayport S (2011) Functional connectome of the striatal medium spiny neuron. J Neurosci 31:1183–1192. CrossRef Medline

Cruikshank SJ, Urabe H, Nurmikko AV, Connors BW (2010) Pathway-specific feedforward circuits between thalamus and neocortex revealed by selective optical stimulation of axons. Neuron 65:230–245. CrossRef Medline

Czubayko U, Plenz D (2002) Fast synaptic transmission between striatal spiny projection neurons. Proc Natl Acad Sci U S A 99:15764–15769. CrossRef Medline

Deans MR, Gibson JR, Sellitto C, Connors BW, Paul DL (2001) Synchronous activity of inhibitory networks in neocortex requires electrical synapses containing connexin36. Neuron 31:477–485. CrossRef Medline

Ding J, Peterson JD, Surmeier DJ (2008) Corticostriatal and thalamostriatal synapses have distinctive properties. J Neurosci 28:6483–6492. CrossRef Medline

Doig NM, Moss J, Bolam JP (2010) Cortical and thalamic innervation of direct and indirect pathway medium-sized spiny neurons in mouse striatum. J Neurosci 30:14610–14618. CrossRef Medline

Dubé L, Smith AD, Bolam JP (1988) Identification of synaptic terminals of thalamic or cortical origin in contact with distinct medium-size spiny neurons in the rat neostriatum. J Comp Neurol 267:455–471. CrossRef Medline

English DF, Ibanez-Sandoval O, Stark E, Tecuapetla F, Buzsáki G, Deisseroth K, Tepper JM, Koos T (2012) GABAergic circuits mediate the reinforcement-related signals of striatal cholinergic interneurons. Nat Neurosci 15:123–130. CrossRef Medline

Gage GJ, Stoetzner CR, Wiltschko AB, Berke JD (2010) Selective activation of striatal fast-spiking interneurons during choice execution. Neuron 67: 466–479. CrossRef Medline

Galarreta M, Hestrin S (1999) A network of fast-spiking cells in the neocortex connected by electrical synapses. Nature 402:72–75. CrossRef Medline

Gibson JR, Beierlein M, Connors BW (1999) Two networks of electrically coupled inhibitory neurons in neocortex. Nature 402:75–79. CrossRef Medline

Gittis AH, Nelson AB, Thwin MT, Palop JJ, Kreitzer AC (2010) Distinct roles of GABAergic interneurons in the regulation of striatal output pathways. J Neurosci 30:2223–2234. CrossRef Medline

Gittis AH, Hang GB, LaDow ES, Shoenfeld LR, Atallah BV, Finkbeiner S, Kreitzer AC (2011) Rapid target-specific remodeling of fast-spiking in-

hibitory circuits after loss of dopamine. Neuron 71:858–868. CrossRef Medline

Gonzales KK, Pare JF, Wichmann T, Smith Y (2012) GABAergic regulation of striatal cholinergic interneurons: synaptic inputs from fastforward parvalbumin-containing interneurons. Soc Neurosci Abstr 38:790.07.

Gunaydin LA, Yizhar O, Berndt A, Sohal VS, Deisseroth K, Hegemann P (2010) Ultrafast optogenetic control. Nat Neurosci 13:387–392. CrossRef Medline

Gupta A, Wang Y, Markram H (2000) Organizing principles for a diversity of GABAergic interneurons and synapses in the neocortex. Science 287: 273–278. CrossRef Medline

Hippenmeyer S, Vrieseling E, Sigrist M, Portmann T, Laengle C, Ladle DR, Arber S (2005) A developmental switch in the response of DRG neurons to ETS transcription factor signaling. PLoS Biol 3:e159. CrossRef Medline

Holmgren C, Harkany T, Svennenfors B, Zilberter Y (2003) Pyramidal cell communication within local networks in layer 2/3 of rat neocortex. J Physiol 551:139–153. CrossRef Medline

Kawaguchi Y, Kubota Y (1997) GABAergic cell subtypes and their synaptic connections in rat frontal cortex. Cereb Cortex 7:476–486. CrossRef Medline

Kawaguchi Y, Wilson CJ, Augood SJ, Emson PC (1995) Striatal interneurones: chemical, physiological and morphological characterization. Trends Neurosci 18:527–535. CrossRef Medline

Kita H, Kosaka T, Heizmann CW (1990) Parvalbumin-immunoreactive neurons in the rat neostriatum: a light and electron microscopic study. Brain Res 536:1–15. CrossRef Medline

Kita H, Tokuno H, Nambu A (1999) Monkey globus pallidus external segment neurons projecting to the neostriatum. Neuroreport 10:1467–1472. CrossRef Medline

Klaus A, Planert H, Hjorth JJ, Berke JD, Silberberg G, Kotaleski JH (2011) Striatal fast-spiking interneurons: from firing patterns to postsynaptic impact. Front Syst Neurosci 5:57. Medline

Koós T, Tepper JM (1999) Inhibitory control of neostriatal projection neurons by GABAergic interneurons. Nat Neurosci 2:467–472. CrossRef Medline

Koós T, Tepper JM (2002) Dual cholinergic control of fast-spiking interneurons in the neostriatum. J Neurosci 22:529–535. Medline

Kubota Y, Kawaguchi Y (1994) Three classes of GABAergic interneurons in neocortex and neostriatum. Jpn J Physiol 44[Suppl 2]:S145–S148.

Ma Y, Hu H, Agmon A (2012) Short-term plasticity of unitary inhibitory-to-inhibitory synapses depends on the presynaptic interneuron subtype. J Neurosci 32:983–988. CrossRef Medline

Mallet N, Micklem BR, Henny P, Brown MT, Williams C, Bolam JP, Nakamura KC, Magill PJ (2012) Dichotomous organization of the external globus pallidus. Neuron 74:1075–1086. CrossRef Medline

Markram H, Lübke J, Frotscher M, Roth A, Sakmann B (1997) Physiology and anatomy of synaptic connections between thick tufted pyramidal neurones in the developing rat neocortex. J Physiol 500:409–440. Medline

Markram H, Wang Y, Tsodyks M (1998) Differential signaling via the same axon of neocortical pyramidal neurons. Proc Natl Acad Sci U S A 95: 5323–5328. CrossRef Medline

Markram H, Toledo-Rodriguez M, Wang Y, Gupta A, Silberberg G, Wu C (2004) Interneurons of the neocortical inhibitory system. Nat Rev Neurosci 5:793–807. CrossRef Medline

Packer AM, Yuste R (2011) Dense, unspecific connectivity of neocortical parvalbumin-positive interneurons: a canonical microcircuit for inhibition? J Neurosci 31:13260–13271. CrossRef Medline

Pakhotin P, Bracci E (2007) Cholinergic interneurons control the excitatory input to the striatum. J Neurosci 27:391–400. CrossRef Medline

Pisani A, Bernardi G, Ding J, Surmeier DJ (2007) Re-emergence of striatal cholinergic interneurons in movement disorders. Trends Neurosci 30: 545–553. CrossRef Medline

Planert H, Szydlowski SN, Hjorth JJ, Grillner S, Silberberg G (2010) Dynamics of synaptic transmission between fast-spiking interneurons and striatal projection neurons of the direct and indirect pathways. J Neurosci 30:3499–3507. CrossRef Medline

Raz A, Feingold A, Zelanskaya V, Vaadia E, Bergman H (1996) Neuronal synchronization of tonically active neurons in the striatum of normal and parkinsonian primates. J Neurophysiol 76:2083–2088. Medline

Reyes A, Lujan R, Rozov A, Burnashev N, Somogyi P, Sakmann B (1998) Target-cell-specific facilitation and depression in neocortical circuits. Nat Neurosci 1:279–285. CrossRef Medline

Shen W, Tian X, Day M, Ulrich S, Tkatch T, Nathanson NM, Surmeier DJ (2007) Cholinergic modulation of Kir2 channels selectively elevates dendritic excitability in striatopallidal neurons. Nat Neurosci 10:1458–1466. CrossRef Medline

Silberberg G, Markram H (2007) Disynaptic inhibition between neocortical pyramidal cells mediated by Martinotti cells. Neuron 53:735–746. CrossRef Medline

Somogyi P, Tamás G, Lujan R, Buhl EH (1998) Salient features of synaptic organisation in the cerebral cortex. Brain Res Brain Res Rev 26:113–135. Medline

Staiger JF, Freund TF, Zilles K (1997) Interneurons immunoreactive for vasoactive intestinal polypeptide (VIP) are extensively innervated by parvalbumin-containing boutons in rat primary somatosensory cortex. Eur J Neurosci 9:2259–2268. CrossRef Medline

Sullivan MA, Chen H, Morikawa H (2008) Recurrent inhibitory network among striatal cholinergic interneurons. J Neurosci 28:8682–8690. CrossRef Medline

Tamás G, Buhl EH, Lörincz A, Somogyi P (2000) Proximally targeted GABAergic synapses and gap junctions synchronize cortical interneurons. Nat Neurosci 3:366–371. CrossRef Medline

Taverna S, Ilijic E, Surmeier DJ (2008) Recurrent collateral connections of striatal medium spiny neurons are disrupted in models of Parkinson's disease. J Neurosci 28:5504–5512. CrossRef Medline

Thomas TM, Smith Y, Levey AI, Hersch SM (2000) Cortical inputs to m2-immunoreactive striatal interneurons in rat and monkey. Synapse 37: 252–261. CrossRef Medline

Tsodyks M, Pawelzik K, Markram H (1998) Neural networks with dynamic synapses. Neural Comput 10:821–835. CrossRef Medline

Tunstall MJ, Oorschot DE, Kean A, Wickens JR (2002) Inhibitory interactions between spiny projection neurons in the rat striatum. J Neurophysiol 88:1263–1269. Medline

Wang Z, Kai L, Day M, Ronesi J, Yin HH, Ding J, Tkatch T, Lovinger DM, Surmeier DJ (2006) Dopaminergic control of corticostriatal long-term synaptic depression in medium spiny neurons is mediated by cholinergic interneurons. Neuron 50:443–452. CrossRef Medline

IV

Manuscript

Modulation of intrastriatal connections by presynaptic membrane potential

H. Planert*, S. N. Szydlowski* and G. Silberberg

Striatal neurons undergo large state-dependent fluctuations in their membrane potential, often spanning tens of millivolts. These fluctuations affect the neuronal conductance, discharge probability and postsynaptic responses. It is however, not known how such voltage fluctuations affect intrastriatal synaptic transmission. In the neocortex, hippocampus, and cerebellum, it has been shown that the membrane potential of the presynaptic neuron can modulate synaptic transmission in a gradual "analog" manner. The striatal microcircuit contains a majority of projection neurons (MSNs) as well as a small yet diverse population of interneurons. Fast spiking interneurons (FSIs) provide strong and depressing GABAergic inhibition onto MSNs in so called feedforward connections. In addition, MSNs are interconnected by feedback connections.
We investigated analog modulation of intrastriatal GABAergic feedforward and feedback transmission in mouse slices from Lhx6-EGFP, virally injected PV-Cre and wild type Swiss Webster mice. We obtained whole-cell patch-clamp recordings simultaneously from pairs, triplets and quadruplets of MSNs and identified interneurons. Changing the baseline membrane potential of the presynaptic cell affected the unitary amplitudes and paired-pulse ratios (PPR) of postsynaptic responses. The degree of PPR modulation was positively correlated with the baseline PPR values, indicating that high initial release probability is associated with smaller possibility for analog modulation of release. We further investigated this hypothesis by testing the effect of external Ca2+ concentration on analog modulation at individual FS-MSN synapses.
Our results show analog modulation in striatal synaptic transmission and that the extent of analog modulation depends on the initial release probability.

Synaptic transmission in the central nervous system is a digital, all-or-nothing event triggered by an action potential at the presynaptic neuron (Clark and Häusser, 2006; Debanne et al., 2012; Marder, 2006). It has long been known that this, however, is not the case in parts of the sensory and in several invertebrate systems (Angstadt and Calabrese, 1991; Burrows and Siegler, 1978; Katz and Miledi, 1967; Maynard and Walton, 1975; Shimahara and Tauc, 1975; Werblin and Dowling, 1969). There, synaptic transmission is conveyed in a gradual, analog manner where small voltage deflections in the presynaptic membrane affect the postsynaptic responses. It has recently been shown that the digital synaptic transmission in mammalian central synapses can be modulated in an analog manner by the presynaptic voltage (Alle, 2006; Christie et al., 2011; Shu et al., 2006; Zhu et al., 2011). These studies were done on excitatory and inhibitory synapses, suggesting that presynaptic voltage modulation may be an overall principle governing the majority of connections. In the cerebellum, inhibitory connections between interneurons showed voltage modulation that was dependent on the initial release probability (Christie et al., 2011).

Striatal projection neurons (medium sized spiny neurons - MSNs) are sparsely interconnected with GABAergic synaptic connections that have varying synaptic dynamics (Czubayko and Plenz, 2002; Koos et al., 2004; Planert et al., 2010; Taverna et al., 2008; Tunstall et al., 2002; Venance et al., 2004). MSNs also receive strong and depressing feedforward GABAergic connections from fast-spiking interneurons (FSIs) (Bennett and Bolam, 1994; Gittis et al., 2010; Kita et al., 1990; Koós and Tepper, 1999; Mallet et al., 2005; Planert et al., 2010; Taverna et al., 2007). Under in vivo conditions, striatal neurons, including both the MSNs and FSIs, undergo large state-dependent rhythmic fluctuations in their membrane potential (Wilson, 1993; Wilson and Groves, 1981; Wilson and Kawaguchi, 1996). These fluctuations between depolarized "up" and hyperpolarized "down" states are believed to be cortically driven (Wilson, 1986; Wilson et al., 1983a; 1983b). The duration in which striatal neurons stay at "up" states may vary between hundreds of milliseconds to several seconds (Mahon et al., 2006). Large voltage fluctuations were also described in awake animals,

Department of Neuroscience, Karolinska Institutet, Stockholm 17177, Sweden
*: These authors contributed equally.

where changes in brain state prolonged the periods spent in up states (Kasanetz et al., 2002; Mahon et al., 2006).

We therefore wanted to investigate whether intrastriatal feedback and feedforward synapses are also modulated in an analog manner by presynaptic membrane voltage. Such modulation of intrastriatal inhibition may be crucial for maintaining the dynamic balance between excitation and inhibition impinging on striatal projection neurons.

METHODS

Slice Preparation and Recordings

All experiments were carried out according to the Guidelines of the Stockholm Municipal Committee for animal experiments. Three different mouse lines were used Lhx6-EGFP 25 and wild type Swiss Webster mice (n = 59) along with AAV2 injected PV-Cre (n = 7) 35. Both the Lhx6-EGFP and Swiss Webster mice were used and sacrificed at postnatal day 18-28 and PV-Cre mice at postnatal day 24-51. The PV-Cre mice were virally injected 10-18 days prior to being used 36. Brains were dissected in ice-cold carbogenated sucrose solution or normal ACSF. The sucrose solution contained the following (in mM) 205 Sucrose, 25 NaHCO3, 10 Glucose, 7.5 MgCl2 6H2O, 2.5 KCl, 1.25 NaH2PO4 H2O, CaCl2 2H2O and the ACSF (in mM) 125 NaCl, 2.5 KCl, 2 CaCl2 2H2O, 1.25 NaH2PO4 H2O, 1 MgCl2 6H2O. Parasagittal slices ,250 µm thick, were cut on a vibratome (Leica VT 1000S Leica Microsystems Nussloch GmbH, Germany). They were incubated in 35°C for 30-60 min after cutting and then transferred to room temperature. Slices were perfused with carbogenated ACSF during recordings, and the temperature was set to 35°C. In some experiments extracellular calcium concentrations were lowered to 1 or 1.5 mM, and magnesium concentrations were elevated in order to maintain the same concentration of divalent ions. Glass pipettes were pulled on a Flaming Brown Micropipette Puller P-1000, (Sutter Instruments, Co, Novato, CA) and had a resistance of 5-10 MΩ. The pipettes were back-filled with intracellular solution containing contained (in mM) 105 mM K_Gluconate, 30 KCl, 10 Na_Phosphocreatine, 10 HEPES, 4 ATP-Mg and 0.3 GTP-Na and in some experiments 0.3% Neurobiotin. Neurons were visualized with IR-DIC microscopy (ZEISS FS Axioskop, Oberkochen, Germany) and the Lhx6-EGFP labeled neurons with a Mercury Vapor Short Arc lamp (X-cite series 120 Q, Lumen Dynamics Group Inc, Ontario Canada) and a green fluorescent filter cube mounted on the same microscope. Whole-cell recordings with up to four cells recorded simultaneously were done in current-clamp mode with access resistance and pipette capacitance compensated throughout the experiments. When access resistance reached above 35 MΩ the recording was discarded. The Liquid Junction Potential was approximately 10mV and was not corrected for. Multiclamp 700 B amplifiers were used and the recordings were filtered at 2KHz and digitized (5-20 KHz) with ITC-18 acquisition board (HEKA Inc. Instrutech Corporation, NY, USA). Recordings were acquired and analyzed using Igor Pro (Wavemetrics, OR, USA). Cells were chosen at random or, in the cases with the Lhx6-EGFP animals, under fluorescence microscopy according to their EGFP expression. They were classified as either Medium Spiny Neurons or Fast-Spiking Interneurons depending on their electrophysiological characteristics 19.

Stimulation protocols and analysis

The neurons were subjected to various stimulation protocols to be able to classify them and extract intrinsic properties. We tested connectivity by evoking action potentials (APs) in the presynaptic neuron with two brief current pulses (pulse duration: 3 ms, interval 100 ms, see Fig. 1), or in some cases a train of five pulses at 20 Hz.. To test for presynaptic voltage modulation, presynaptic neurons were depolarized for a duration of 4-5 s before evoking APs every second sweep. The baseline holding potential was about -80mV (-81± 0.61 mV) in control sweeps and depolarized by ~20mV (-56 ± 1.1 mV) during the prepulse. The prepulse duration was chosen according to the modulation time constant observed for neocortical synapses 10. Traces were discarded from analysis if the presynaptic neuron discharged spontaneous APs during the prepulse. The postsynaptic responses were averaged with at least 5 sweeps in each condition, and within conditions, only traces that did not deviate by more than 10 mV were used. The membrane potential prior to the responses in both conditions was comparable (-81.18 ± 1.53 and -81.19 ± 1.53, paired t test p = 0.31, n = 20). Synaptic amplitudes were automatically extracted using IgorPro. In order to extract the second amplitude, the synaptic decay was fitted by an exponential curve and was subtracted from the response to correct for the previous response. Paired Pulse Ratios (PPR) were calculated and classified as facilitating if they were above 1 and depressing if they were below 1.

$$PPR = IPSP2 / IPSP1 \quad (1)$$

The coefficient of modulation (Mc) was calculated as

$$Mc = PPRcondition1 / PPRcondition2 \quad (2)$$

Statistical analysis and associated figures were made using Graph Pad Prism and figures were edited using Adobe Illustrator. Linear Regression was made between the PPR of condition 1 and Mc with a test of non-zero slope with a significance level of 95%. The value of r2 was obtained and any value above 0.64 (r = 0.8) was considered a strong correlation and values above 0.25 (r = 0.5) moderate correlations. The different data sets were tested for normality, and if normal distribution could be assumed a paired t test (two-tailed) was conducted, otherwise a paired Wilcoxon signed rank test (two-tailed). Other values are reported as mean ± SEM.

RESULTS

Connections between Fast Spiking Interneurons and Medium Spiny Neurons are modulated by presynaptic voltage

To test the presence of modulation of intrastriatal connections by presynaptic voltage, we focused on the feedforward connections between FSIs and MSNs (Koós and Tepper, 1999; Mallet et al., 2005). We simultaneously recorded from single FSIs and single, pairs, and triplets of MSNs (FS-MSN pairs, n = 49). To target FSIs we used Lhx6-EGFP transgenic mice and EGFP expressing cells were classified as FSIs according to their intrinsic properties including high firing rate, fast and deep afterhyperpolarization, non-accommodating firing pattern and narrow action potentials (n = 25, fig 1B). We recorded from 17 FSIs and 49 FSI-MSN pairs. To test for connectivity, we elicited

pairs of action potentials in the presynaptic cell. We recorded 18 such connections and their average unitary amplitude was 2.52 ± 1.19 mV and paired-pulse ratio 0.88 ± 0.18 (fig 2B-D). We tested if presynaptic voltage affected the connections by depolarizing the presynaptic cell 5 s prior to stimulation. The average amplitudes from these experiments are 2.92 ± 1.22 mV and they are significantly larger than the ones in the control condition ($p = 0.013$, paired Wilcoxon signed rank test, fig 2B-C). The paired-pulse ratios were 0.76 ± 0.16 and were smaller than the ones in the control condition ($p = 0.028$, paired t test, fig 2D). To also test whether the modulation of FSI-MSNs connections was influenced by initial release probability, we did a linear regression between the paired-pulse ratio in the control condition and the Modulation coefficient (see Materials & Methods). This showed a moderate correlation that is statistically significant ($r2 = 0.32$, $p = 0.014$, fig 2E). In summary, depolarizing the presynaptic FSI enhanced synaptic amplitudes and increased synaptic release probability. Modulation of the release probability was associated with the initial PPR of the recorded synapse.

Changing the synaptic dynamics of connections may alter the modulation by presynaptic voltage

To examine whether initial release probability indeed is correlated to the degree of modulation, we altered the initial release probability of recorded connections by decreasing the extracellular Calcium concentrations (Katz and Miledi, 1970). Thereby the driving force is altered and less Calcium enters the presynaptic terminals, thus resulting in a decrease of release probability. We altered extracellular Calcium concentrations from 2 mM to half ([Ca2+]=1 mM), and to three fourths (1.5 mM) (n = 5). An example from one of those experiments is shown in fig 3A. We then examined if altering the initial release probability influenced the amount of modulation by correlating the Modulation coefficient with the initial PPR ($r2 = 0.95$, $p < 0.0001$, fig 3B), showing that the degree of voltage modulation is indeed strongly associated with the initial release probability.

Connections between Fast Spiking Interneurons and Medium Spiny Neurons in PV-Cre mice show a modulation that is strongly correlated to initial release probability

To test if there was any difference between transgenic mouse lines we also targeted FSIs in a PV-Cre line and simultaneously recorded from MSNs (fig 1C). The PV-Cre mice were injected with an Adeno Associated Viral vector (AAV2) that expressed a mCherry-ChR2 fusion protein in a Cre-dependent manner. The PV-expressing (FSIs) cells thus expressed ChR2 and mCherry (fig 1C)(Cardin et al., 2009). MCherry positive cells had intrinsic properties of typical FSIs and MSNs were identified as explained above (see also fig 1B,D). Connectivity was tested with a train of four pulses (fig 4A). We recorded from 10 connections and the average first amplitude of these in the control condition was 1.83 ± 0.52 mV (fig 4B). The Paired-Pulse Ratio was 0.83 ± 0.09 and two of the connections were facilitating (PPR > 1, fig 4D). To test if the connections were modulated by presynaptic voltage, a 4.4 s pulse that depo-

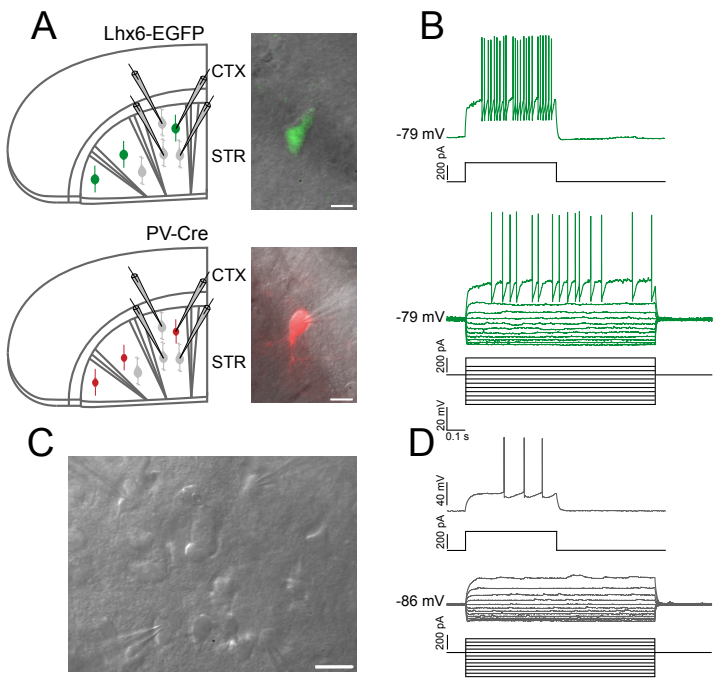

Figure 1. Classification of recorded neurons. A, Schematic showing the experimental set-up (Top Left). Merged photomicrographs taken with fluorescent and Ir microscopy respectively of a GFP-positive recorded neuron from the Lhx6-EGFP mouse (Top right), Scalebar = 10 µm. Schematic showing the experimental set-up (Bottom Left). Merged photomicrographs taken with fluorescent and Ir microscopy respectively of a mCherry-positive recorded neuron from the PV-Cre mouse (Bottom right), Scalebar= 10 µm B, The response of the GFP positive depicted neuron to a subthreshold current injection (Top) and a series of hyperpolarizing and depolarizing current steps (bottom). C, Photomicrograph of a quadruple of recorded MSNs, Scalebar= 20 µm. D, The response of one of the depicted MSNs to a subthreshold current injection (Top) and a series of hyperpolarizing and depolarizing current steps (Bottom).

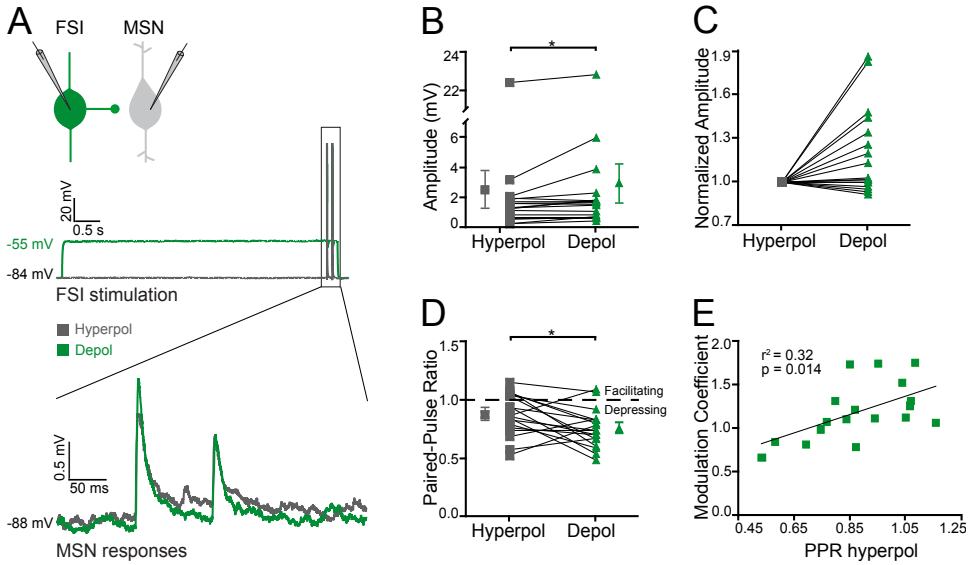

Figure 2. Effect of presynaptic voltage modulation of connections between GFP+ FSIs and MSNs. A, Schematic showing the presynaptic and postsynaptic neuron. (Top) Average trace from a presynaptic FSI showing the paired pulse stimulation and the 5.1 s prepulse that in this case depolarized the cell to -55 mV (depol or condition 2). In the control (hyperpol) condition, the membrane potential was -84 mV(Middle). The response to this stimulation of the postsynaptic MSN, the membrane potential of the cell was -88 mV (Bottom). B, Amplitude (mV) in the two conditions from all recorded FSI-MSN connections (n=18). There was a statistical difference between the amplitudes in the two conditions (p = 0.013). Average (hyperpol) = 2.52 ± 1.19 mV. Average(depol) = 2.92 ± 1.22. C, Normalized 1st amplitudes from all recorded connections. D, Paired-pulse ratios between the 2 conditions. Average(hyperpol)= 0.88 ± 0.18, Average(depol)= 0.76 ± 0.16. The difference in paired-pulse ratio between the two conditions was statistically significant (p = 0.028) . E, Linear regression of the PPR in the hyperpolarized condition versus the Modulation coefficient (Mc = PPRcondition1/PPRcondition2) showing a statistically significant correlation with r = 0.32 and p = 0.014.

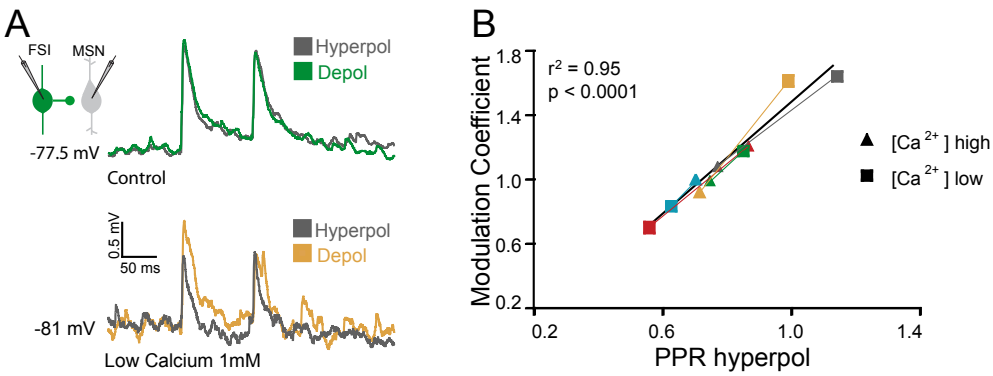

Figure 3. Effect of decreasing initial release probability, by lowering extracellular [Ca2+], on modulation of FSI-MSN connections by presynaptic voltage. A, Schematic showing the presynaptic and postsynaptic cell (Top). Example Responses to presynaptic FSI stimulation (see fig 3 for details on stimulation protocol) of the postsynaptic MSN in control conditions (Middle). Responses to the presynaptic FSI stimulation of the postsynaptic MSN when [Ca2+] were lowered to 1 mM (same neurons recorded as in Middle traces. Notice the decreased release probability (decreased amplitude) in the hyperpolarized condition and the strongly depressing synaptic dynamics in the depolarized condition (Bottom). B, Linear regression of the PPR in the hyperpolarized condition versus the Modulation coefficient in both the control (high Calcium) and low Calcium concentrations. The individual experiments from the two concentrations are paired and color-coded. The linear regression shows a strong and statistically significant correlation with r =0.95 and p < 0.0001.

larized the presynaptic cell was given prior to the stimulation (fig 5A). The average first amplitude in the depolarized condition was 2.00 ± 0.71 mV and there was no significant difference between the amplitudes in the two different conditions (paired t test, p = 0.46). We also compared the paired-pulse ratios (0.75 ± 0.03) and the differences were also found to be insignificant (paired t test, p = 0.33, fig 4D). As was the case with feedforward connections in the LHX6-EGFP mice, the modulation coefficient was positively correlated to the initial PPR (r2 = 0.86, p = 0.0001, fig 4E). This strong and highly significant correlation indicates that the degree of presynaptic voltage modulation is strongly associated with the initial release probability of the synapse.

Presynaptic voltage possibly alters release probability in connections between Medium Spiny Neurons

To further test presynaptic voltage modulation of intrastriatal connections we also recorded from feedforward connections formed between MSNs. We obtained whole-cell patch-clamp recordings in current-clamp mode from pairs, triplets and quadruplets of MSNs in both wild type (Swiss Webster) and Lhx6-EGFP mice. MSNs were classified according to their intrinsic properties; hyperpolarized resting membrane potential (-77 ± 0.4 mV), inward rectification in response to hyperpolarizing and depolarizing current steps, and delayed AP discharge with a ramp to the first action potential, (fig 1 D). We tested the recorded pairs (n = 380) for connectivity and synaptic dynamics by eliciting paired action potentials in the presynaptic cell. 5 of the recorded pairs of neurons were connected (n = 5/288; 1.7 %). An example of such a connection is shown in fig 5A. The unitary amplitude of the connections in the hyperpolarized or control condition was 0.91 ± 0.18 mV (fig 5B). We tested the effect of presynaptic voltage on the connections by keeping the presynaptic cell at a more depolarized membrane potential 5 s prior to the stimulus. The amplitude in this condition was 1.00 ± 0.24 mV (fig 5A-C). There was no significant voltage modulation of the amplitude (paired t test, p = 0.51). The paired-pulse ratios were 0.76 ± 0.11 for the hyperpolarized and 0.63 ± 0.09 in the depolarized condition, respectively (n = 4, Fig 5D). The connections exhibited varying synaptic dynamics, as described previously (Planert et al., 2010), and one of the connections were facilitating with a PPR of 1.09. The facilitating connection showed a robust decrease in PPR in the depolarized condition (fig 5D). Again, there is a strong correlation with the initial release probability (r2 = 0.72), so that it appears to us that modulation by presynaptic voltage in MSN-MSN connections, as in the FS-MSN ones, may be associated with release probability of the connection. However, we can still not draw any conclusions due to the small number of connections (p = 0.15) (fig 5E).

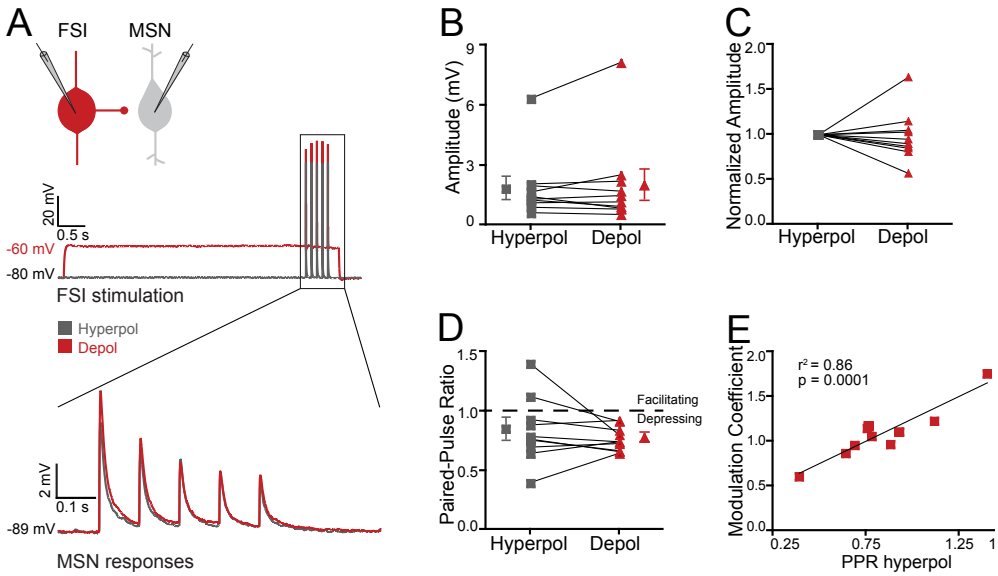

Figure 4. Effect of presynaptic voltage modulation of connections between PV+ FSIs and MSNs. A, Schematic showing the presynaptic and postsynaptic cell (Top), An average trace from a presynaptic FSI showing a train of stimulation and the 4.4 s prepulse that in this case depolarized the cell to -60 mV (depol or condition 2). In the control (hyperpol) condition the membrane potential was -80 mV (Middle). The response to this stimulation of the postsynaptic MSN. The membrane potential of the cell was -89 mV(Bottom). B, The amplitude (mV) in the two conditions from all recorded FSI-MSN connections (n = 10). Average(hyperpol) = 1.83 ± 0.52 mV, Average(depol) = 2.00 ± 0.71(p = 0.46) C, Normalized 1st amplitudes from all recorded connections. D, Paired-pulse ratios between the 2 conditions (n = 10). Average(hyperpol)= 0.83 ± 0.09 mV, Average(depol) = 0.75 ± 0.03 mV (p = 0.33). E, Linear regression of the PPR in the hyperpolarized condition versus the Modulation coefficient showing a strong and statistically significant correlation with r =0.86 and p = 0.0001.

DISCUSSION

We showed here that intrastriatal GABAergic synaptic connections between striatal projection neurons (MSN-MSN) and interneurons (FS-MSN) can be modulated by changing the presynaptic membrane potential. Such analog transmission has been shown to modulate synapses in the neocortex, hippocampus and cerebellum(Alle, 2006; Christie et al., 2011; Shu et al., 2006; Zhu et al., 2011). In particular, feedforward connections were shown to be modulated by analog transmission. In these connections, amplitudes were increased and PPRs were decreased. Furthermore the extent of the modulation depended on the initial release probability of the synapse. This is in agreement with a previous study of GABAergic synapses between Molecular Layer interneurons (MLIs) in the cerebellum(Christie et al., 2011). The phenomenon has also been studied at inhibitory synapses in the neocortex, between FSIs and Pyramidal cells and Low threshold spiking interneurons and pyramidal cells (Zhu et al., 2011). A portion of these synapses also exhibited this type of modulation, thereby further agreeing with our findings. The synaptic dynamics of the cerebellar MLI connections were varying with both facilitating and depressing synapses (Christie et al., 2011). The feedforward connections between FSIs and MSNs are mainly depressing, but the rules governing the modulation seem to be similar, indicating that it may be a principle common to GABAergic synapses.

The hypothesis of the underlying mechanism of modulation is that subthreshold presynaptic depolarization travels from the soma to the axon (Alle, 2006; Shu et al., 2006). In the neocortex and cerebellum this is believed to trigger Ca2+ entry into the presynaptic terminal (Christie et al., 2011; Shu et al., 2006). More conflicting evidence has been presented in the hippocampus and the Ca2+ involvement is not resolved (Scott et al., 2008). In the cerebellum, Ca2+ entry is believed to be mediated by voltage-sensitive calcium channels(Christie et al., 2011). Although we cannot prove or disprove these hypotheses, our study supports the idea that Calcium entry to presynaptic terminals is indeed enhanced by somatic depolarization.

Surprisingly, we found different results of the modulation of the feedforward connections between the two different animal models used. Both the amplitudes and PPR were unchanged during modulation in the FSI-MSN connections recorded in PV-Cre mice. The percentage of FSIs in the Lhx6-EGFP transgenic mouse in the striatum has been showed to be 41 %. 34 % of all GFP+ cells are immunoreactive for PV(Gittis et al., 2010). It is therefore likely that FSIs recorded in the Lhx6-EGFP mouse are also PV expressing and thereby not from a generally different population of FSIs compared to the ones recorded in the PV-Cre

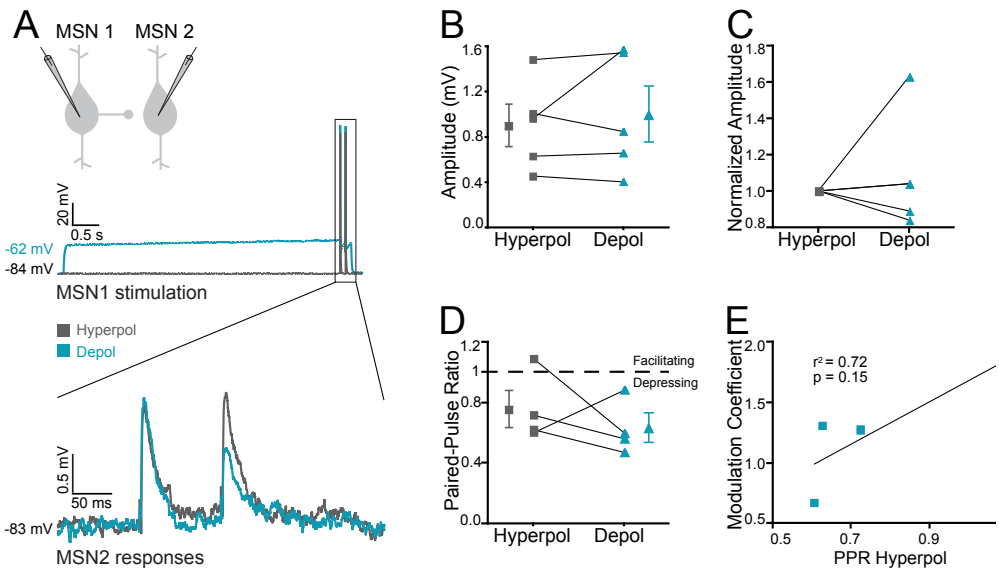

Figure 5. Presynaptic voltage modulation of connections between MSNs. A, Schematic showing the presynaptic and postsynaptic neuron (Top),. Average trace from a presynaptic MSN showing the paired pulse stimulation and the 5.1 s prepulse that in this case depolarized the cell to -62 mV (depol or condition 2). In the control (hyperpol) condition, the membrane potential was -84 mV (Middle). The response to this stimulation of the postsynaptic MSN. The membrane potential of the cell was -83 mV (Bottom). B, A diagram of the Amplitude (mV) in the two conditions from all recorded MSN-MSN connections (n=5). Average (hyperpol) = 0.91 ± 0.18 mV. Average(depol) = 1.00 ± 0.24 mV. C, Normalized 1st amplitudes from all recorded connections. D, Paired-pulse ratios in the 2 conditions (n=4). Average(hyperpol)= 0.76 ± 0.11, Average(depol)= 0.63 ± 0.09. E, Linear regression of the PPR in the hyperpolarized condition versus the Modulation coefficient showing a strong but statistically insignificant correlation with r = 0.72 , and p = 0.15

mouse. There could however be a difference in relative expression levels of PV in the FSIs due to a bias in cell selection based on fluorescence, or an actual difference of PV expression of the FSI populations in the different animal models. An alternative explanation could be that the transfection of interneurons with ChR2 affected their properties by photo-excitation during the experiment. The fact that the correlation between the PPR and initial release probability still holds (and is indeed strong in this sample) indicates that the basic mechanism for analog transmission is present but the selection, state, or synaptic connections of these FSIs may possibly be altered.

Striatal neurons undergo fluctuations in their membrane potential and the most studied of these fluctuations, the up-and down states, are cortically driven (Wilson, 1986; 1993; Wilson and Groves, 1981; Wilson and Kawaguchi, 1996; Wilson et al., 1983a; 1983b). The cycles in which the neurons spend in each state are 0.1-3 s but can be longer in some other behaviorally relevant states (Kasanetz et al., 2002; Mahon et al., 2006). In the periods in which the presynaptic cell is depolarized, synaptic transmission could be modulated by analog transmission. This would suggest an important functional role to analog transmission and would also ascribe an important modulatory role for the up- and down states. It implies the way in which the cortex can affect intrastriatal connectivity and it can also explain how the striatum can match the cortical excitation with an increase in inhibition. Interconnectivity between striatal projection neurons has been reported to be sparse and if our findings will hold for a larger part of the MSN connections it could explain a way in which different states can make these connections more reliable and temporally precise.

We have shown that analog transmission modulates intrastriatal connections, that modulation is associated with release probability of the synapse and we hypothesize that presynaptic depolarizations could make connections more reliable and time locked indicating an important functional role for this type of modulation.

ACKNOWLEDGEMENTS

We thank Marie Carlén and Dinos Meletos for providing the PV-Cre mice and the virus and Iskra Pollak Dorocic for doing all virus injections.

REFERENCES

Alle, H. (2006). Combined Analog and Action Potential Coding in Hippocampal Mossy Fibers. Science (New York, NY) 311, 1290–1293.

Angstadt, J.D., and Calabrese, R.L. (1991). Calcium currents and graded synaptic transmission between heart interneurons of the leech. The Journal of Neuroscience : the Official Journal of the Society for Neuroscience 11, 746–759.

Bennett, B.D., and Bolam, J.P. (1994). Synaptic input and output of parvalbumin-immunoreactive neurons in the neostriatum of the rat. Neuroscience 62, 707–719.

Burrows, M., and Siegler, M.V. (1978). Graded synaptic transmission between local interneurones and motor neurones in the metathoracic ganglion of the locust. The Journal of Physiology 285, 231–255.

Cardin, J.A., Carlén, M., Meletis, K., Knoblich, U., Zhang, F., Deisseroth, K., Tsai, L.-H., and Moore, C.I. (2009). Driving fast-spiking cells induces gamma rhythm and controls sensory responses. Nature 459, 663–667.

Christie, J.M., Chiu, D.N., and Jahr, C.E. (2011). Ca(2+)-dependent enhancement of release by subthreshold somatic depolarization. Nature Neuroscience 14, 62–68.

Clark, B., and Häusser, M. (2006). Neural coding: hybrid analog and digital signalling in axons. Current Biology 16, R585–R588.

Czubayko, U., and Plenz, D. (2002). Fast synaptic transmission between striatal spiny projection neurons. Proceedings of the National Academy of Sciences of the United States of America 99, 15764–15769.

Debanne, D., Bialowas, A., and Rama, S. (2012). What are the mechanisms for analogue and digital signalling in the brain? Nature Reviews Neuroscience 14, 63–69.

Gittis, A.H., Nelson, A.B., Thwin, M.T., Palop, J.J., and Kreitzer, A.C. (2010). Distinct Roles of GABAergic Interneurons in the Regulation of Striatal Output Pathways. The Journal of Neuroscience : the Official Journal of the Society for Neuroscience 30, 2223–2234.

Hippenmeyer, S., Vrieseling, E., Sigrist, M., Portmann, T., Laengle, C., Ladle, D.R., and Arber, S. (2005). A developmental switch in the response of DRG neurons to ETS transcription factor signaling. PLoS Biology 3, e159.

Kasanetz, F., Riquelme, L.A., and Murer, M.G. (2002). Disruption of the two-state membrane potential of striatal neurones during cortical desynchronisation in anaesthetised rats. The Journal of Physiology 543, 577–589.

Katz, B., and Miledi, R. (1967). A study of synaptic transmission in the absence of nerve impulses. The Journal of Physiology 192, 407–436.

Katz, B., and Miledi, R. (1970). Further study of the role of calcium in synaptic transmission. The Journal of Physiology 207, 789–801.

Kita, H., Kosaka, T., and Heizmann, C.W. (1990). Parvalbumin-immunoreactive neurons in the rat neostriatum: a light and electron microscopic study. Brain Research 536, 1–15.

Koos, T., Tepper, J.M., and Wilson, C.J. (2004). Comparison of IPSCs evoked by spiny and fast-spiking neurons in the neostriatum. The Journal of Neuroscience : the Official Journal of the Society for Neuroscience 24, 7916–7922.

Koós, T., and Tepper, J.M. (1999). Inhibitory control of neostriatal projection neurons by GABAergic interneurons. Nature Neuroscience 2, 467–472.

Mahon, S., Vautrelle, N., Pezard, L., Slaght, S.J., Deniau, J.-M., Chouvet, G., and Charpier, S. (2006). Distinct patterns of striatal medium spiny neuron activity during the natural sleep-wake cycle. Journal of Neuroscience 26, 12587–12595.

Mallet, N., Le Moine, C., Charpier, S., and Gonon, F. (2005). Feedforward Inhibition of Projection Neurons by Fast-Spiking GABA Interneurons in the Rat Striatum In Vivo. The Journal of Neuroscience : the Official Journal of the Society for Neuroscience 25, 3857–3869.

Marder, E. (2006). Neurobiology: extending influence. Nature 441, 702–703.

Maynard, D.M., and Walton, K.D. (1975). Effects of maintained depolarization of presynaptic neurons on inhibitory transmission in lobster neuropil. Journal of Comparative Physiology ? A 97, 215–243.

Planert, H., Szydlowski, S.N., Hjorth, J.J.J., Grillner, S., and Silberberg, G. (2010). Dynamics of synaptic transmission between fast-spiking interneurons and striatal projection neurons of the direct and indirect pathways. The Journal of Neuroscience : the Official Journal of the Society for Neuroscience 30, 3499–3507.

Scott, R., Ruiz, A., Henneberger, C., Kullmann, D.M., and Rusakov, D.A. (2008). Analog modulation of mossy fiber transmission is uncoupled from changes in presynaptic Ca2+. Journal of Neuroscience 28, 7765–7773.

Shimahara, T., and Tauc, L. (1975). Multiple interneuronal afferents to the giant cells in Aplysia. The Journal of Physiology 247, 299–319.

Shu, Y., Hasenstaub, A., Duque, A., Yu, Y., and McCormick, D.A. (2006). Modulation of intracortical synaptic potentials by presynaptic somatic membrane potential. Nature 441, 761–765.

Szydlowski, S.N., Pollak Dorocic, I., Planert, H., Carlén, M., Meletis, K., and Silberberg, G. (2013). Target selectivity of feedforward inhibition by striatal fast-spiking interneurons. The Journal of Neuroscience : the Official Journal of the Society for Neuroscience 124, 1678–1683.

Taverna, S., Canciani, B., and Pennartz, C.M.A. (2007). Membrane properties and synaptic connectivity of fast-spiking interneurons in rat ventral striatum. Brain Research 1152, 49–56.

Taverna, S., Ilijic, E., and Surmeier, D.J. (2008). Recurrent collateral connections of striatal medium spiny neurons are disrupted in models of Parkinson's disease. The Journal of Neuroscience : the Official Journal of the Society for Neuroscience 28, 5504–5512.
Tunstall, M.J., Oorschot, D.E., Kean, A., and Wickens, J.R. (2002). Inhibitory interactions between spiny projection neurons in the rat striatum. Journal of Neurophysiology 88, 1263–1269.
Venance, L., Glowinski, J., and Giaume, C. (2004). Electrical and chemical transmission between striatal GABAergic output neurones in rat brain slices. The Journal of Physiology 559, 215–230.
Werblin, F.S., and Dowling, J.E. (1969). Organization of the retina of the mudpuppy, Necturus maculosus. II. Intracellular recording. Journal of Neurophysiology 32, 339–355.
Wilson, C.J. (1986). Postsynaptic potentials evoked in spiny neostriatal projection neurons by stimulation of ipsilateral and contralateral neocortex. Brain Research 367, 201–213.
Wilson, C.J. (1993). The generation of natural firing patterns in neostriatal neurons. Progress in Brain Research 99, 277–297.
Wilson, C.J., and Groves, P.M. (1981). Spontaneous firing patterns of identified spiny neurons in the rat neostriatum. Brain Research 220, 67–80.
Wilson, C.J., and Kawaguchi, Y. (1996). The origins of two-state spontaneous membrane potential fluctuations of neostriatal spiny neurons. The Journal of Neuroscience : the Official Journal of the Society for Neuroscience 16, 2397–2410.
Wilson, C.J., Chang, H.T., and Kitai, S.T. (1983a). Disfacilitation and long-lasting inhibition of neostriatal neurons in the rat. Experimental Brain Research Experimentelle Hirnforschung Expérimentation Cérébrale 51, 227–235.
Wilson, C.J., Chang, H.T., and Kitai, S.T. (1983b). Origins of post synaptic potentials evoked in spiny neostriatal projection neurons by thalamic stimulation in the rat. Experimental Brain Research Experimentelle Hirnforschung Expérimentation Cérébrale 51, 217–226.
Zhu, J., Jiang, M., Yang, M., Hou, H., and Shu, Y. (2011). Membrane potential-dependent modulation of recurrent inhibition in rat neocortex. PLoS Biology 9, e1001032.
Spontaneous Subthreshold Membrane Potential Fluctuations and Action Potential Variability of Rat Corticostriatal and Striatal Neurons In Vivo.